

https://dspace.org/

Landslide classification, characterization and susceptibility modeling in KwaZulu-Natal

Singh, Rebekah Gereldene

2010-03-04T12:27:45Z
http://hdl.handle.net/10539/7624

Downloaded from a DSpace repository. https://dspace.org/

LANDSLIDE CLASSIFICATION, CHARACTERIZATION AND SUSCEPTIBILITY MODELING IN KWAZULU-NATAL.

by

Rebekah Gereldene Singh

Supervisors: Prof T McCarthy and Dr G.A. Botha

A dissertation submitted to the Faulty of Science, University of the Witwatersrand, Johannesburg, in fulfillment of the requirements for the Degree of Master of Science

2009

DECLARATION

I declare that this dissertation is my own, unaided work. It is being submitted for the Degree of Master of Science in the University of the Witwatersrand, Johannesburg. It has not been submitted before for any degree or examination in another University. The information used in the dissertation has been obtained while employed by the Council for Geoscience.

_____
(Signature of candidate)

_____ day of _____ 200_____

ABSTRACT

In eastern South Africa landslides are widespread owing to the dramatic topographic-, climatic-, geological- and geomorphological-gradients across the region. In the KwaZulu-Natal (KZN) province numerous landslides and associated deposits are geohazards that represent threats to development and strategic infrastructure.

The regional landslide inventory and susceptibility mapping project, following international classification systems and modeling techniques, has revealed the widespread occurrence of landslides. Landslide types mapped include; falls, topples, flows, translational and rotational slides. The bivariate statistical landslide susceptibility modeling method and Analytical Hierarchy Process (AHP) was used to evaluate landslide susceptibility, using a Geographic Information System (GIS).

The huge size of some palaeo-landslides mapped is a revelation in the context of KwaZulu-Natal where recent landslide events are mainly small features triggered by intense rainfall events affecting embankments and steep hillslopes. Radiocarbon dating of organic material derived from sag ponds yielded minimum ages for the large middle to late Holocene landslide events.

ACKNOWLEDGEMENTS

I would like to express my heartfelt gratitude to the following individuals who have made this work possible:

- My supervisors, Prof Terence McCarthy and Dr Greg Botha, who provided scientific guidance, and encouragement.

- Many thanks to all individuals who completed the preference rating questionnaire.

- Thank you to all my colleagues at the KZN unit of the Council for Geoscience for providing moral and academic support during this project. A special thank you to Dr Nick Richards who provided academic guidance during early stages of the project.

- The Chief Executive Officer of the Council for Geoscience, Mr. Thibedi Ramontja and Dr Peter Zawada, Executive Manager of the regional mapping division for their support of this project.

- My husband, Rakesh and my family for their constant support, encouragement and inspiration.

TABLE OF CONTENTS

ABSTRACT I

ACKNOWLEDGEMENTS II

LIST OF FIGURES VI

LIST OF TABLES XI

CHAPTER ONE 1

1. INTRODUCTION, OBJECTIVES AND METHODOLOGY 1

1.1 Introduction 1

1.2 Research objectives 4

1.3 Previous landslide studies in the KZN region 7

1.4 Methodology 8

CHAPTER TWO 15

2. REGIONAL SETTING 15

2.1 Physiography 15

2.2 Climate 16

2.3 Regional geology 18

2.4 Terrain morphology and geomorphology of KZN 22

CHAPTER THREE 27

3. LANDSLIDE TYPES, CLASSIFICATION, MAPPING AND DATING 27

3.1 Overview 27

3.2 Overview of landslide classification systems 31

3.3 Classification system derived for the KZN context 32

3.4 Landslide mapping 34

3.5 Landslide dating 40

3.6 Site Investigations 44

3.6.1 Undated sites 44

3.6.2 Dated sites 47

3.7 Interpretation of landslide ages 60

3.8 Ground truthing 64

3.9 Landslide characteristics 69

CHAPTER FOUR 70

4. LANDSLIDE SUSCEPTIBILITY MAPPING 70

4.1 Overview 70

4.2 Previous landslide susceptibility maps 70

4.3 Landslide causal factors 72
4.3.1 Slope angle 72
4.3.2 Seismicity 74
4.3.3 Lithostratigraphy and rock type 76
4.3.4 Rainfall 77
4.3.5 Dolerite intrusion contact zones 80
4.3.6 Lineaments 80
4.3.7 Terrain morphology 80
4.3.8 Aspect 81

4.4 Landslide susceptibility methodologies 82

4.5 Evaluation of methodologies 83

4.6 Bivariate statistical susceptibility analysis 84
4.6.1 Calculation of ranking values of Pertinent Sub–Classes 85
4.6.2 Analytical Hierarchy Process evaluation of weighting values 90
4.6.3 Model computation using the ArcGIS Spatial Analyst 93

4.7. Landslide susceptibility evaluation 94

4.8 Landslide Susceptibility Map 97

4.9 Landslide Susceptibility Map Description and Verification 98

CHAPTER FIVE 106

5. DISCUSSION 106

CHAPTER SIX 109

6. CONCLUSION 109

REFERENCES 111

APPENDIX 1: Landslide inventory 130

APPENDIX 2: Graphs showing ranking values of all considered landslide causal factors 140

APPENDIX 3: Consistency ratio calculation 152

APPENDIX 4: Analytical hierarchy process calculation 155

LIST OF FIGURES

Figures		Pages
Figure 1	Locality map showing the KZN Province and key road infrastructure.	3
Figure 2	Anaglyphs and aerial photographic interpretations of the Mount Currie and Dilston palaeo-landslides.	14
Figure 3	Regional geology of KZN (Whitmore et al., 1999).	19
Figure 4	An idealized landslide block diagram (Varnes, 1978).	29
Figure 5a-e	The five basic types of landslides based on the mode of movement (Cruden and Varnes, 1996).	30
Figure 6	Distribution of the regions initially investigated in KZN showing key landslide sites, the closest urban nodes and arterial roads. a: Matatiele–Cedarville–Kokstad; b: Ukhahlamba–Drakensberg; c: Ladysmith–Dundee–Vryheid–Utrecht; d: Central Zululand regions.	38
Figure 7	Shaded relief map based on the 90m SRTM digital elevation model showing the widespread occurrence of various types of landslides in areas studied within KZN. Occurrences were identified through aerial photographic interpretation, field mapping and from literature reviews.	*
Figure 8	Recent superficial flows (centre left) occurring on the steep slopes north of the public picnic site in the Giant's Castle Nature Reserve.	39
Figure 9	Rockfalls are a typical occurrence in the Drakensberg. Weathering of an argillaceous layer below a resistant sandstone bed or enhanced groundwater seepage results in formation of a hanging block of sandstone. Disengagement of these hanging blocks from the rock face is along fracture and joint planes.	40

* Find figure in the pocket sleeve located at the back of the dissertation.

Figure 10a-c	(a) A translational slide occurred in the sandstones of the Vryheid Formation on an eastward facing slope in the Molletshe Tribal Authority area in 1991. (b) View of the translational slide in 1991 showing sharp morphological landslide features. (c) View of the slide in 2006 showing similarities in the morphological landslide features since the landslide event.	43
Figure 11a, b	(a) Aerial view showing characteristic hummocky topography indicative of palaeo-landslides on the slopes of the Bushman's River valley. (b) GIS – based, geomorphological map of the Bushman's River valley palaeo-landslides.	46
Figure 12a-d	(a) Panoramic view of the Mount Currie landslide taken from the southern slopes of Bushy Ridge (b) Sketch of the Mount Currie landslide, located northeast of Kokstad, showing the zones of depletion and accumulation. (c) Digital elevation model (DEM) of the Mount Currie landslide based on a 20m grid interval. Vertical exaggeration x1.6. The X and Y scales are in decimal degrees. (d) Cross-section through the Mount Currie palaeo-landslide showing the geomorphic features and geometry.	49
Figure 13	GIS - based, detailed geomorphological map of the Mount Currie palaeo-landslide (centre) and the dominant features are illustrated in the surrounding photographs.	50
Figure 14a, b	(a) Digital elevation model (DEM) of the 1.4 km^2 Knostrope palaeo-landslide based on a 90m grid interval. The landslide area includes the zones of depletion and accumulation. Vertical exaggeration x4.2. The X and Y scales are in metres. (b) Cross-section through the Knostrope palaeo-landslide showing the geomorphic features and geometry.	52
Figure 15a-c	(a) Random joint pattern in dolerite observed at outcrop scale,	53

	approximately 8 km northeast of Helpmekaar. (b) Lower hemisphere equal angle stereographic projection of joints. (c) Rose diagram of joints.	
Figure 16	Wide bedrock cracks parallel to the scarp above landslides, near Helpmekaar, represent classic geoindicators of future slope instability.	54
Figure 17a-c	(a) GIS - based, detailed geomorphological map of the Meander Stream palaeo-landslide and the dominant features are illustrated in the adjacent photographs. (b) The Meander Stream rotational palaeo-landslide, located in the Giant's Castle Nature Reserve, had a profound influence on drainage development. Immediately upstream an anomalous meandering stream floodplain has developed in an area where the deeply incised tributary valleys are typically drained by steep gradient, linear or dendritic channels. (c) Cross-section through the Meander Stream palaeo-landslide showing the geomorphic features and the geometry.	57
Figure 18a, b	(a) Aerial view of the Gobela palaeo-landslide, located in the Giant's Castle Nature Reserve. (b) Cross-section through the Gobela flow palaeo-landslide showing the geomorphic features and geometry.	58
Figure 19	Sag ponds within the hummocky topography of the Gobela palaeo-landslide.	58
Figure 20a-c	(a) Aerial photograph of the Mooihoek palaeo-slide showing typical hummocky terrain forms. Symbol (○) refers to the locality at which the photograph shown in Figure 20b was taken. (b) Incision through a hummock exposing unsorted, angular dolerite and shale blocks in a reddish-brown clayey sand. (c) Cross-section through the Mooihoek palaeo-landslide, located north of Babanango, showing the geomorphic features and geometry.	59
Figure 21	Age estimates of the various palaeo-landslides superimposed on the palaeo-	63

climatic proxy record from the Cold Air Caves speleothem (Lee-Thorp et al., 2001; Holmgren et al., 2003). There is no clear correlation with warmer, relatively more humid periods

Figure 22 Seismicity map of the Matatiele-Cedarville-Kokstad region showing relatively large magnitude seismic events in the Mount Currie area (Seismology Unit, Council for Geoscience, 2005). 64

Figure 23 Digital elevation model (DEM) of the Poplars landslide based on a 20m grid interval. The landslide area includes the zones of depletion and accumulation. Vertical exaggeration x2.3. The X and Y scales are in decimal degrees. 67

Figure 24a-c (a) Digital elevation model (DEM) of the landslides in Royal National Park based on a 90m grid interval. Vertical exaggeration x2.5. The X and Y scales are in decimal degrees. (b) A flow debris palaeo-landslide (Mudslide) in the Royal Natal National Park, view to the northeast (Thomas, 1985). (c) Aerial view of the flow debris palaeo-landslide. 68

Figure 25 Landslide susceptibility map of southern Africa based on geology, geomorphology, water and historical landslide events (Paige–Green, 1985). 71

Figure 26 A compilation of the various regional landslide causal factors initially selected. 73

Figure 27 Map illustrating the relationship of bedding dip in shales of the Pietermaritzburg Formation with slopes in the Durban area. High values indicate concordant relationship of bedding with slope dip. 79

Figure 28 Flowchart showing the various critical steps in the bivariate statistical analysis (modified after Soeter and Van Westen, 1996). 86

Figure 29 Graph showing landslide polygon density versus slope class. 87

Figure 30 Graph showing ranking values per slope angle class 89

Figure 31	Illustration on how map algebra uses mathematical operators and functions to derive new information on a cell by cell basis.	93
Figure 32	Illustration on the utilisation of the Reclassify and Raster calculator functions of Spatial Analyst.	95
Figure 33	Illustration showing how the landslide susceptibility coefficient data was evaluated on a cell by–cell basis.	96
Figure 34	Landslide susceptibility of KZN.	*
Figure 35	The large Dilston landslide is an undifferentiated palaeo-landslide with an areal extent of approximately 3.0 km^2, located in the Umkomaas valley, approximately 50 km SSW of Pietermaritzburg.	99
Figure 36	Toppling in vertically jointed shales in the vicinity of Helehele**.**.	100
Figure 37	The landslide susceptibility map shows good correspondence with the slope instability identified by Richards et al., (2008) during the Pietermaritzburg geotechnical mapping programme.	102
Figure 38	Shallow flows associated with the "Berea Red Sand" in the La Lucia area, north of Durban.	104
Figure 39	The landslide susceptibility map shows strong correlation with the regional slope instability inventory data.	105

* Find figure in the pocket sleeve located at the back of the dissertation.

LIST OF TABLES

Tables		Pages
Table 1	Summary of research objectives, hypotheses and approaches adopted.	6
Table 2a	Durban average monthly temperatures and rainfall for the 30-year period 1961 – 1990 (South African Weather Service, 2007).	17
Table 2b	Ladysmith average monthly temperatures and rainfall for the 30-year period 1961 – 1990 (South African Weather Service, 2007).	18
Table 3	Stratigraphic subdivision of the Natal Group showing the dominant rock types (Marshall, 1994, 2003a, b; Marshall and Von Brunn, 1999).	21
Table 4	Summary of major stages in the geomorphic evolution of Southern Africa, comparing the models of King 1972 and Partridge and Maud 1987 (after Boelhouwers, 1987)	26
Table 5	Abbreviated landslide classification scheme employed in this study (modified after Cruden and Varnes, 1996).	33
Table 6	Landslide size classification based on the areal extent of the failure zone (*after* van Schalkwyk and Thomas, 1991).	33
Table 7	Localities of landslides that were sampled for organic rich sediment on which radiocarbon dating was done.	47
Table 8	Radiocarbon ages derived from organic deposits in sag ponds of palaeo-landslides in KZN.	61
Table 9	The Natal Provincial Administration industry standards for development planning.	74
Table 10	Overview of methodologies and recommendations of their use at three most relevant scales (Soeter and Van Westen, 1996)	84
Table 11	Ranking values of each sub-class	88
Table 12	Preference rating values	91

Table 13 The pairwise comparisons of each decision–maker 91

Table 14 Landslide causal factor comparison matrix 92

Table 15 Weighting values of each landslide causal factor 94

CHAPTER ONE

1. INTRODUCTION, OBJECTIVES AND METHODOLOGY

1.1 Introduction

Landslides are an important form of mass movement responsible for hillslope development and long-term evolution of landscapes. This geomorphic process is often abrupt and is caused by unconstrained movement of large volumes of material downslope with catastrophic force. Landslide debris deposits also represent a residual geomorphological threat due to risks of secondary slope instability. Throughout the world landslides and their associated debris deposits are significant geomorphological threats responsible for large socio–economic losses.

Landslides annually destroy or damage industrial or residential developments, forest and agricultural lands and are often responsible for numerous human casualities and fatalities. Many Asian countries such as Pakistan, China, Taiwan and Japan have also suffered major devastation due to rainfall and/or earthquake induced-landslides. Some examples of large landslides around the world that caused such devastation are described below. The 2005 La Conchita landslide in California killed 10 people, destroyed 13 houses and severely damaged 23 others (Randall, 2005). Widespread landslides occurred as a result of an earthquake in the mountainous Kashmir region of Pakistan during October 2005. Approximately 10976 landslide-related deaths associated with the 2005 Kashmir earthquake have been recorded (Petley and Rosser, 2007). During 2006 the Southern Leyte landslide in the Philippines caused widespread damage and the loss of more than 1000 lives (International Federation of the Red Cross and Red Crescent Societies, 2007). According to Petley and Rosser (2007) a total of 394 landslide events were recorded, inducing 3017 deaths worldwide during 2007. A series of heavy rainfall events has triggered numerous landslides in southwestern China during the past two years. Currently, extreme rainfall associated with Typhoon Morakot has initiated a large mudslide that has buried up to 300 villagers in mountainous southern Taiwan.

Japan has been severely affected by landslides and suffers estimated landslide losses of $4 billion annually (Schuster, 1996). In the United States, landslides are estimated to cause an annual loss of about $1.5 billion and at least 25 fatalities (United States Search and Rescue Task Force, 2000).

In South Africa landslides have been responsible for fatalities on the Chapman's Peak drive along the Cape Peninsula Atlantic coastline prompting extensive structural improvements and removal of loose rock from the steep slopes. The catastrophic failure of a mine tailings dam in Merriespruit, a suburb of Virginia in the Free State goldfields, was initiated by heavy rainfall in February 1994. The Merriespruit mud flow devastated the residential suburb resulting in the death of seventeen people which prompted a review of the Mine Health and Safety legislation and an introduction of a new code of practice in 1997. In the KZN Province (Fig. 1) landslides most often affect urban developments and strategic communication infrastructure. The risk of slope failure excludes large areas around urban nodes from formal development and many areas of informal housing are potentially at risk.

Many areas in eastern South Africa are prone to slope failure due to diverse terrain morphology comprising high mountains and steep valley slopes, high intensity summer rainfall, deep weathering associated with the humid climate and ancient landsurface remnants, combined with a range of geological and structural influences. In KZN there have been no isolated, large–scale, catastrophic, natural landslide events in recent history. However, numerous recent landslide events in the province have been mainly small features triggered by high intensity rainfall events and the cumulative costs to society associated with these small slides may be as great as a large catastrophic

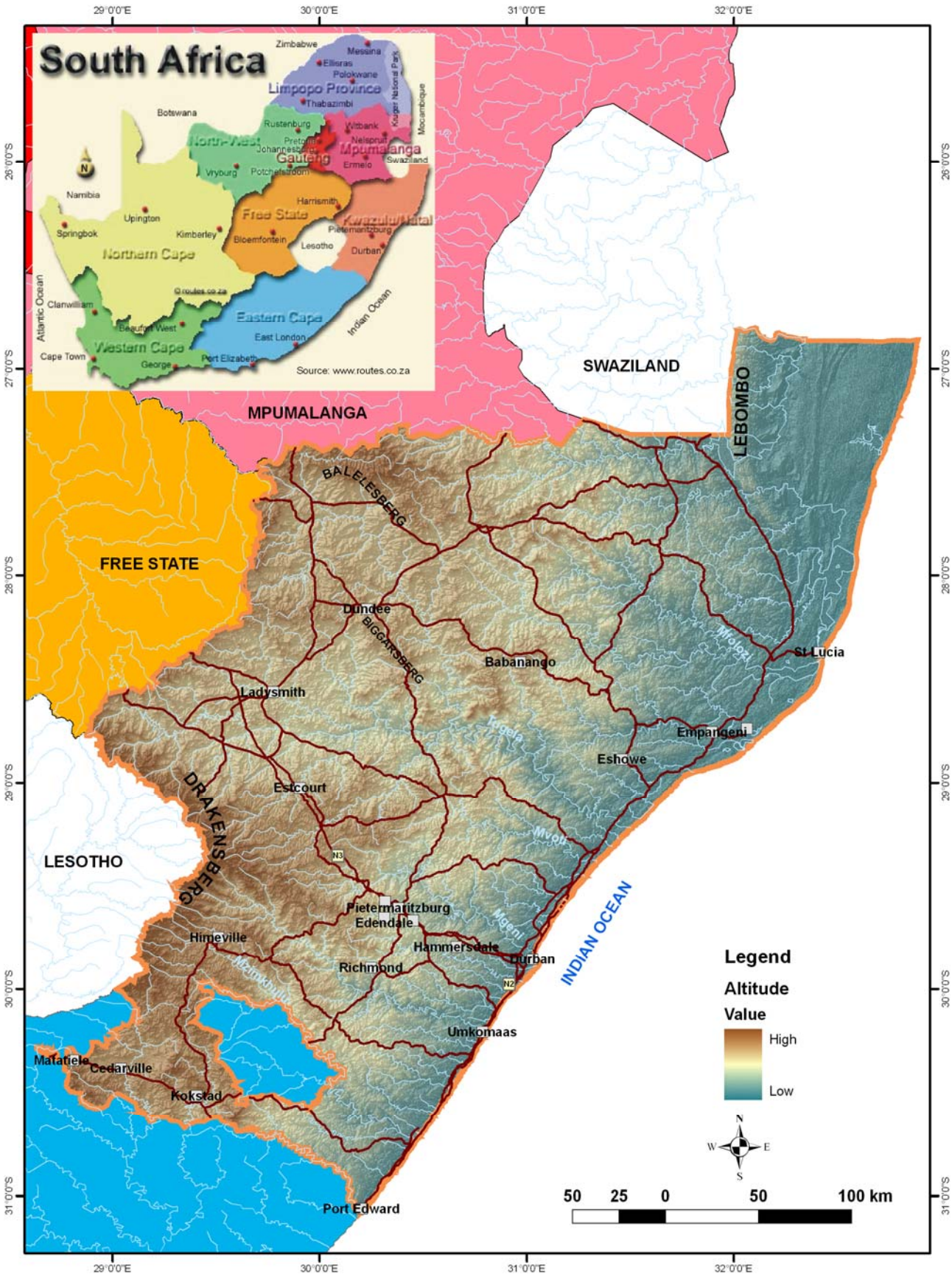


Figure 1 Locality map showing the KZN Province and key road infrastructure

landslide. In 1987, heavy summer rainfall in the greater Durban area resulted in landsliding with estimated costs amounting to approximately $2.5 million (Paige–Green, 1989).

Losses such as impairment to ecosystems have not been widely documented in current literature but may have devastating consequences on natural habitats especially in pristine World Heritage sites such as the uKhahlamba–Drakensberg Park through landslide induced stream blockage and slope denudation which promotes erosion. Such devastation of the priceless natural environment may have unrecoverable costs. The 2km–long Lake Fundudzi located in the Soutpansberg Range, Limpopo, is an inland freshwater lake formed by a huge palaeo-landslide which blocked the course of the Mutale River (Janisch, 1931). From a short–term perspective it is difficult to envisage the benefits of natural landslide events. However, in terms of a geological time scale framework, mass movement is a fundamental geomorphic mechanism responsible for landscape development in KZN.

Although landslides remain difficult to predict it is possible through the process of detailed landslide inventory mapping and statistical modeling techniques to identify areas that are at highest potential for slope failure. This project aimed to generate a detailed landslide susceptibility model for the KZN province that can be used by provincial and municipal planners to identify areas which can be studied further or avoided during spatial development framework planning.

1.2 Research objectives

There are huge initiatives to develop rural areas both in South Africa and elsewhere on the African continent. In KZN landslides and their associated debris deposits often represent geohazards that impose significant threats and risk on development of strategic infrastructure. The ongoing instability factors associated with the palaeo–landslide deposits below the World's View

escarpment and the Rickivy area on the western escarpment slopes around Pietermaritzburg highlights the geohazard potential. Landslide deposits therefore should be one of the primary considerations in town planning and landuse zonation.

Landslide susceptibility maps are one of the fundamental products of slope instability investigations which rank the slope stability of an area into categories that range from stable to unstable. Susceptibility maps highlight areas where landslides may form and provide information of potential devastation. A holistic–approach to regional mapping of landslides and their associated debris deposits has not been systematically adopted in KZN. This pioneering project represents the first holistic approach to regional scale investigation of landslides covering the most susceptible areas in KZN.

The mapping and classification of these landslide deposits highlighted the fact that these Quaternary disequilibrium geomorphic features are more widespread than is commonly appreciated. The creation of a provincial landslide susceptibility map aimed at providing a critical town planning tool for future decision making in regional and urban development projects. The research objectives are summarized below (Table 1):

Table 1 Summary of research objectives, hypotheses and approaches adopted.

Research Objective	Research Hypothesis	Research Approach
Does geology determine the landslide type?	Although landslides are associated with all bedrock types, the type of landslide is dependent on geology. Slides and flows are frequently associated with the softer rocks that generally weather deeply whilst rock falls are associated with rocks that are more resistant to deep weathering.	Aerial photograph interpretations overlaid on a regional geological map permit assessment of the association between rock type and slope instability.
Does the widespread intrusion of dolerite influence slope failure?	Differential weathering between dolerite and sedimentary country rocks creates areas of steep topography. Dolerite intrusions alter the dip of the country rocks locally. Bedding planes may become concordant with the slope gradient. The contact zone between dolerite and country rock, and dense vertical jointing within dolerite act as zones of groundwater migration. Groundwater saturation may increase pore pressures within the weathering profile associated with these zones and thus reduce strength.	By overlaying aerial photographic interpretations on a regional geological map the association of dolerite with slope failure can be assessed.
What landslide classification system should be employed?	The Varnes' (1978) classification, including amendments from Cruden and Varnes (1996), has been adopted. This approach is consistent with the UNESCO Working Party on World Landslide Inventory (WP/WLI, 1990)	Review of various classification systems to assess the most appropriate scheme for KZN and modify if necessary.
Are large landslides across the province coeval?	Similarities in the morphology, degree of degradation, soil profile development and significant accumulation of organic rich sediment in back–tilted pond areas of the large landslides indicate that they occurred at a similar period in geological history.	Radiocarbon dating of suitable organic material derived from back tilted ponds of landslide deposits, described by Stout (1969, 1977) and McCalpin (1989), is a suitable technique for providing a minimum age for some landslides.
Are the larger landslides triggered by climatic, slope threshold or seismic influences?	The three primary triggering factors of heavy and prolonged rainfall, high slope gradients and seismicity interacted simultaneously to create large landslides of very similar morphology.	By overlaying regional maps of each causal factor with a landslide inventory distinctive trends may be determined.

Which landslide susceptibility methodology should be adopted in a regional study?	The qualitative or direct mapping approach includes the landslide inventory and heuristic analyses, which are generally based on personal experience or knowledge, are considered as subjective. Some qualitative approaches, however, incorporate the idea of ranking and weighting, and may evolve to be semi–quantitative in nature. The quantitative methods such as statistical methods and deterministic approaches can be considered as more objective due to the data–dependent character of the methodologies rather than experience driven knowledge.	Review of landslide methodologies. Application of appropriate methodologies and production of landslide susceptibility map in a GIS by inter–relating the landslide causal parameters.
How accurate is the derived KZN landslide susceptibility map?	Applying the suitable susceptibility methodology to the KZN province will ensure that the landslide susceptibility map is most appropriate.	The quality of the resultant KZN landslide susceptibility map at a regional scale will be examined by overlaying the regional landslide inventory data to verify map accuracy.

1.3 Previous landslide studies in the KZN region

Although little is known about the regional distribution of landslides in South Africa (Beckedahl et al., 1988), there have been a number of case studies based on recent landslide events in KZN and neighbouring areas. The association between landslides and various lithostratigraphic units has been investigated by Bell and Maud (1996a, b) who studied landslide occurrences in areas underlain by Natal Group sandstone and Pietermaritzburg Formation shale around Durban. According to Bell and Maud (2000) the majority of the most recent landslides have occurred in thick, sandy colluvial deposits that accumulated on slopes formed of Ordovician Natal Group sandstone bedrock. Many site–specific investigations have been carried out with respect to slope stability problems in the region (Maurenbrecher and Booth, 1975), and in particular slope instability problems associated with the construction of the N3 highway in the Rickivy area of Pietermaritzburg (Maurenbrecher, 1973; Maud, 1985). The Mayat Place landslide, studied extensively by the firm D.L.Webb and Associates (1975) and summarized by Webb (1983), occurred in an area underlain by Pietermaritzburg Formation shale where the bedding dips concordantly with the hillslope. Studies focusing on the geomorphological context of landslides include Boelhouwers (1988a), Garland and

Olivier (1993), Olivier et al., (1993) and Sumner (1993). A regional study of the nature and distribution of slope failures associated with the extreme rainfall and flood events of September 1987 and February 1988 in KZN (van Schalkwyk and Thomas, 1991) employed the Varnes (1978) classification system. Also, a predictive landslide modeling study was carried out in the Injisuthi Valley, Drakensberg by Bijker (2001) to highlight the spatial distribution of shallow slope failures. Aspects of this research have been published in the South African Journal of Geology (Singh et al., 2008) and also presented at the XVII congress of the International Union for Quaternary Research (Singh et al., 2007).

1.4 Methodology

Central to the research methodology was the recognition of past landslides since the landslide susceptibility modeling followed the hypothesis which suggests slope-failures in the future will be more likely to occur under those conditions which led to slope instability and failure in the past.

The research programme was implemented in six phases:

(a) Literature review and background data

The initial phase involved a desktop study during which published technical work on slope instability was collated from international scientific and technical journal articles, geotechnical site reports and other unpublished work was investigated. The wealth of literature concerning landslides contributed the background data concerning mapping and classification systems, landslide dating techniques as well as landslide susceptibility modeling protocols used elsewhere in the world. Landslides in KZN were also identified from published literature (Bell and Maud, 1996a, b; van Schalkwyk and Thomas, 1991) and responses to appeals to local authorities and geotechnical consultants yielded valuable information which supplemented the regional aerial photographic interpretation.

(b) Aerial photographic interpretation

A regional aerial photographic interpretation was undertaken for specific terrain morphological regions (Kruger, 1983) in KZN. The initial focus was on areas of high relief and steep slopes in mountainous areas and the steep valley slopes of the main river basins traversing the province. The use of ~1:30 000 scale aerial photographs, viewed using stereographic projection, proved to be an effective technique for identification and delineation of medium to very large landslides (Fig. 2).

The larger landslides were mapped, differentiating the scarp failure plane, the zone of depletion and the accumulation zone. Where landslides appeared to have blocked streams or rivers the influences on river morphology up- and downstream were studied to identify possible terrace deposits. The more detailed, small scale aerial photographs were used for the compilation of the comprehensive landslide inventory. The landslide delineation and areal extent of observed features were checked during subsequent field investigations.

(c) Field reconnaissance and sampling

Field reconnaissance mapping and investigation was limited to the larger palaeo-landslides due to the large areal extent of the study region. During the field inspection phase, locations and extents of smaller landslides outside the coverage of the aerial photography were mapped using a Garmin III+ Gobal Positioning System (GPS) and plotted onto the relevant base map. Ground truthing of landslides identified through aerial photographic interpretation involved the detailed mapping of the well-preserved landslides within the various mapping regions. Key localities were also mapped in detail to understand and illustrate critical morphological relationships. All structural data was measured according to standard conventions and recorded using a compass clinometer. The co-ordinates of various critical landslides, key morphological features and radiocarbon dating sample localities were recorded by a GPS set on the WGS 84 datum.

The field reconnaissance was necessary to confirm the aerial photographic interpretations, assist in the modification of the amended classification system (Cruden and Varnes, 1996) to develop a system that more appropriately represents the range of slope failure types in the province, and provided insight into primary landslide causal factors.

Well-preserved medium to very large landslides with characteristic hummocky topography and sag pond deposits were identified on aerial photographs and targeted for onsite investigation as well as for the recovery of potentially datable organic material. The radiocarbon dating technique was performed on organic sediment derived from sag ponds of palaeo-landslide deposits across the province to assess whether these geomorphic events were coeval or if they were triggered at different times.

A representative landslide sag pond deposit in each study region was dated using C^{14} from organic-rich pond sediments to establish a minimum age estimate for those landslide events. Radiocarbon dating was performed on organic-rich samples derived from the base of the sag pond infill sediments that lie immediately above the landslide debris surface. These palaeo-landslide sag pond deposits were carefully augered by hand to collect basal bulk organic material. Sampling depth varied according to the morphology of the individual sag ponds and contained sediments which are from ~1.0 – 3.5m thick. Precautions were taken to limit modern carbon contamination of the organic deposits. Radiocarbon dating was conducted by the Council for Scientific and Research (CSIR)-Environmentek Quaternary Dating Research Unit and Beta Analytic Inc. radiocarbon dating laboratories. Both laboratories reported that the samples provided sufficient amounts of carbon for an accurate measurement and the analysis proceeded normally. The radiocarbon ages were reported as "years Before Present (BP)" and calibrated using the Pretoria programme (after Talma and Vogel, 1993) with a 1-sigma range. The single radiocarbon date produced by Beta Analytic Inc. used the AMS dating technique.

(d) Inventory map compilation

Each landslide and its affected area mapped through aerial photographic interpretations or identified in the field was manually plotted onto the latest 1: 50,000 topocadastral base maps. Digitising of the boundaries of each landslide feature i.e. main scarp and accumulation body, was initially carried out in ArcView 3.2 using a digitising tablet but was subsequently performed directly on screen in ArcGIS 9 to create a spatial database/inventory map. Other landslide data were recorded into the spatial database by digitising information from geological/engineering geological maps, using co–ordinates provided in the literature, or downloaded from GPS.

(e) Data modeling

A digital elevation model (DEM) was created using Surfer 8 software for each of the landslides that were targeted for further investigation. The DEM made it possible to explore each landslide and its affected area in three-dimensions and greatly facilitated the visual interpretation process. Onsite knowledge gained during the field investigations also assisted in the interpretation of the landslide causal parameters. ArcGIS software allowed for better insight into the spatial distribution of various mass movement types and facilitated the comparison of a series of thematic map layers and data tables. Procedures regarding utilization of GIS in the various landslide susceptibility methodologies have been discussed by Soeters and van Western (1996). The semi-quantitative, bivariate statistical landslide susceptibility method (refer to Chapter 4), was used to assess the landslide susceptibilty of the KZN province. During the implementation of the Bivariate statistical analysis the following GIS procedures were carried out:

- Categorisation of each parameter map into various pertinent sub–classes.
- Calculation of cross tabulation data defining the spatial correlations between a parameter sub–class and the landslides.
- Assignment of weighting values to each parameter sub–class based on the cross tabulation data. This is achieved by ranking each sub-class according to increasing mass movement polygon density.

- Assignment of weighting values to each parameter map. The decision criteria of the weighting values of individual parameter maps were obtained by using a multi–criterion decision making technique.
- Conversion of parameter vector maps (source data) to ranked raster maps using Spatial Analyst.
- Raster Calculator function of ArcGIS Spatial Analyst evaluated landslide susceptibility using map algebra, the resultant map highlighted various susceptibility classes.

A multi-criterion decision making technique based on the fuzzy set theory was utilised to effectively evaluate relative weighting values associated with landslide causal parameters. The landslide susceptibility modeling approach investigated the inter-relationships between the various landslide causal factors as well as their sub-classes. Weighting values of the landslide causal factors were derived using a multi–criterion decision making technique, the Analytical Hierarchy Process (AHP) (Saaty 1980, 1986, 1995) to reflect the relative importance of factors. The inter-relationship of various sub-classes of the individual landslide causal factors was evaluated from polygon densities. The polygon densities were calculated by ArcGIS 9 using a script downloaded from the Esri website (Schaub, 2004). The Raster Calculator function of ArcGIS Spatial Analyst evaluated landslide susceptibility using advanced map algebra, which involves the cell by cell combination of raster layers (landslide causal factor maps) using mathematical operations.

(f) Map verification

A quality control assessment to assess the accuracy of the landslide susceptibility map was performed in ArcGIS 9 by overlaying landslide inventory data that was not incorporated in the susceptibility modeling and an inspection of the areas delineated on the landslide susceptibility map as having a high landslide potential, but not previously considered to be landslide prone. Secondary aerial photographic interpretations of these highly susceptible areas, followed by further field

reconnaissance, identified some large landslides in areas that were not initially regarded as being landslide prone.

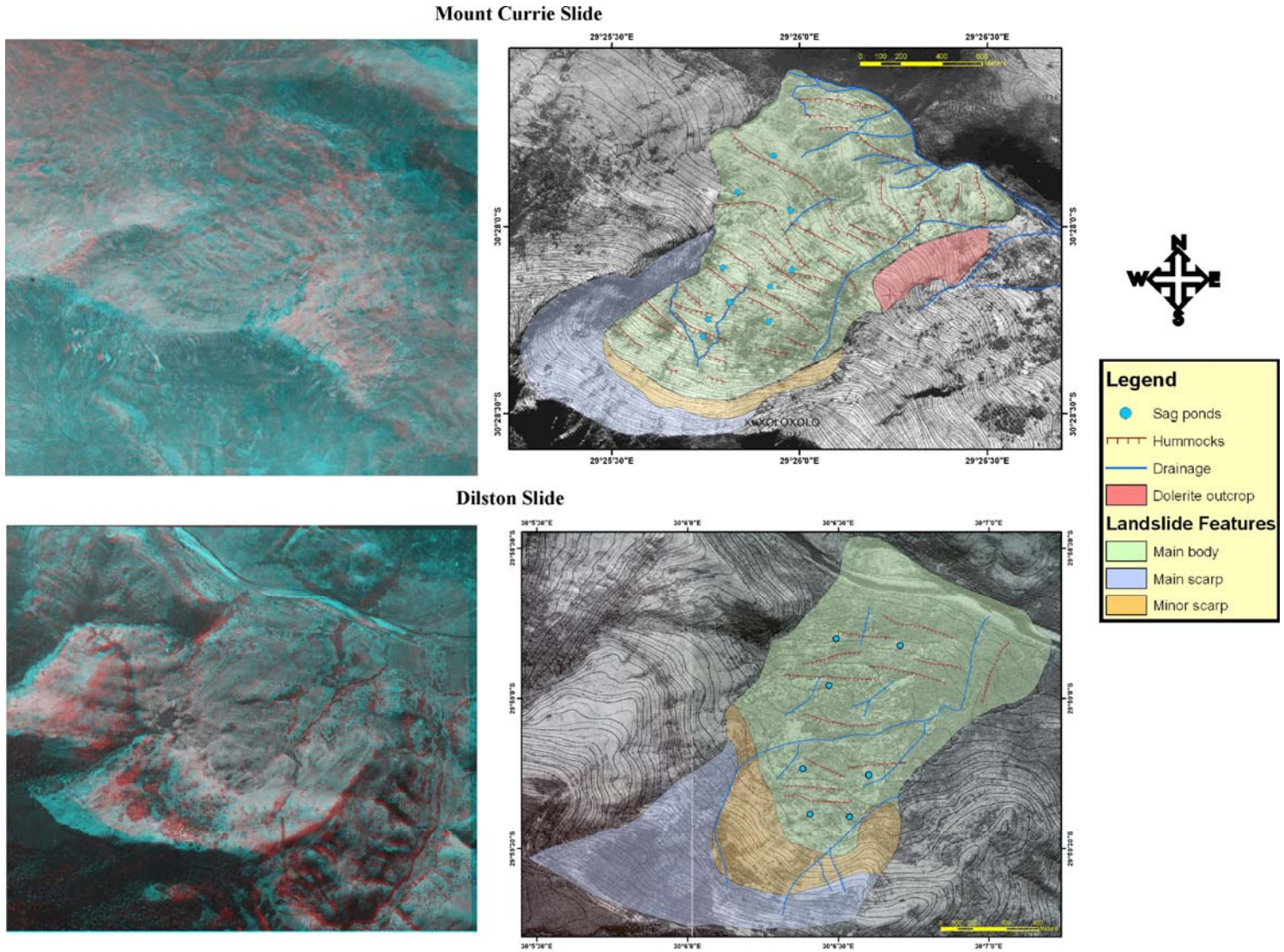


Figure 2 Anaglyphs and aerial photographic interpretations of the Mount Currie and Dilston palaeo-landslides.

Use 3D glasses provided in the pocket sleeve at the back of the report.

CHAPTER TWO

2. REGIONAL SETTING

2.1 Physiography

The KZN Province is bounded by the Eastern Cape in the south, Mpumulanga, Mozambique and Swaziland in the north, Free State and Lesotho in the west and the warm Indian Ocean in the east, with an areal extent of approximately 93 000 km^2 (Fig. 1). Major urban centres include the city of Durban, the Richards Bay/Empangeni industrial hubs and the capital city, Pietermaritzburg. Other important urbanized areas include Ulundi, Dundee, Ladysmith, Newcastle, Port Shepstone, Kokstad and Vryheid. Excluding the eThekweni Metropolitan Municipality the KZN region is subdivided into 10 District Municipalities and 50 Local Municipalities, which exercise administrative control at the local government level. The provincial economy thrives on agriculture, forestry, mining and tourism.

A high portion of the KZN populace is concentrated around the urban centres within municipal areas such as Durban. There is, however, a significant proportion of the populace that resides in non–urban areas resulting in a large number of poorly developed rural communities being scattered around the province. In terms of linear infrastructure, KZN has a well developed road network, comprising the N3 and N2 national highways, arterial routes, main roads, and tarred or graveled secondary roads together with an adequate rail system which facilitates easy access to most of the towns, rural settlements and harbours.

The KZN Province can be divided broadly into three geographic regions; i) lowland plains along the Indian Ocean, (ii) rolling hills in the central regions, (iii) mountainous areas in the west and north (Kruger, 1983). Some of the major rivers that drain the province include the

Tugela, Mfolozi, Mgeni, Msunduzi, Mkomaas and Mzimkulu (Fig. 1). In terms of mass movements the areas of steep relief e.g along the Drakensberg Mountains, Biggarsberg and Balelesberg ranges and Lebombo Mountains, and steep parts of the main river basins and valleys are thought to be most significant.

2.2 Climate

The KZN province lies between the Indian Ocean in the east and the high Drakensberg escarpment in the west. The weather patterns experienced in KZN are strongly influenced by the South Indian anticyclone which controls the general airflow over the region (Tyson, 1969; Schulze, 1972). During winter (dry season) there is a subsidence of air which results in atmospheric stability. However, in summer a subsidence inversion, if present, frequently rises above the escarpment resulting in an influx of humid air from the Indian Ocean by southeasterly winds.

In KZN summer rainfall (Table 2a, b) often results from convective thunderstorms or is orographically–induced along escarpments. Many of the flood events in eastern South Africa are caused by cut–off low pressure systems, which are an important synoptic-scale weather system (Tennant and Heerden, 1994; Hunter, 2007). The weather system responsible for the KZN floods of September 1987, one of the most devastating natural disasters in recent South African history, was a cut-off low that developed in the upper air accompanied by a strong surface high-pressure system that ridged across south of the country (Tennant and Heerden, 1994). According to Hunter (2007) the cut-off low of September 1987 caused more flood damage than the Tropical Cyclone Demoina in January 1984. Intense rainfall associated with these types of prolonged precipitation events or storms are often erosive and are directly associated with slope failure (van Schalkwyk and Thomas, 1991). Numerous slope failures were caused during the 120-150 year return rainfall event of September 1987 (Badenhorst et al., 1989).

The undulating terrain results in localised climatic variations. Generally, the coastal areas are sub-tropical with inland regions becoming progressively colder. Coastal areas such as Durban often experience hot, wet and very humid weather during the summer months. During the winter months very mild weather is encountered along the coastal belt. Durban has an annual rainfall of 1009 mm, with daytime maxima peaking from January to March at 28 °C with a minimum of 21 °C, dropping to daytime highs from June to August of 23 °C with a minimum of 11 °C (Table 2a). In KZN, the Zululand north coast experiences the warmest climate and highest humidity. Temperatures begin to drop toward the midland areas, with Pietermaritzburg being much cooler than coastal areas in winter. The very cool hinter-land regions including Ladysmith and the Drakensberg escarpment experiences very dry, cold - very cold conditions in winter with occasional frost and snow often falling in the higher elevation areas. In the summer Ladysmith reaches 30 °C but in winter temperature may drop below freezing point (Table 2b).

Table 2a Durban average monthly temperatures and rainfall for the 30-year period 1961 – 1990 (South African Weather Service, 2007)

Month	**Temperature (° C)**		**Precipitation**
	Average Daily Maximum	**Average Daily Minimum**	**Average Monthly (mm)**
January	28	21	134
February	28	21	113
March	28	20	120
April	26	17	73
May	25	14	59
June	23	11	28
July	23	11	39
August	23	13	62
September	23	15	73
October	24	17	98
November	25	18	108
December	27	20	102
Year	**25**	**17**	**1009**

Table 2b Ladysmith average monthly temperatures and rainfall for the 30-year period 1961 – 1990 (South African Weather Service, 2007)

Month	**Temperature (° C)**		**Precipitation**
	Average Daily Maximum	**Average Daily Minimum**	**Average Monthly (mm)**
January	30	17	145
February	29	16	106
March	28	15	90
April	25	11	39
May	23	6	14
June	20	2	6
July	21	3	5
August	23	6	26
September	25	10	38
October	26	12	77
November	27	14	91
December	29	16	112
Year	**25**	**11**	**749**

2.3 Regional geology

The geological evolution of KZN extends back in time to approximately 3 500 million years (Fig. 3). The Kaapvaal Craton (~3000Ma) predominantly comprises granitoids with subordinate gneisses. These Archaean rocks have intruded the ancient basaltic and ultramafic lavas (~3500 Ma) of the Greenstone Belt. According to Gold (2006) in South Africa the Pongola Supergroup appears to have formed two separate basins but probably accumulated in a single depositional basin which possibly was influenced by a structural high during deposition. The basal part of the

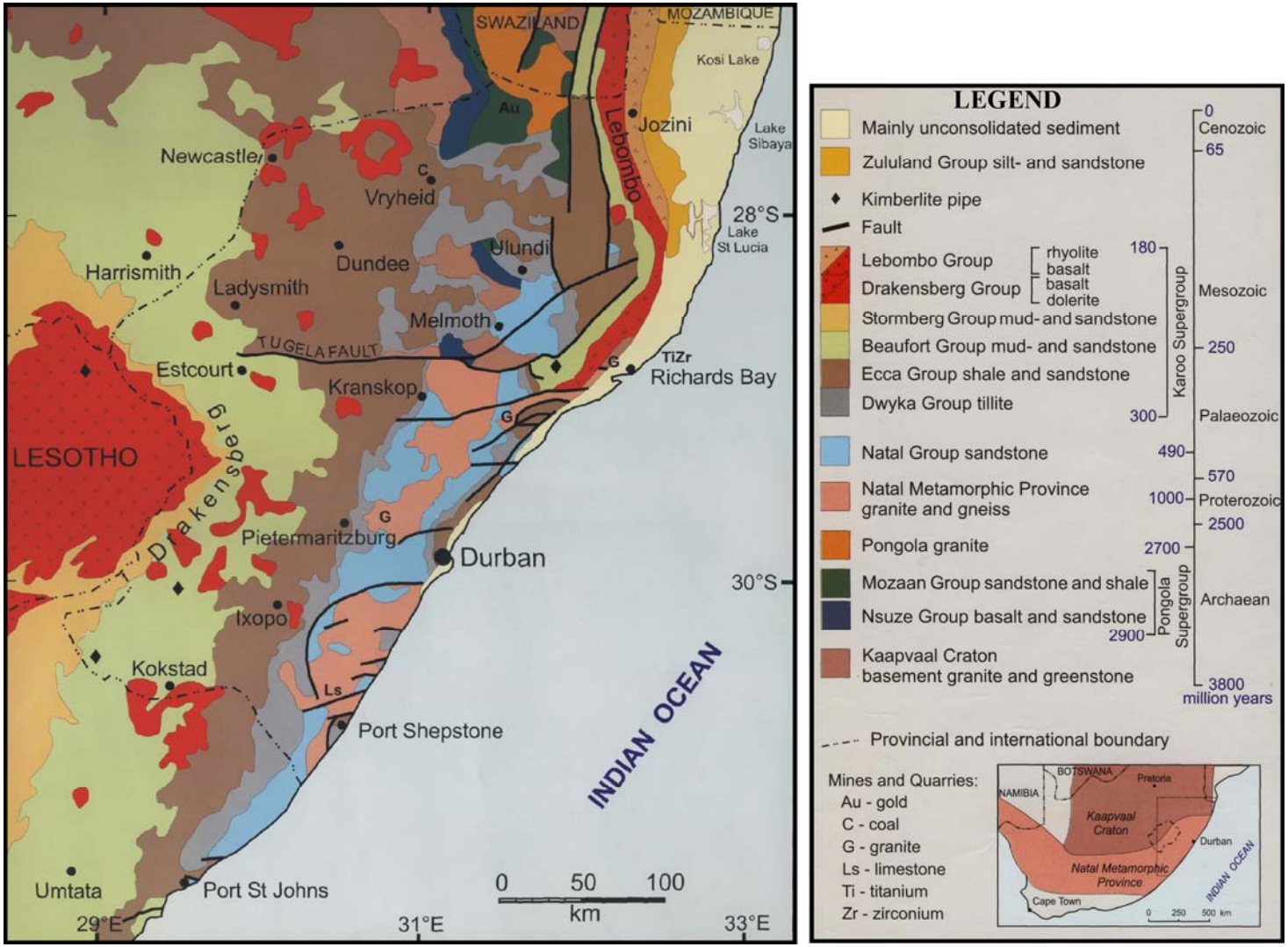


Figure 3 Regional geology of KZN (Whitmore et al., 1999).

Pongola Supergroup, the volcano-sedimentary Nsuze Group, unconformably overlies the Archaean basement. This volcano-sedimentary stratigraphic unit is overlain by the Mozaan Group which is characterized by a thick sedimentary succession of predominantly argillaceous and arenaceous sedimentary rocks.

During the Namaqua Orogeny approximately 1200-1000 Ma intense tectonism along the southern margin of the Kaapvaal Craton gave rise to the crystalline rocks of the Natal Sector of Natal Metamorphic Province (NMP). These Meso–proterozoic rocks are exposed as a series of basement inliers and can be subdivided from north to south into three terranes (Tugela, Mzumbe and Margate). Each terrane consists of lithostratigraphically different assemblages of supacrustal and intrusive rocks (Thomas, 1989).

The early Palaeozoic Natal Group comprising arkosic and quartz–arenitic sandstones, conglomerates and subordinate argillaceous rocks unconformably overlies the Archaean and Proterozoic basement rocks. Recent research has indicated that there is no correlation of the Natal Group rocks in KZN with the Late Devonian (Anderson and Anderson, 1985) Msikaba Formation south of the province and the revised stratigraphy of the Natal Group consists of two formations and eight members as summarized in Table 3 (Marshall, 1994, 2003 a, b; Marshall and Von Brunn, 1999).

Table 3 Stratigraphic subdivision of the Natal Group showing the dominant rock types (Marshall, 1994, 2003a, b; Marshall and Von Brunn, 1999)

Natal Group	**Mariannhill Formation**	Westville Member		matrix-supported conglomerate
		Newspaper Member		arkosic sandstone and shale
		Tulini Member		small-pebble conglomerate
	Durban Formation	Dassenhoek Member	Melmoth	silicified quartz arenite
		Situndu Member		coarse arkosic sandstone
		Kranskloof Member		silicified quartz arenite
		Eshowe Member		arkosic sandstone and shale
		Ulundi Member		coarse monomict clast-supported conglomerate

Disconformably overlying the Natal Group is the Karoo Supergroup. The Karoo Supergroup preserves a wide spectrum of depositional paleoenvironments ranging from glacial to deep marine, deltaic, fluvial and aeolian (Smith, 1990; Smith et al., 1993). The deposition of the basal Dwyka Group was associated with the Permo-Carboniferous glaciation of Gondwana, which lasted some 60 Ma (Visser, 1990). With the melting of the ice sheet a major transgression occurred, resulting in the formation of the marine Ecca basin (Johnson et al., 2006). In KZN the Ecca Group is represented by the Pietermaritzburg, Vryheid and Volksrust Formations. Stratified, carbonaceous shales and siltstones of the basal Pietermaritzburg Formation are overlain by the Vryheid Formation. The Vryheid Formation is a fluviodeltaic deposit, comprising sandstone, shales, siltstones and subordinate coal beds. The overlying Volksrust Formation is a predominantly argillaceous unit comprising silty shale with thin siltstone and sandstone lenses and beds, mainly in the upper and lower boundaries. Cairncrosss et al., (1998) found a large pelecypod bivalve with marine affinities in this formation. However, according to Taverner-Smith et al., (1988), the upper and lower parts of the Volkrust formation may have been deposited in lacustrine to possibly lagoonal and shallow coastal embayment environments.

These sediments are in turn overlain by the argillaceous and arenaceous rocks of Permian–Triassic Beaufort Group. These sandstones and mudstones form the foothill of the Drakensberg escarpment

and were deposited in predominantly fluvial environment under semi–arid climatic conditions. Overlying the Beaufort Group is the Molteno Formation comprising alternating medium-to coarse–grained sandstone with secondary siliceous cement, form prominent scarps in the lower Drakensberg. The Molteno Formation is in turn overlain by 'red–bed' succession (thinly–bedded mudstone and sandstone) of the Elliot Formation which represents fluvial deposits (Visser and Botha, 1980). The distinctive, overhanging cream to maroon, fine–grained sandstone cliffs of the Drakensberg constitutes the Clarens Formation. These fine-grained sandstones of the Late Triassic/ Early Jurassic Clarens Formation were deposited during a period of progressive warming and desiccation which is reflected by the fine-grained aeolian sand and associated ephemeral streams and flood plain playas (Beukes, 1970; Eriksson, 1981). With the break up of the Gondwana supercontinent approximately 183 Ma, massive lava outpourings occurred forming the Drakensberg and Lebombo Groups. Fractures and planes of weaknesses in rocks acted as conduits to the lava. Crystallisation of the magma within these fractures formed dolerite sills and dykes.

Following the regional volcanism, uplift and faulting resulted in the separation of Africa and Antarctica. The marine sediments of the Cretaceous Zululand Group were subsequently deposited in the newly opened Indian Ocean. Fluctuations in sea level resulted in the formation of a series of parallel dune complexes along the KZN coastline, such as the Berea and Bluff ridges. The geology of the KZN province is completed by erosion to present topography and this process of erosion continues to be active.

2.4 Terrain morphology and geomorphology of KZN

The significance of the Great Escarpment, forming the Ukhahlamba – Drakensberg escarpment and foothills, in the development of the landscape of KZN has been stressed repeatedly in the literature since the pioneering studies by Suess (1904) and Penck (1908) as cited in Partridge and Maud

(1987). Other early studies focusing on the South African landscape include work published by King (1941; 1944) and Dixey (1938; 1942, 1945).

Early geomorphical studies used geological theory based on the existence of the Natal monocline that formed at the breakup of Gondwana to explain the evolution of KZN (King and King, 1959 and King, 1974, 1982). The geomorphic history of the southern African subcontinent can be traced through a series of major evolutionary events since the fragmentation of Gondwana in the early Cretaceous (Table 4). These landscape development hypotheses invoked erosion cycles generated by intermittent uplift followed by long periods of stability during which pediplains developed. The seminal study of Partridge and Maud (1987) provided a spatial representation of the areal extent of a variety of ancient landsurfaces that can be characterised by terrain morphology, weathering profiles and a range of duricrusts. Dating of the period of formation of each landsurface is, however, subjective due to limited absolute dating control.

Escarpment retreat has been suggested in earlier studies to be the main mechanism for the evolution of the Great Escarpment. An average retreat rate of approximately 1km Ma^{-1} has been suggested for southern Africa (King, 1944). However, Fleming et al., (1999) have utilised cosmogenic nuclides to estimate average summit denudation rates on the Drakensberg escarpment at 6m Ma^{-1}, and escarpment retreat rates at 50-95 m Ma^{-1}over the past 10^4-10^6 years. According to Fleming et al., (1999) the rate of summit lowering is sufficient to prevent long term survival of erosion cycle surfaces, which were previously inferred for this region. The results of some fission-track studies have indicated that when the African and South American plates drifted apart, the rifted continental margins were subjected to a period of major denudation immediately following the breakup of Gondwana which occurred at about 120 Ma, (Brown et al., 1990, 2000). This observation is in disagreement with previous ideas concerning the very long-term survival of erosion surfaces in these areas and severely undermines a strategy of reconstructing landscape histories that rely on a record of tectonic uplift and base-level change reflected in the erosion surfaces that remain in the

modern landscape (Brown et al., 2000). A debate on the origin and age of physiographic features is still ongoing. Burke (1996) believes that the highlands of South Africa are predominantly Cenozoic in age.

The continental interior and coastal hinterlands areas east of the Great Escarpment responded to different base level controls with the co-existence of surfaces of the same age at different elevations across the country (Partridge and Maud, 1987, 2000). During the warm, humid Cretaceous period weathering rates were high and aggressive river erosion caused the rapid retreat of the escarpment from the emerging coastline. The 'African surface' developed from the breakup event until the early Miocene with remnants preserved as isolated plateau remnants forming inselbergs or interfluve ridges within dissected drainage basins inland from the coast. Extensive areas defining the elevated coastal hinterland stretching along the KZN coast have been characterised as "Post-African I surface" which is extensively dissected by drainage rejuvenation (Partridge and Maud, 1987, 2000). Much of the province has been characterised as "other dissected areas" where deep river incision and the structural control imposed by diverse rock types has controlled the landscape development. It is the high relief and steep slopes created by dissection of these ancient landsurface remnants that represents one of the major controls on slope instability in the river valleys and high hills or mountainous terrain.

The steep mountain slopes shed sediment cover rapidly but there is also evidence that frequent landslides and blockfalls have been effective in shaping the river gorges. Sumner and Meiklejohn (2000) suggested that deep seated landslides occurred during the Pliocene uplift as a result of fluvial incision resulting in the rejuvenation of streams that caused slope over steepening. In this study radiocarbon dating of organic sediments from sag ponds on some deep seated landslides in the Giant's Castle Game Reserve has provided much younger minimum ages. Although in KZN the processes of erosion such as mass movements continue to be active (especially evident in the

Drakensberg), according to Sumner (1997) the contribution of landslides to geomorphology of the Drakensberg is apparently little understood.

Table 4 Summary of major stages in the geomorphic evolution of Southern Africa, comparing the models of King 1972 and Partridge and Maud 1987 (after Boelhouwers, 1988a)

Event	Geomorphic manifestation	Age	Event	Geomorphic manifestation	Age
Intermission VI (youngest landscape)	Backward erosion giving rise to stream dissection in the Little Berg		Climatic and sea level fluctuations	Marine benches, coastal dune deposits, river terraces, Kalahari sands.	Late Pliocene to Holocene
Active episode E	1800m uplift with seaward tilting	Late Pliocene	Post–African II cycle of erosion	Formation of Post–African II surface, incision of gorges, downcutting and formation of terraces along interior rivers.	
Intermission V (widespread landscape)	Scarp retreat and pedimentation. 1350m planation surface in Natal Midlands				
			Major uplift	Asymmetrical uplift of subcontinent, major westward tilting of interior landsurface, monoclinal warping along southern and eastern coastal margins.	Late Pliocene (~2.5 Ma)
Active episode D	600m uplift with pronounced seaward tilting	Late Miocene			
Intermission IV (rolling landscape)	Incomplete planation 200-300m below the Moorland landscape. 1800m planation surface in the Little Berg		Post–African I cycle of erosion	Formation of Post–African I surface, major deposition of the Kalahari basin.	Early mid Miocene to late Pliocene
Active episode C	Gentle uplift of a 'few hundred' metres over entire Natal	Early Miocene	Moderate uplift	Westward tilting of African surface with limited coastal monoclinal warping. Subsidence of Bushveld basin.	End of early Miocene (~18 Ma)
Intermission III (Moorland landscape)	Extensive planation, retreat of the 1200-1500m high Drakensburg scarp over most of Natal. Summit level at 1950m in Little Berg.		African cycle of erosion	Advance planation throughout subcontinent (at two levels above and below Great Escarpment). Development of laterite, silcrete profiles and Kalahari basin.	Late Jurassic/early Cretaceous to end of early Miocene
Active episode B	1200m uplift of the interior of Natal, origin of the Great Escarpment.	Middle Cretaceous			
Intermission II (Cretacic landscape)	Backward erosion giving rise to 500m scarp. Planation surface in Lesotho Mountains above 2800m		Fragmentation of Gondwana	Initiation of Great Escarpment.	Late Jurassic/early Cretaceous
Active episode A	Break up of Gondwanaland, origin of Natal Monocline. 300-500m uplift	Early Cretaceous			
Intermission I (Gondwana landscape)	Extensive erosional surface following the outpour of Drakensberg lavas. Summit level of Lesotho Mountains at +/- 3300m.				

CHAPTER THREE

3. LANDSLIDE TYPES, CLASSIFICATION, MAPPING AND DATING

3.1 Overview

A landslide is defined as, “the movement of a mass of rock, debris, or earth down a slope” (Cruden, 1991). The widely accepted terminology (WP/WLI 1990, 1991, 1993a, b) describing features of typical landslides are depicted in Fig. 4. The term "landslide" encompasses events such as rock falls, topples, slides, spreads, and flows. These five types of landslides are illustrated in Figures 5a–e and described below according to the classification of Cruden and Varnes (1996);

(a) *Falls* involve the detachment of material (rock, debris or earth) from a near–vertical slope along a surface on which there is little or no shear displacement. The detachment often occurs along planes of weakness such as fractures and joints. Rock falls are often strongly influenced by gravitational forces on discrete rock blocks or joint-bounded rock masses, mechanical weathering, undercutting or erosion, and the pore pressure associated with interstitial water. The rapid movement of material occurs by free-fall, bouncing and rolling, or sliding (Fig. 5a) which results in accumulation of fallen material at the bottom of the slope. The fallen material forms a talus deposit which often comprises rock fragments of various sizes due to breakage of the displaced mass during the fall.

(b) *Topples* are rock masses that rotate forward (Fig. 5b) about a pivotal point then detach from the main mass under the influence of gravity and/or forces exerted by adjacent blocks or interstitial fluids which eventually cause the displaced material to bounce and/or rolls down the slope. The initial process of overturning is usually slow but the final detachment of the material is instant.

(c) *Slides* require a slip plane (surface of rupture) between the mass in momentum and underlying stable ground and are caused by shear failure. Slides are subdivided according to the geometry of the surface of rupture into rotational slides and translational slides. *Translational slides* comprise a roughly planar, two dimensional slip surface along which the landslide mass moves with little rotation or back tilting (Fig. 5c(i)). *Rotational slides* have a concave upward

curved surface of rupture and the slide movement is roughly rotational about an axis which is parallel to the ground surface and transverse across the slide hence there is a backward rotation of the displaced mass (Fig. 5c(ii)).

(d) *Flows* involve a spatially continuous movement in which surfaces of shear are short-lived, closely spaced, and usually not preserved. The distribution of velocities in the displacing mass resembles that in a viscous liquid. The lower boundary of the displaced mass may be a surface along which appreciable differential movement has taken place or a thick zone of distributed shear (Cruden and Varnes, 1996) (Fig. 5d).

(e) *Spreads* are distinctive slides which involve lateral/horizontal movements on very gentle terrains. The failure is triggered by rapid ground motion such as earthquakes which cause liquefaction of the loose, cohesionless sediments underlying a firmer, more cohesive lithological layer (Fig. 5e).

Landslides can be triggered by many different natural causes including increases or decreases in loading forces on slopes, changes in moisture content of soils or increased pore pressure in regolith or fractured bedrock, seismicity, steeply dipping bedding, changes between shear stress and shear strength in potential slip zones and groundwater seepage. Anthropogenic influences such as excavations that reduce the lateral support of regolith of rock masses through excavation for road works, trenching, cut-and-fill terracing and the erosion of the slope toe can also trigger landslides.

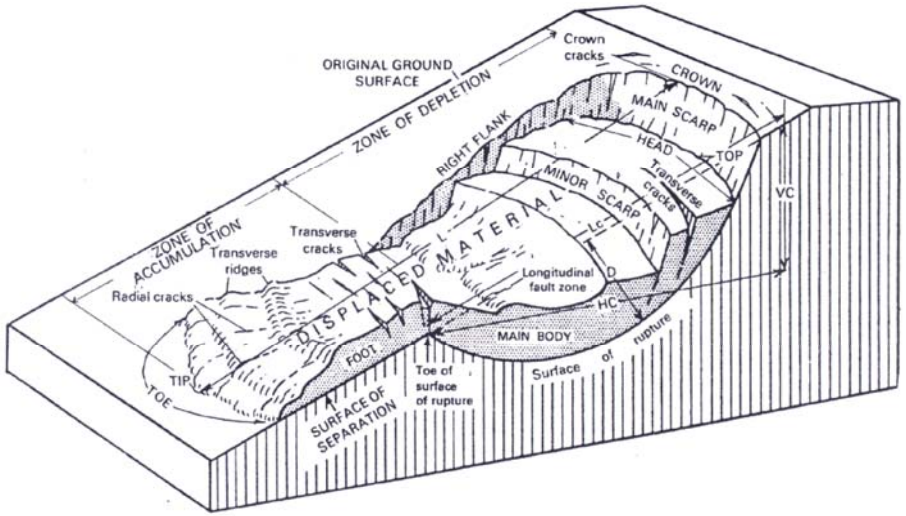
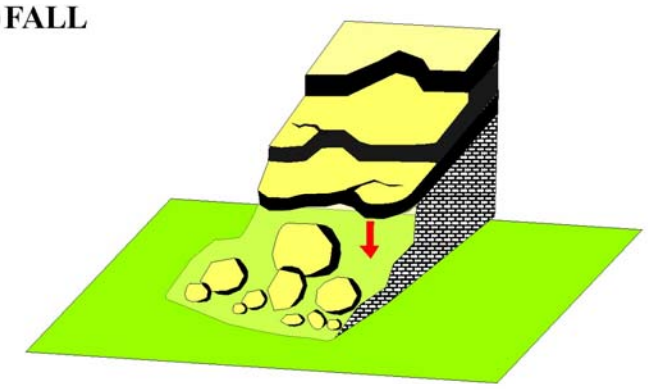


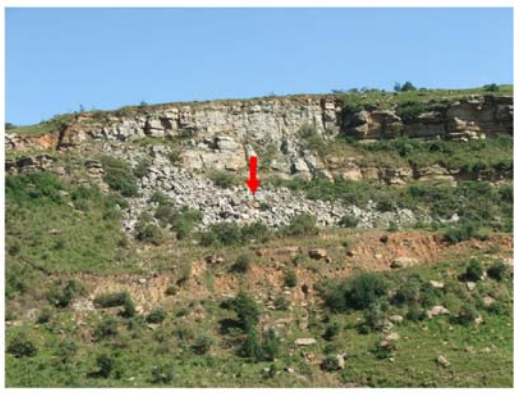
Figure 4 An idealised landslide block diagram (Varnes, 1978).

NOMENCLATURE

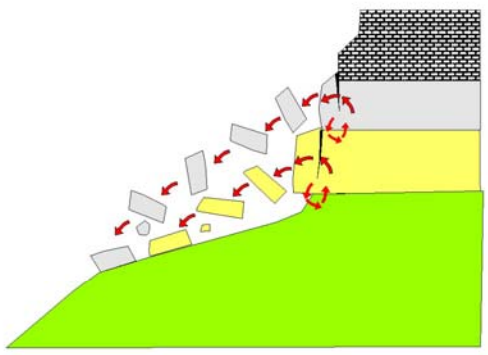
Main Scarp: A steep surface on the undisturbed ground around the periphery of the slide, caused by the movement of slide material away from undisturbed ground. The projection of the scarp surface under the displaced material becomes the surface of rupture.
Minor Scarp: A steep surface on the displaced material produced by differential movements within the sliding mass.
Head: The upper parts of the slide material along the contact between the displaced material and the main scarp.
Top: The highest point of contact between the displaced material and the main scarp.
Toe of Surface of Rupture: The intersection (sometimes buried) between the lower part of the surface of rupture and the original ground surface.
Toe: The margin of displaced material most distant from the main scarp.
Tip: The point on the toe most distant from the top of the slide.
Foot: The portion of the displaced material that lies downslope from the toe of the surface of rupture.
Main Body: That part of the displaced material that overlies the surface of rupture between the main scarp and toe of the surface of rupture.
Flank: The side of the landslide.
Crown: The material that is still in place, practically undisplaced and adjacent to the highest parts of the main scarp.
Original Ground Surface: The slope that existed before the movement which is being considered took place. If this is the surface of an older landslide, that fact should be stated.
Left and Right: Compass directions are preferable in describing a slide, but if right and left are used they refer to the slide as viewed from the crown.
Surface of Separation: The surface separating displaced material from stable material but not known to have been a surface of which failure occurred.
Displaced Material: The material that has moved away from its original position on the slope. It may be in a deformed or unreformed state.
Zone of Depletion: The area within which the displaced material lies below the original ground surface.
Zone of Accumulation: The area within which the displaced material lies above the original ground surface.
Runout: The horizontal travel distance achieved by a landslide

(a) FALL



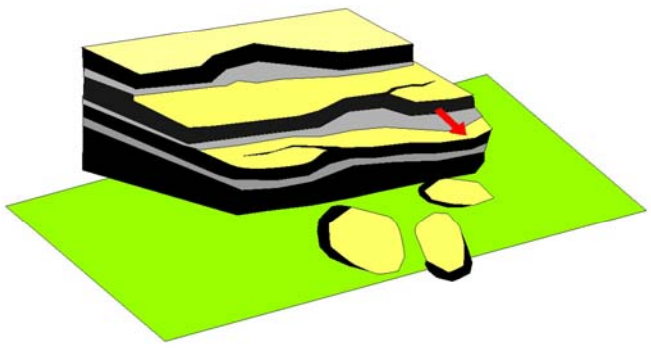


(b) TOPPLE



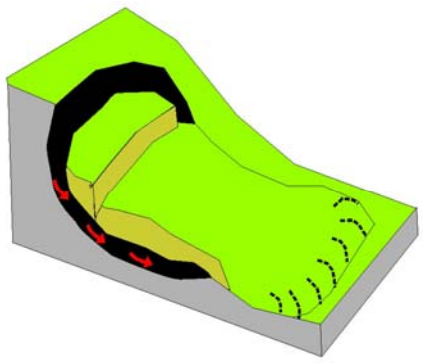


(c) SLIDE



(i) TRANSLATIONAL

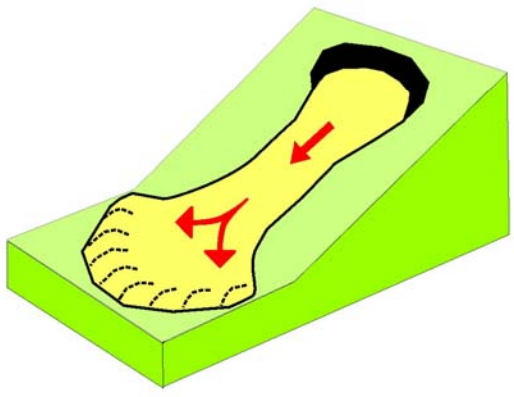


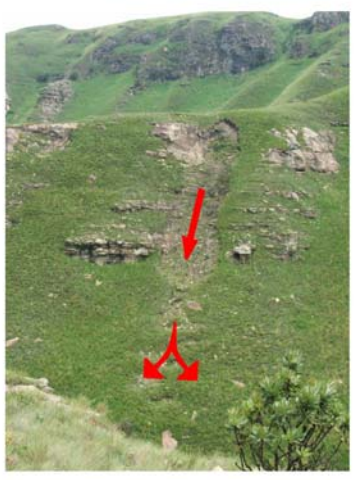


(ii) ROTATIONAL



(d) FLOW





(e) SPREAD

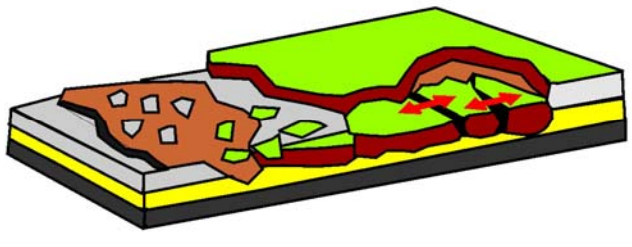




Figure 5a-e. The five basic types of landslides based on the mode of movement (Cruden and Varnes, 1996).

3.2 Overview of landslide classification systems

Hansen's (1984) discussion of strategies employed for the numerous and varied landslide classification schemes emphasized the underlying concept of classification systems; they are descriptive tools which ideally reflect the requirements of the user. This is clearly evident from the numerous systems developed since the first landslide classification by Dana (1862) which was based on the type of movement (Cruden, 2003). Other classification systems use various differentiating factors such as;

- age of movement (Popov, 1946; Zaruba and Mencl, 1969);
- degree of activity (Erskine, 1973);
- geographic type (Reynolds, 1932, Reiche, 1937);
- geographic location (Reynolds, 1932);
- climate type (Sharpe, 1938);
- type and size of material (Baltzer, 1875; Heim, 1882; Howe, 1909; Sharpe, 1938; Zaruba and Mencl, 1969; Coates, 1977; Varnes, 1978);
- underlying geology (Ladd, 1935; Savarenskii, 1937; Zaruba and Mencl, 1969);
- type of movement (Sharpe, 1938; Ward, 1945; Varnes, 1958, 1978; Hutchinson, 1968; Skempton and Hutchinson, 1969; Zaruba and Mencl, 1969; Coates, 1977);
- velocity of movement (Sharpe, 1938 and Varnes, 1978);
- water content, air or ice (Sharpe, 1938);
- triggering mechanisms (Terzaghi, 1950 and Brunsden, 1979);
- morphology of deposited material and failure surface (Blong, 1973a, b and Crozier, 1973).

For many years the most commonly used classification schemes were those of Hutchinson (1968); Skempton and Hutchinson, (1969) and Varnes (1958, 1978). In these classification systems the type of movement is the primary classificatory factor.

Since various classification systems have been devised from different perspectives, similar landsliding events may be classified differently, motivating the need for a global terminology. The International Association of Engineering Geology (IAEG) Commission on Landslides and Other Mass Movements has developed landslide terminology. The declaration of the United Nations of the International Decade for Natural Disaster Reduction (1990-2000) motivated the IAEG Commission's Suggested Nomenclature for Landslides (1990) and the establishment of the WP/WLI by the International Geotechnical Societies and the United Nations Educational, Scientific and Cultural Organization (UNESCO).

3.3 Classification system derived for the KZN context

For the purpose of this investigation Varnes' (1978) classification, including amendments from Cruden and Varnes (1996), has been adopted. This approach is consistent with the UNESCO Working Party on World Landslide Inventory (WP/WLI, 1990). The advantage of using this approach is the interpretation of the type of movements in a landslide with more than one movement type is essential. The classification system by Varnes (1978) grouped many of the palaeo-landslide forms in KZN into the "complex" landslide category with no interpretation of the sense of movement. This category has been dropped from the formal classification scheme adopted here.

Minor adaptations of the amended classification system (Cruden and Varnes, 1996) have been made to develop a landslide classification system that accommodates the kind of slope failures that occur across a range of climatic and topographic settings within KZN. If the morphology of the recent landslides or palaeo-landslides has been modified by pedogenic weathering and erosional degradation to the point where the geometry of the failure can not be identified, these geomorphic forms are classified as "undifferentiated" (Table 5). This adaptation of the amended classification system also facilitates integration of slope instability data from other sources. Selected landslides were ground-truthed and other more remote slope failures that were mapped from the aerial

photography have been classified as "undifferentiated" slope failures until the type of slope movement can be qualified on the basis of site investigations (Table 5).

Table 5 Abbreviated landslide classification scheme employed in this study (modified after Cruden and Varnes, 1996).

Type of movement	Type of material		
	Bedrock	Engineering soils	
		Predominantly coarse	Predominantly fine
Fall	Rock fall	Debris fall	Earth flow
Topple	Rock topple	Debris topple	Earth topple
Slide	Rock slide	Debris slide	Earth slide
Spread	Rock spread	Debris spread	Earth spread
Flow	Rock flow	Debris flow	Earth flow
Undifferentiated	Type of movement not qualified		

In addition to classifying slope failures according to the type of movement and material, an attempt has been made to further classify these sites in terms of size and age. According to Zaruba and Mencl (1982) landslides that have remained visible in the landscape for thousands of years after they have moved and stabilized are referred to as ancient or fossil occurrences. Ancient slope failures that are modified by erosion, stream incision, development of soil profiles and generally uniformly vegetated are classified as "palaeo-landslides". All other failures are broadly classed as "recent-landslides". Five size categories are used to classify slope failures: very small; small; medium; large and, very large, according to the areal extent of the failure zone (Table 6).

Table 6 Landslide size classification based on the areal extent of the failure zone (*after* van Schalkwyk and Thomas, 1991).

Size		Description
□	0.01-10.00 m^2	Very small
□	10.01-1000.00 m^2	Small
□	1000.01-100 000.00 m^2	Medium
□	100 000.01-1 000 000.00 m^2	Large
□	>1 000 000.00 m^2	Very large

3.4 Landslide mapping

During recent regional geological and geotechnical mapping programmes carried out by the Council for Geoscience (Botha and Botha, 2002 and Richards, 2008) it was revealed that landslide deposits represent a significant proportion of the Quaternary regolith cover on hillslopes in the Durban and Pietermaritzburg regions.

This investigation extended the mapping of landslides to cover areas of the province regarded as being most susceptible to slope failure. These pilot study regions were known to have widespread landslide deposits associated with steep, irregular topography and diverse geology. Hummocky topography on upper to mid-slope areas in these regions is often indicative of historic landslides. Aerial photographic interpretation and field mapping focused on four pilot study regions (Fig. 6);

(a) Matatiele–Cedarville–Kokstad (M-C-K)

The Matatiele–Cedarville–Kokstad region is characterized by plains, undulating hills and lowlands, as well as mountainous areas (Kruger, 1983), with elevations ranging from 1500 m above mean sea level (amsl) along the Cedarville flats to 2224 m amsl at Mount Currie, resulting in steep relief of up to 720 m. The region is characterized by convex, concave and straight slope forms. Drainage densities are low to medium, from 0 to 2 km/km^2, and stream frequency is highly variable (0 to 10.5 streams/km^2). The mean annual rainfall is in the 620–1265 mm range and annual temperature means range from 2.2°C to 27.4°C. Approximately 80% of the rain falls during the summer months and winter snowfalls are a frequent occurrence.

The low–lying areas of the region are underlain by mudrocks and siltstones of the Permian–age Tarkastad Subgroup of the Beaufort Group, dipping at approximately 5° to the northwest. The southeastern sector of the study region is underlain by the Adelaide Subgroup argillites. These rocks have been extensively intruded by dolerite sills and dykes that weather positively and create the steep topography and high relief. Thick alluvial soils and wind–blown sand deposits

characterize the broad flats around the Mzimvubu River floodplain, known as the "Cedarville Flats".

(b) Ukhahlamba–Drakensberg mountains (U-D)

In terms of terrain morphology, the Ukhahlamba–Drakensberg area is classified in broad terms as closed hills and mountains with moderate and high relief (Kruger, 1983). The terrain comprises high mountains with a combination of convex, concave and straight slope forms. The percentage of area with slopes of less than 5% (approximately 3°) is less than 20%. Drainage densities are medium, from 0.5 to 2 km/km^2, and stream frequency is medium high (1.5 to 10.5 streams/km^2).

The Drakensberg escarpment experiences very dry, cold - very cold conditions in winter with occasional frost and snow often falling in the higher elevation areas. Summer rainfall often results from convective thunderstorms or is orographically–induced along escarpments.

The topography and slope characteristics in the Drakensberg region are directly controlled by geology and geomorphological processes. The steep main Ukhahlamba–Drakensberg escarpment incises the sequence of flood basalt flows comprising the Drakensberg Group and has an average altitude of approximately 2900 m amsl. The Clarens Formation comprising light yellowish-brown or red, fine to medium grained, quartz-rich sandstones forms a prominent, lower level escarpment at an altitude of about 2200 m amsl, known as the 'Little Berg'. The steep, grassy slopes beneath the Clarens Formation aeolian sandstone are underlain by alternating beds of sandstone and red argillites of the Elliot Formation. Underlying the Elliot Formation is the conspicuous Molteno Formation scarp comprising beds of pebbly feldspathic sandstone with thin interbedded shale and mudstone units. The bottom slopes are predominantly formed by the argillaceous rocks of the Beaufort Group.

(c) Ladysmith–Dundee–Vryheid–Utrecht (L-D-V-U)

The terrain morphology of this region is broadly classified as lowlands, hills and mountains with moderate to high relief (Kruger, 1983) and elevation ranging from 1100 m amsl at Ladysmith in the south to 2291 m amsl in the Nshele area, ~40 km north west of Utrecht. The Ladysmith–Dundee–Vryheid–Utrecht region is characterized by convex, concave and straight slope forms. Drainage densities are low to medium, from 0 to 2 km/km^2, and stream frequency is highly variable (0 to 10.5 streams/km^2).

Very hot, wet summers are characteristic of this area and the mean annual rainfall is approximately 750 mm. The driest months of the year are from May to August when frost and winter snowfalls can be expected.

The Permian Ecca Group, comprising argillaceous and arenaceous rocks of the Vryheid and Volkrust Formations, characterises the bedrock over most of the area. The Permian age sedimentary rocks of the Adelaide Subgroup (Beaufort Group) conformably overly the rocks of the Volkrust Formation. Within the study region these sedimentary rocks are extensively intruded by Jurassic age dolerite sills and dykes which account for many of the topographic highs of the area.

(d) Central Zululand region (CZ)

The greater part of the region is an upland plateau at an average elevation of 1200 m drained by the Mhlatuze, White Mfolozi, and Black Mfolozi River catchments. Mountains such as Babanango, Brandwagkop and Nhlazatshe rise above the plataeau surface to elevations in excess of 1400 m amsl. The escarpments of the Babanango and Melmoth plateaus form an amphitheatre around part of the lowland basin where Ulundi is situated.

The terrain morphology of the area is classified in broad terms as plains, lowlands, hills and mountains with moderate and high relief (Kruger, 1983). The region is characterized by convex, concave and straight slope forms and some deeply incised valleys. Both drainage densities (0 to 3.5) km/km^2, and stream frequency are highly variable (0 to 10.5 streams/km^2).

The climate of this southern Zululand area is characterised by warm, wet summers and cold, dry winters. Mean temperatures for January are around 22°C with a mean maximum of 29°C. During winter mean annual temperatures in July are about 10°C with a mean minimum of about 3°C. The area has a mean annual rainfall of 890 mm, falling predominantly between October and March.

The region is underlain by diverse lithologies ranging in age from Archaean to Cenozoic. The Kaapvaal Craton high grade crystalline basement granite–gneisses are overlain by the steeply dipping sedimentary rocks and lavas of the Pongola Supergroup. The relatively flat lying sandstones of the Ordovician Natal Group and the Karoo Supergroup sandstone/mudrock, shale successions overlie the basement rock units. Dolerite dykes and sills have extensively intruded all rock types, particularly the Karoo strata, and generally weather positively to create steep topography and slopes with high relief.

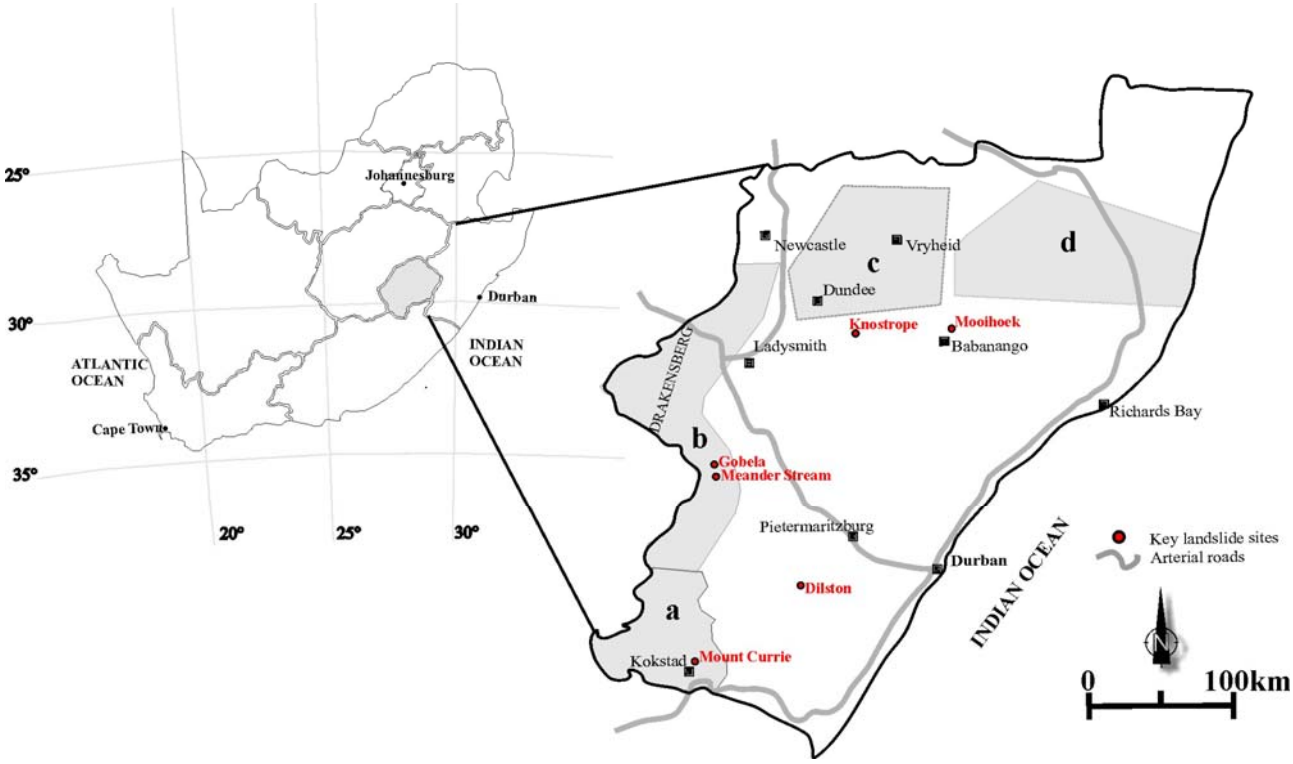


Figure 6 Distribution of the regions initially investigated in KZN showing key landslide sites, the closest urban nodes and arterial roads. a: Matatiele–Cedarville–Kokstad; b: Ukhahlamba–Drakensberg; c: Ladysmith–Dundee–Vryheid–Utrecht; d: Central Zululand regions.

Landslide mapping in the various pilot study regions revealed that historically landslides included very large failures as opposed to the present day mass wasting activity which is in the form of rockfalls and smaller scale slides. Isolated, recent landslide events are mainly small to medium-sized features triggered by high intensity, prolonged rainfall events, such as those during the summer of 1987/1988 (Paige-Green, 1989; van Schalkwyk and Thomas, 1991) that affected embankments and steep hillslopes. The landslide types identified include; fall, topple, flow, translational and rotational slides, as well as some of uncertain origin (undifferentiated), which occur across climatic gradients and a range of terrain morphological contexts (Fig. 7 and Appendix 1). Surficial landslides commonly occur on many steep slopes in KZN but their shallow based characteristic results in poor preservation (Fig 8). Thus, the manifestation of these geomorphic features in the landscape is ephemeral.

Find figure 7 in the pocket sleeve located at the back of the report



Figure 8. Recent superficial flows (centre left) occurring on the steep slopes north of the public picnic site in the Giant's Castle Nature Reserve.

Within the KZN region it appears that geology, or more specifically, the terrain morphological expression of different rock types has a direct association with the movement type of the slope failure. Falls are often associated with bedrock that is resistant to deep weathering. Disengagement of blocks from the near-vertical rock face is along fracture and joint planes (Fig. 9). Conversely, flows are frequently associated with deeply weathered rocks on steep slopes, and often occur preferentially on slopes with a southerly aspect. Topples are generally associated with near-vertical jointed or steeply dipping bedrock. Translational and rotational slides are associated with a range of bedrock types. Mass movements are associated with all bedrock types within the study regions. There are definite associations between slope gradient, rainfall, geological structure, seismicity, and geomorphic terrain.



Figure 9. Rockfalls are a typical occurrence in the Drakensberg. Weathering of an argillaceous layer below a resistant sandstone bed or enhanced groundwater seepage results in formation of a hanging block of sandstone. Disengagement of these hanging blocks from the rock face is along fracture and joint planes

Many of the landslides identified from the literature or aerial photographs were ground truthed to confirm the API and served in testing the adopted classification system. Those palaeo-landslides with characteristic sag pond deposits were targeted for onsite investigation with the expectation of ascertaining datable material.

3.5 Landslide dating

The determination of landslide event chronology is essential for understanding of the causes of these mass movements through association with known environmental conditions or periods of rapid climate change.

The clustering of landslides ages during specific periods may relate to climatic conditions or to other external triggering factors such as seismic activity. There are several methods for determining landslide chronologies and the selection of the most appropriate dating method is often not a simple task. Landslides may be dated by different techniques, depending on a variety of factors such as local climate, type of landslide material, degree of internal disruption etc. and the availability of material suitable for dating. Classic landslide dating techniques include historical records, dendrochronology, radiocarbon dating, pollen analysis, lichenometry, weathering rinds and

geomorphic analysis. New dating techniques such as cosmogenic nuclides, uranium-series techniques, Ar-Ar dating, optically-stimulated-luminescence, alpha-recoil-track dating methods have been outlined by Lang et al., (1999). According to Lang et al., (1999) none of the new methods can yet be considered routine whilst the established dating methods (radiocarbon dating, lichenometry and dendrochronology) have proven useful for dating landslides in the Late Quaternary.

A common characteristic of many palaeo-landslides in the study regions is the well defined sag ponds developed on back-tilted landslide surfaces or inter-hummock depressions. Since the pond infill comprises organic-rich sediment and/or peat deposited on a surface of landslide debris the radiocarbon dating method was favoured. Radiocarbon dating of organic matter and peat from the infill at the base of sag ponds has yielded reliable age estimates of pond formation following the stabilisation of the hummocky landslide surface (Stout, 1969, 1977; McCalpin, 1989) thus providing a minimum age for the landslide event.

The possibility of using other dating techniques such as geomorphic analysis for landslides in KZN should be investigated in the future once a regional radiocarbon dating framework has been established but have not been tested during this investigation. The geomorphic analysis technique uses the degree of preservation or degradation of landslide morphological features to assign relative age estimate classes to landslides with very similar morphologies, occurring in similar geological, geomorphological and climatic contexts. An analysis of degradation was carried out using the landslide in the Molletshe Tribal Authority since a precise date of the landslide event is known. This translational landslide occurred in the sandstones of the Vryheid Formation on an eastward facing slope in the Molletshe Tribal Authority area in 1991. The average dip of the slope is 15° (Fig. 10a) and Wilson (1992), who described the site soon after the event, noted that the movement of the sandstone mass occurred along a shale horizon which appears to dip concordantly with the slope direction. However, observations during the field work phase of this investigation revealed the influence of a thin porphyritic dyke running up the slope, and a fine-grained dolerite sill above

the sandstone below the hill crest. The landslide still displays many of the morphological features (Fig. 10b-c) created by the original event and highlights the limited degree of degradation that has occurred within the intervening 15 year period.

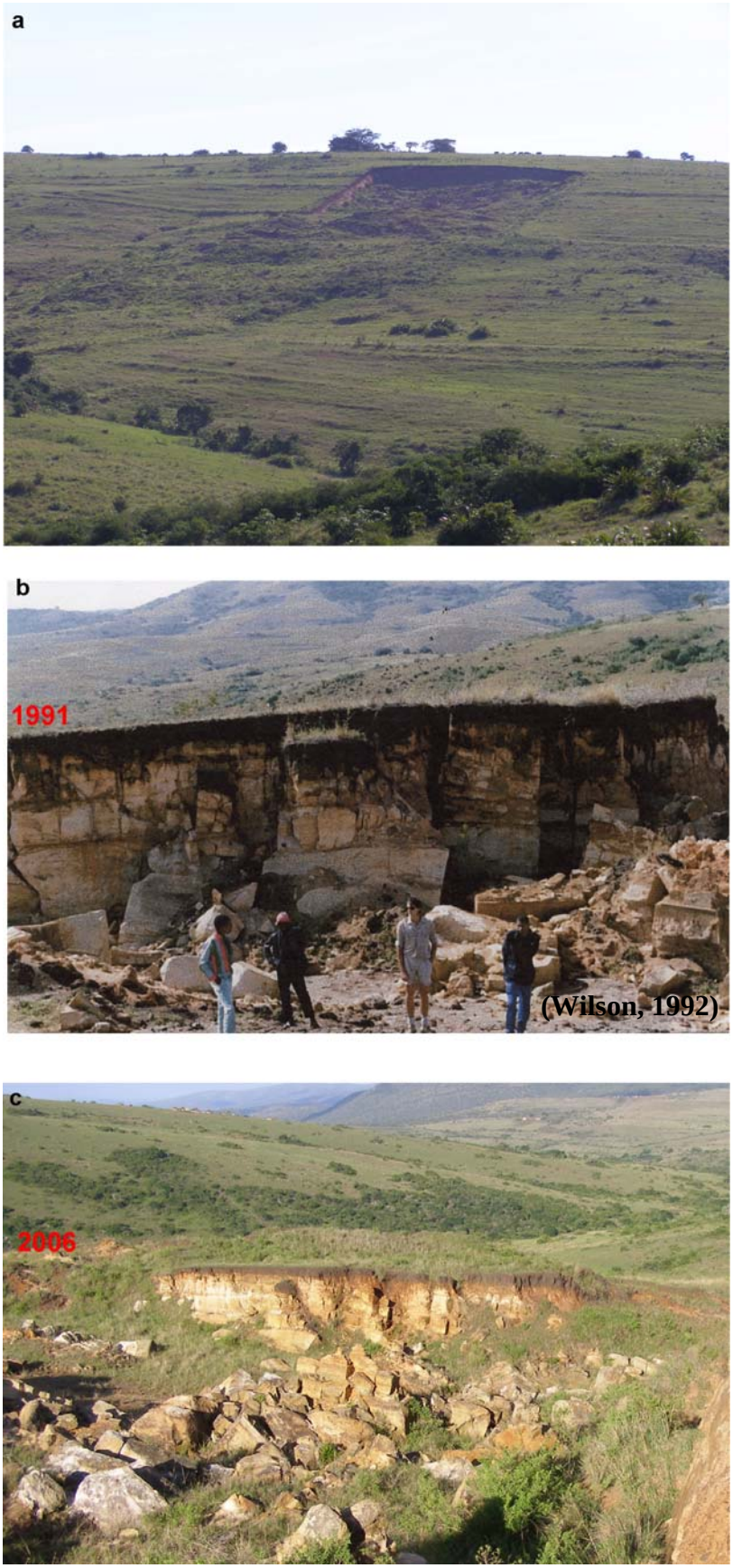


Figure 10a-c. (a) A translational slide occurred in the sandstones of the Vryheid Formation on an eastward facing slope in the Molletshe Tribal Authority area in 1991. (b) View of the translational slide in 1991 showing sharp morphological landslide features. (c) View of the slide in 2006 showing similarities in the morphological landslide features since the landslide event.

3.6 Site Investigations

Medium to very large landslide deposits with characteristic sag pond deposits initially identified on aerial photographs were targeted for onsite investigation. A representative landslide sag pond deposit in each study region was dated using radiocarbon from organic-rich pond sediments to establish a minimum age estimate for those landslide events. The pond infill was hand augered to ascertain if radiocarbon datable organic-rich sediment occurs. Where spring seepage or small streams drain the slopes above the failure plane, sag ponds commonly preserve organic-rich infill deposits. However, landslides with well defined back-tilted blocks and sag ponds filled with reddish brown, clayey colluvium are characteristic of dry backslope areas. The possibility of dating the silty clay sag pond infill at most of these sites using luminescence dating techniques is being investigated. These investigations served to test the application of the classification system adopted.

3.6.1 Undated sites

Numerous other palaeo-landslides (Appendix 1) were mapped and ground-truthed but their terrain forms were highly degraded through erosion or the sag ponds deposits were dominated by silty clay hillwash deposits. Some of these palaeo-landslides include the three ancient mass movement deposits (Fig 11a-c) situated on both sides of the Bushman's River valley about 1 km north-east of the Giant's Castle camp, identified by Boelhouwers (1988a). Palaeo-landslides in the Bushmans River valley (Fig 11a-c) includes a rotational slide occurring on the south east facing slope at the transition from the Elliot Formation to the Clarens Formation. The landslide debris comprises blocks of sandstone in a clayey sand matrix. The strata of the palaeo–scarp dip gently to the north whereas the displaced sandstone blocks remain relatively intact and dip at up to 51° toward the palaeo–scarp. The sag pond and back-tilted area immediately below the scarp (Fig. 11a) is drained efficiently by streams incised along the flanks of the disturbed area. Reddish brown, sticky clay with sandstone granules was augered from the back tilted surface. The landslide has a runout of 350m into the river valley and areal extent of 92360 m^2. A fluvial terrace 2m above stream level

(a.r.l) occurs at the landslide toe. Continual fluvial undercutting along the toe has lead to secondary shallow slumping. A mass of bedrock forming a secondary scarp has been vertically displaced from the primary palaeo–scarp surface (Fig. 11a). Associated with this secondary scarp are a series of deep bedrock, vertical cracks (2.4–4.0 m deep and 1.0–3.0 m wide) that parallel the palaeo–scarp that are classic geoindicators of the original failure event and represent sites of potential secondary slope movement. Complete detachment of material from this displaced mass will be likely through a series of toppling events along vertical cracks. The total estimated volume of the material that will be displaced by the potential toppling is in the order of 22500 m^3. According to Boelhouwers (1988a) the scarp of the palaeo–landslide shown in Fig 11b comprises alternating sandstone and siltstone layers that exhibit a straight profile indicative of translational movement, while the displaced material displays an irregular lobate form characteristic of slump failure. Immediately below the scarp recent talus rests upon the palaeo–landslide deposit. Undercutting by the Bushman's River exposes landslide debris down to 0.3 m a.r.l on the upstream side of the palaeo–landslide (Boelhouwers, 1988a). This palaeo–landslide has an areal extent of 31609 m^2 and a runout of 250 m. Immediately downstream is another rotational palaeo–landslide with an areal extent of 88138 m^2 (Fig. 11c). In situ, horizontally bedded Elliot Formation is exposed in the vicinity of the right flank. The strata forming the back–wall of the failure has highly varying dips of to 35° in a northerly direction that indicates the area was subjected to multiple disturbances.

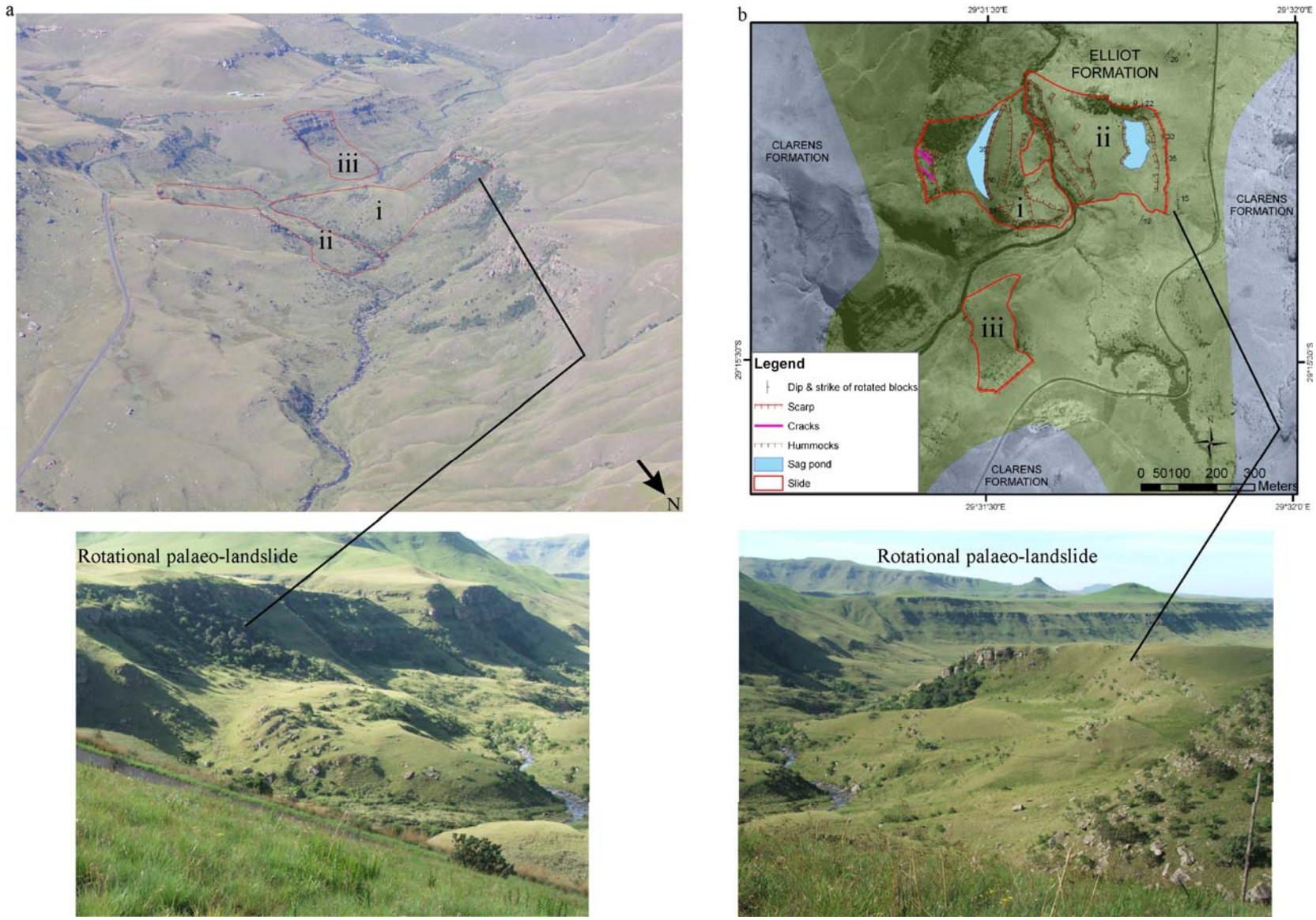


Figure 11a, b. (a) Aerial view showing characteristic hummocky topography indicative of palaeo-landslides on the slopes of the Bushman's River valley. (b) GIS - based, geomorphological map of the Bushman's River valley palaeo-landslides.

3.6.2 Dated sites

The radiocarbon dating technique was performed on organic sediment derived from sag ponds of palaeo-landslide deposits across the province to assess if these ancient geomorphic events were coeval or if they were triggered at different times. The following section describes dated palaeo-landslides investigated within each region, outlining the classification, geological, soil, and drainage context across the landslide deposit (Table 7) and presents longitudinal sections through the slopes (Fig. 12d, 14b, 17c, 18b, 20c).

Table 7 Localities of landslides that were sampled for organic rich sediment on which radiocarbon dating was done.

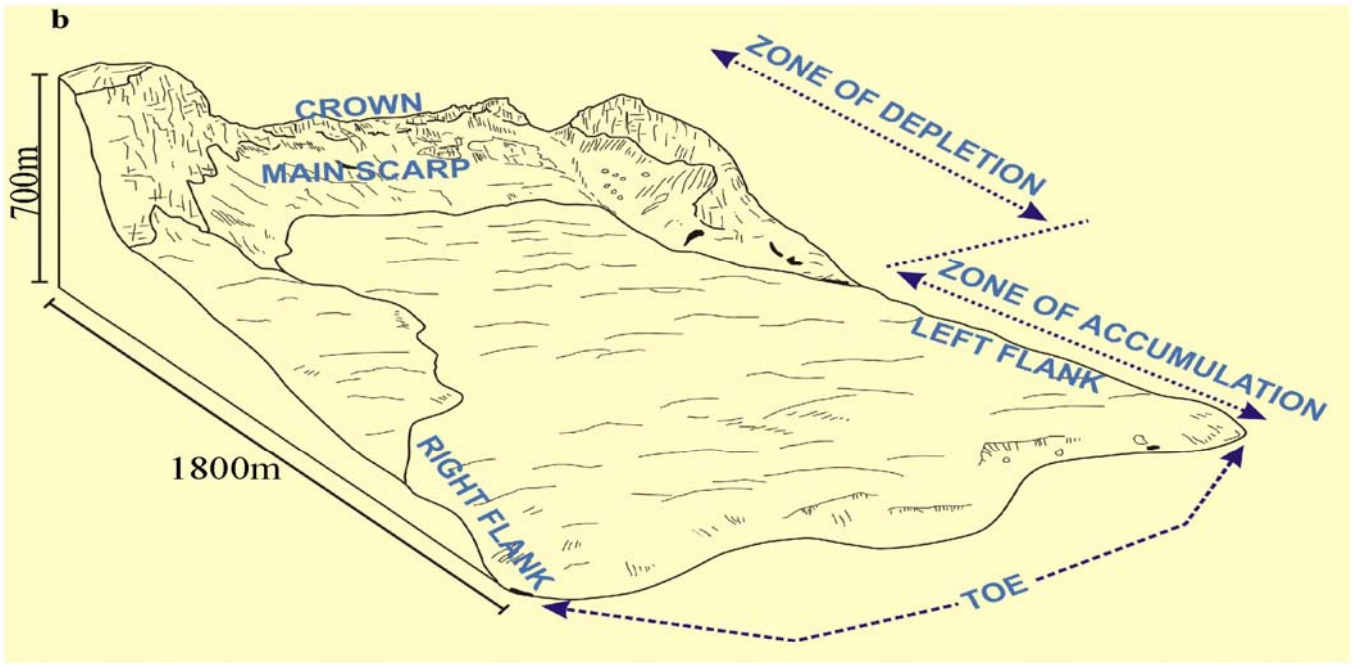
Site name	Region	Co-ordinates
Mount Currie	Matatiele-Cedarville-Kokstad	30°28'04"S ; 29°25'55"E
Knostrope	Ladysmith-Dundee-Vryheid-Utrecht	28°22'40"S ; 30°27'11"E
Meander Stream	Ukhahlamba-Drakensberg	29°17'00"S ; 29°34'15"E
Gobela	Ukhahlamba-Drakensberg	29°12'46"S ; 29°33'21"E
Mooihoek	Central Zululand	28°20'51"S ; 31°03'56"E

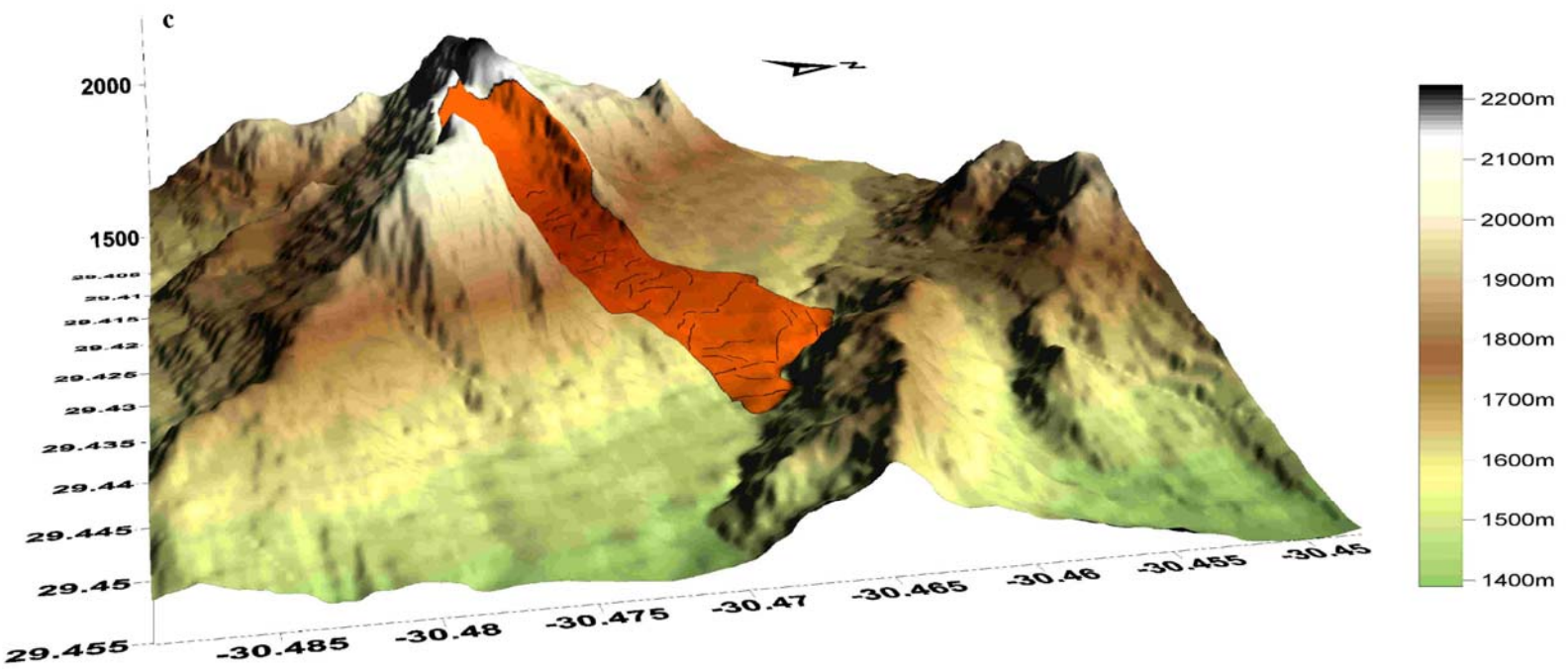
(a) Mount Currie landslide

The Mount Currie landslide forms a component of a larger mass movement complex on the northeast–facing slopes of the prominent Mount Currie (2224 m amsl) northeast of Kokstad**.** The landslide has created a backscarp with 220 m relief (2120–1900 m amsl) and the debris runout relief is 340 m (1900–1560 m amsl). Widespread hummocky topography characterises the palaeo–landslide debris which extends downslope over an area of approximately 1.80 km^2 and has a total runout of 2050 m into the river valley (Fig. 12a–d). Shallow scars have developed where minor adjustments have occurred within the hummocky slope topography. A combination of subterranean and surface drainage occurs in this landslide debris deposits. The development of well–defined soil profiles and deeply incised streams cutting through some debris hummocks provides the evidence for classification as a palaeo–landslide**.** Transverse hummocks, with long axes parallel to the slope

contours (Fig. 13) range in height from 10 to 20 m and comprise angular to rounded cobble and boulder debris (up to 2 m in diameter) in a reddish brown clayey sand matrix. This terrain form is classified as a debris slide. The volume of the ground displaced by the landslide has been estimated to be in the order of $2x10^7$ m^3. Organic-rich sag pond infill deposits on inter- hummock depressions were identified as potential sampling localities where radiocarbon dating could provide a minimum age for the mass movement event. A well developed sag pond was augered and a sample of organic-rich mud retrieved from above the landslide debris surface. The samples yielded a radiocarbon age of 2770 ± 60 yr BP (Pta-9420).







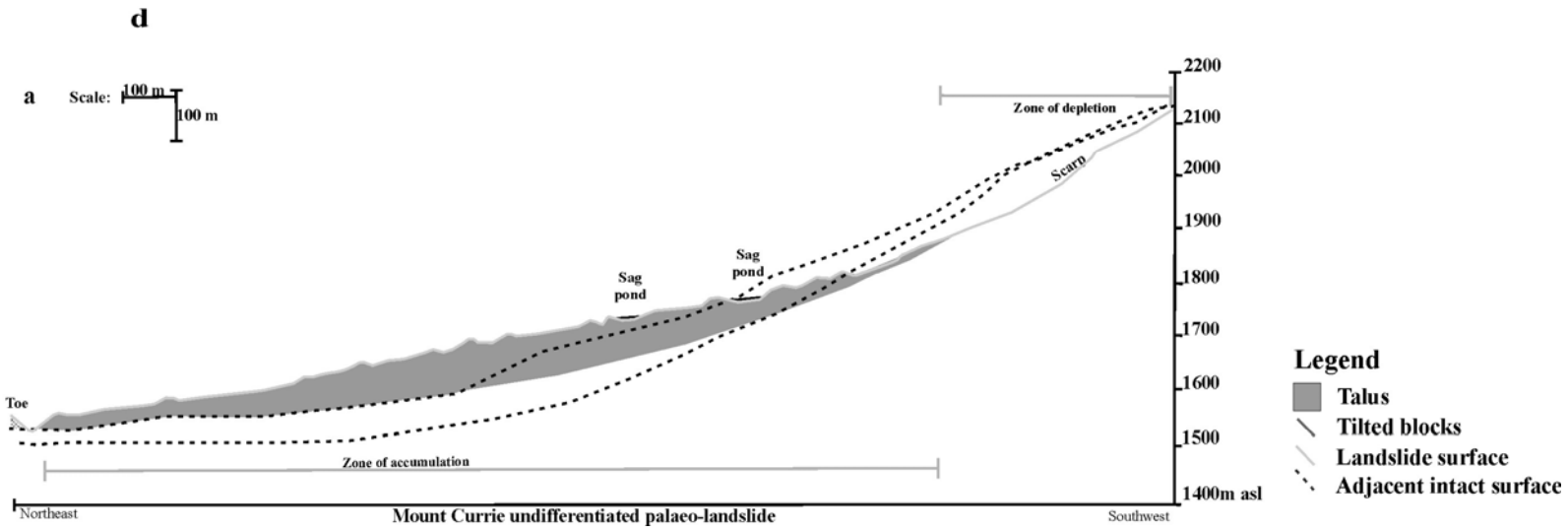


Figure 12a-d. (a) Panoramic view of the Mount Currie landslide taken from the southern slopes of Bushy Ridge (b) Sketch of the Mount Currie landslide, located northeast of Kokstad, showing the zones of depletion and accumulation. (c) Digital elevation model (DEM) of the Mount Currie landslide based on a 20m grid interval. Vertical exaggeration x1.6. The X and Y scales are in decimal degrees. (d) Cross-section through the Mount Currie palaeo-landslide showing the geomorphic features and geometry.



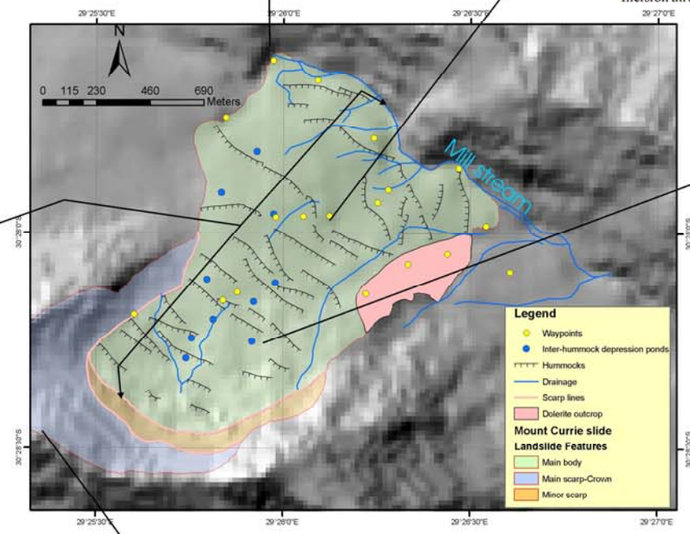
View of the left flank toe incised by Mill Stream exposing landslide debris comprising angular to rounded cobbles and large boulders in a reddish brown clayey sand matrix.



Incision through a typical hummock

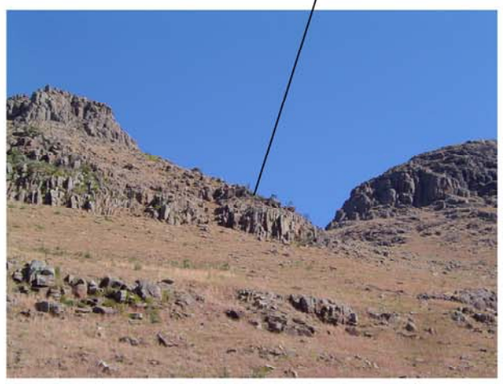


View of the landslide foot displaying the typical widespread hummocky topography.





A typical inter-hummock depression pond containing organic rich material indicative of poor drainage.



Vertical jointing in dolerite outcrop in the main scarp area.

Figure 13. GIS - based, detailed geomorphological map of the Mount Currie palaeo-landslide (centre) and the dominant features are illustrated in the surrounding photographs.

(b) Knostrope landslide

Below the escarpment defining the Biggersberg plateau, approximately 8 km northeast of Helpmekaar, a well-preserved undifferentiated debris palaeo-landslide covers 1.40 km^2 on the farm Koostrofe 3316. . The mass movement deposit is characterised by transverse hummocks ranging in height from 5–10 m, comprising angular to sub-rounded dolerite cobble- and boulder-sized blocks in a reddish brown clayey matrix. The landslide runout deposited debris onto sub-horizontally bedded sandstone on the lower-lying slopes. Recent rock-scree accumulations occur just below the scarp region of this palaeo-landslide, demonstrating the often complex nature of these slope failures and secondary process that are generated following the landslide event. The hummocky landslide surface created a series of inter-hummock depressions forming seasonal wetlands. The back-tilted surface with associated wetland preserves sag pond sediments just below the scarp (100 m relief, 1500–1400 m amsl) (Fig. 14a, b). These organic-rich sediments yielded an AMS radiocarbon age of 2960 ± 40 yr BP (Beta-229408). Closely-spaced vertical jointing characterises the dolerite sill defining the rim of the steep scarp. Association of the mass movement with structural control exerted by a specific joint orientation pattern is not possible due to the range of lineament orientations in the area (Fig. 15a-c).

An interesting phenomenon on the margin of the plateau to the south of the pass is the preservation of tension cracks 4 m wide extending over 100 m along the escarpment face (Fig. 16). These structures represent relicts from the landslide which occurred on the western side of the scarp.

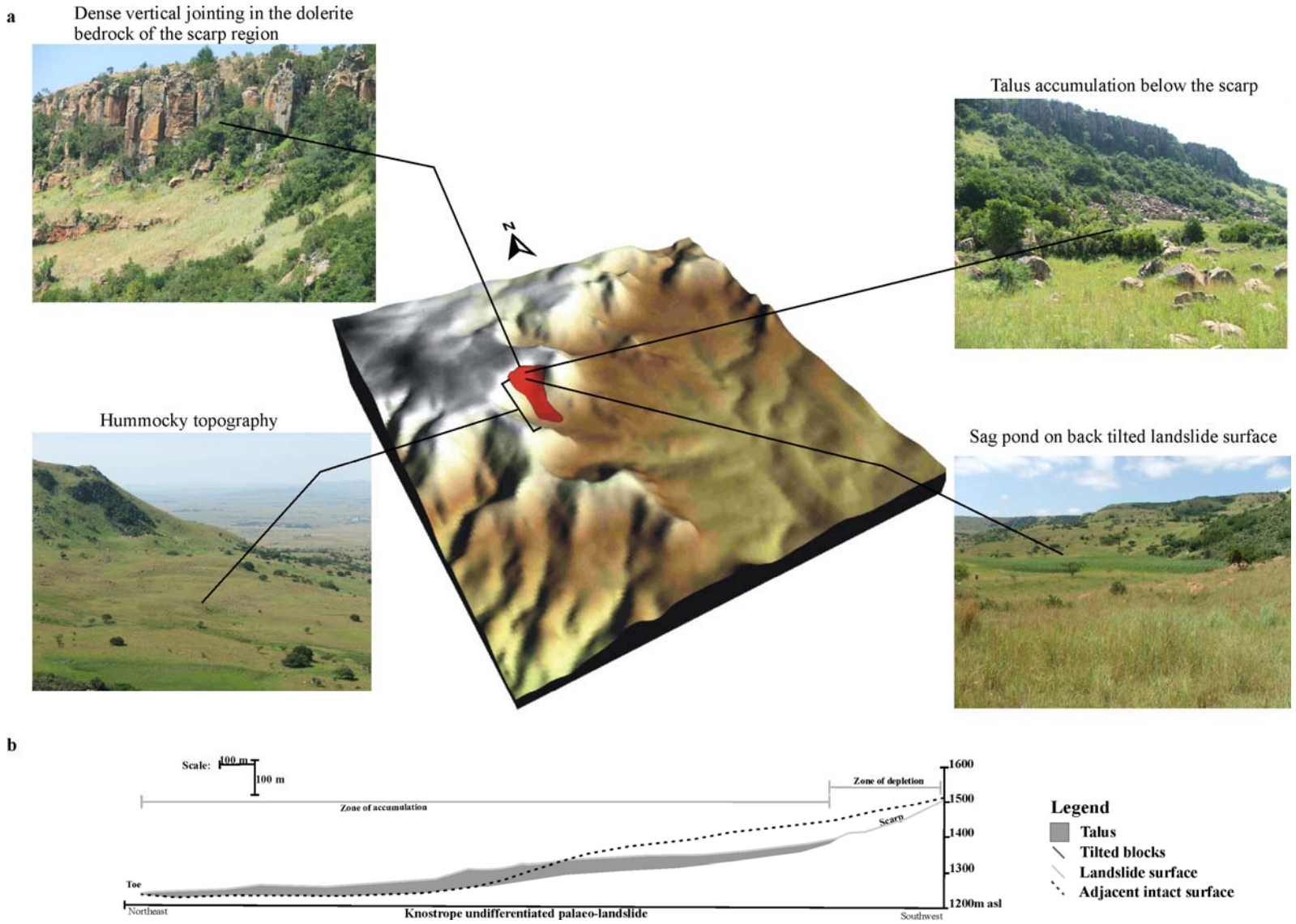


Figure 14a, b. (a) Digital elevation model (DEM) of the 1.4 km^2 Knostrope palaeo-landslide based on a 90m grid interval. The landslide area includes the zones of depletion and accumulation. Vertical exaggeration x4.2. The X and Y scales are in metres. (b) Cross-section through the Knostrope palaeo-landslide showing the geomorphic features and geometry.

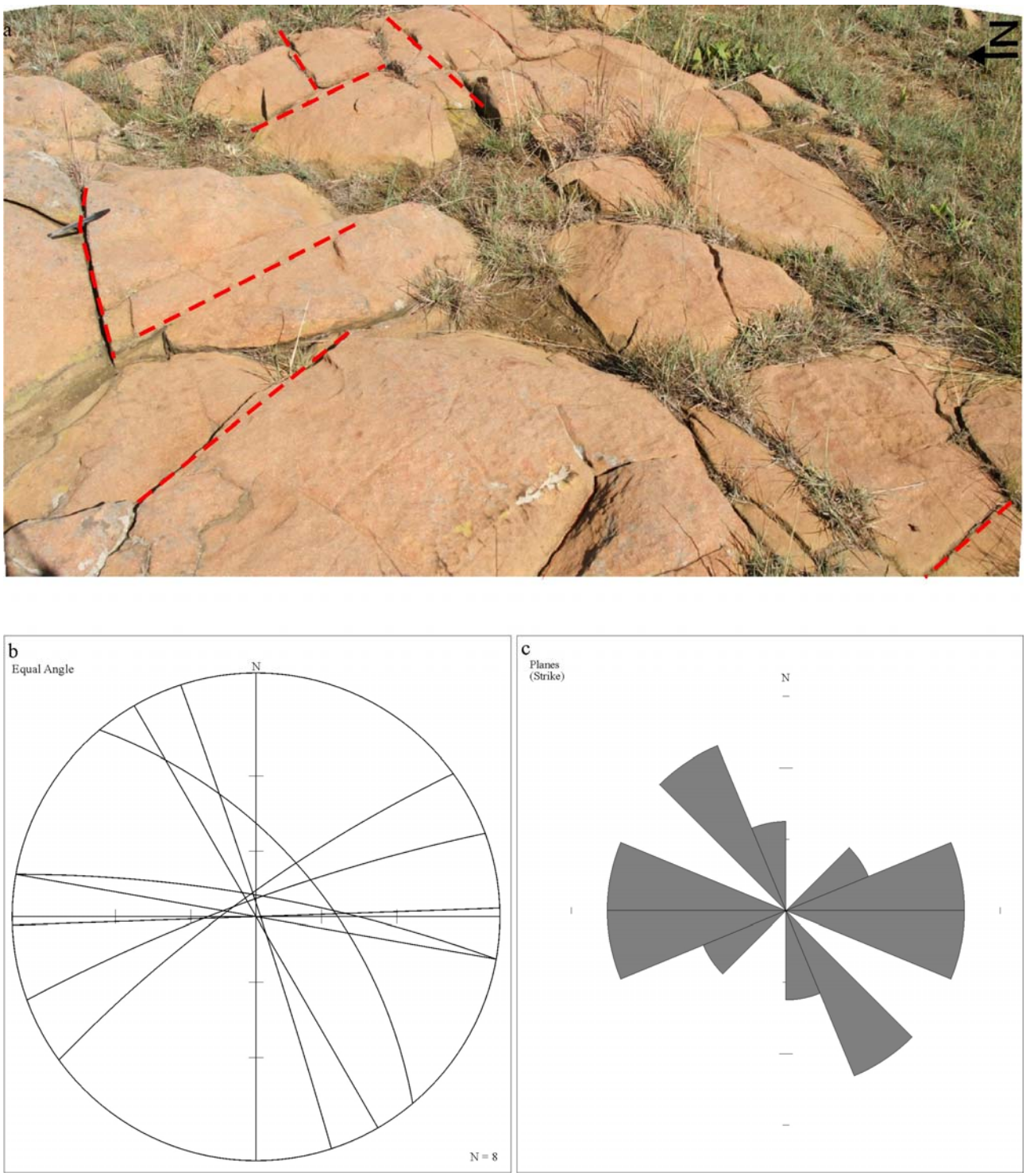


Figure 15a-c. (a) Random joint pattern in dolerite observed at outcrop scale, approximately 8 km northeast of Helpmekaar. (b) Lower hemisphere equal angle stereographic projection of joints. (c) Rose diagram of joints.



Figure 16. Wide bedrock cracks parallel to the scarp above landslides, near Helpmekaar, represent classic geoindicators of future slope instability.

(c) Meander Stream landslide

The Meander Stream rotational, large palaeo-landslide is located in the Giant's Castle Nature Reserve in the "Little 'Berg" foothills below the Ukhahlamba–Drakensberg escarpment (Fig. 17a-c). The site preserves a palaeoscarp that exposes a well-defined joint pattern in the alternating mudstone and thin sandstone beds of the Elliot Formation. The cliff line marking the southeastern margin of the landslide corresponds with the orientation of a thin dolerite dyke that can be traced up the hillside above the scarp towards the southwest. A small stream discharges over a waterfall at the landslide head. The landslide debris extends over an area of approximately 0.12 km^2 and the volume of the ground displaced by the landslide has been estimated to be in the order of $1x10^7$ m^3. The landside surface is formed of transverse hummocks from 2 to 15 m high comprising angular to

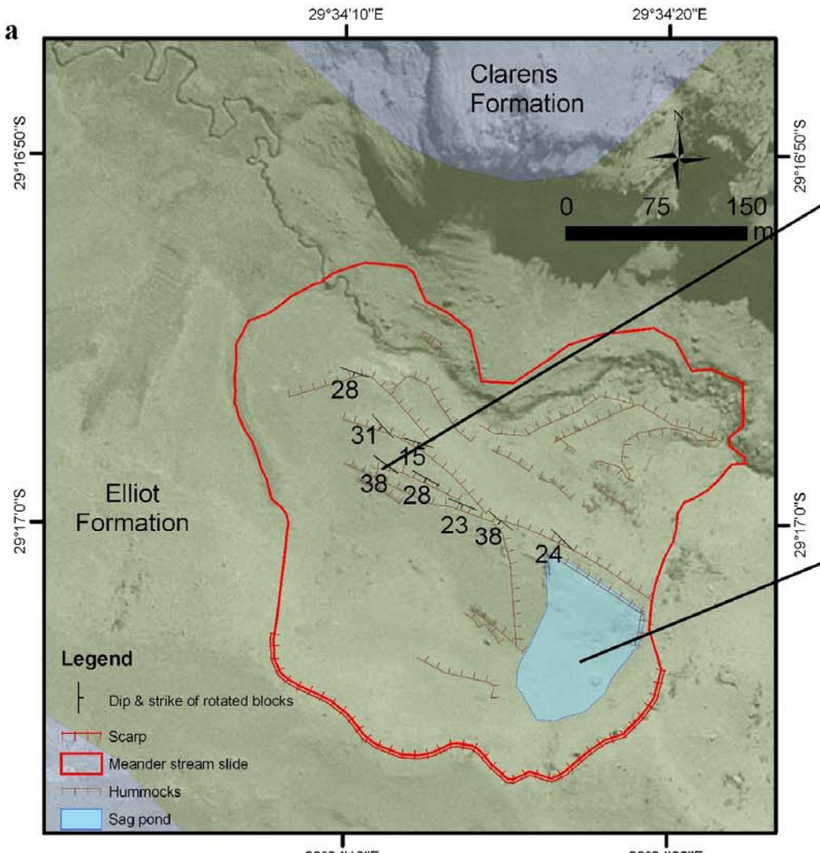
sub-rounded sandstone blocks. A series of large, relatively intact, rotated sandstone/mudstone blocks dip into the slope at up to 38°, each rotated block tilted at a slightly different angle relative to the adjacent block (Fig. 17a), indicating that this is a rock slide. The stream cascading over the steep back–slope scarp has formed an alluvial fan below the waterfall. The sag pond (Fig. 17a) infill comprises fibrous peat inter-bedded with organic-rich clay, silt and sand that has accumulated on the well preserved back-tilted rock surface. Radiocarbon dating of peat from the base of the wetland deposit, augered from the deposit adjacent to a deep gully that incises the deposit, yielded an age of 3420 ± 90 yr B.P (Pta-9635), providing a minimum age estimate for the landslide event.

This landslide has had a profound influence on drainage development of the Meander Stream close to the confluence with the Ncibidwana River valley. The landslide debris forms a knick point on the stream profile, the incised stream dropping ~10 m to the confluence. In the Drakensberg region, most low-order tributary channels exhibit straight profiles with limited floodplain development whereas the reach of the Meander Stream immediately upstream of the palaeo-landslide deposit displays uncharacteristic meandering morphology across a broad floodplain where the channel drops only 40 m over a distance of 1300 m (Fig. 17a, b). The flood plain is underlain by up to 3 m of inter-bedded clay and sandy alluvium. Small alluvial fans prograde off the steep valley footslopes onto the margins of the floodplain. The Meander Stream gradient was altered after the palaeo-landslide runout of 400 m into the valley. Temporary blockage of the valley by the landslide toe reduced the stream channel gradient and resulted in a meandering channel that led to aggradation of fine sand and silty clay alluvium on the floodplain.

The most likely hypotheses for the evolution of a meandering stream landscape in a previously steep incised valley, in close proximity to a large palaeo–landslide, are discussed below;

(i) The history of the meandering reach of the Meander Stream may have been the result of reduced gradient in response to altered hydrological regime that was initiated by the landslide damming. The impaired drainage caused by a rise in the base level led to a rapid decrease in stream velocity

that resulted in deposition of stream bedload sediment. Thereafter the valley floor aggraded vertically as the meandering stream migration pattern developed, depositing thin layers of overbank sediments and small point bars within the narrow incised channel.





Large, relatively intact, rotated sandstone/mudstone blocks dip into the slope at up to 38°



Sag pond situated on a well preserved back-tilted surface.



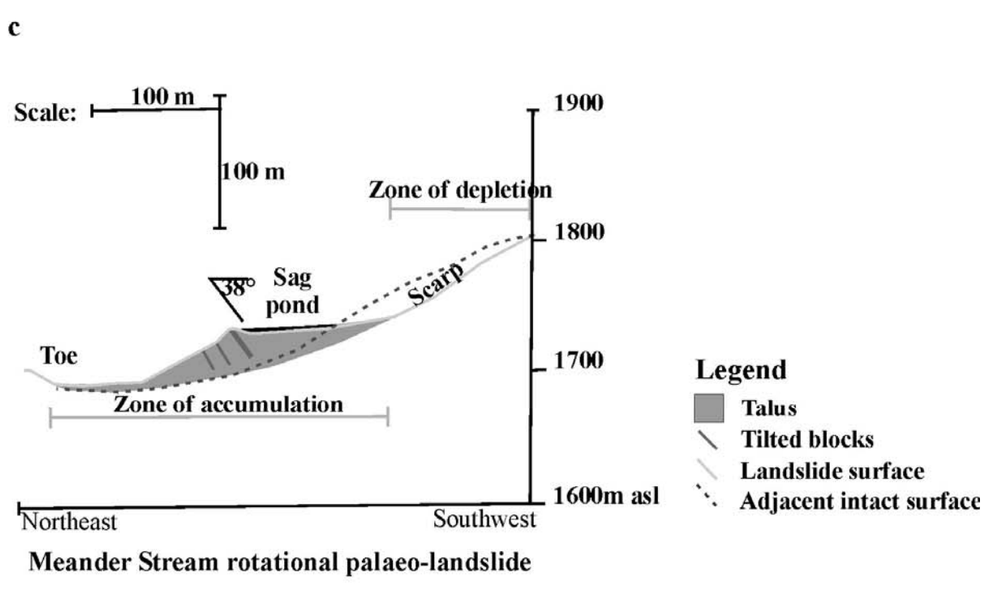


Figure 17a-c. (a) GIS - based, detailed geomorphological map of the Meander Stream palaeo-landslide and the dominant features are illustrated in the adjacent photographs. (b) The Meander Stream rotational palaeo-landslide, located in the Giant's Castle Nature Reserve, had a profound influence on drainage development. Immediately upstream an anomalous meandering stream floodplain has developed in an area where the deeply incised tributary valleys are typically drained by steep gradient, linear or dendritic channels. (c) Cross-section through the Meander Stream palaeo-landslide showing the geomorphic features and geometry.

(d) Gobela landslide

A medium-sized, debris flow palaeo-landslide is located in a tributary valley of the Bushman's River approximately 0.5 km north of the entrance gate to Giant's Castle Nature Reserve. The mass movement deposit is characterised by 1 to 3 m high transverse hummocks and has a runout zone extending 375 m from the upper hillslope failure zone (Fig. 18a, b). Organic-rich pond infill deposits with an areal extent of ~10 m^2 have accumulated within the inter-hummock depressions (Fig. 19). Radiocarbon dating of organic-rich sediment sampled using a hand auger yielded an age of 600 ± 50 yr B.P (Pta-9591), providing an minimum age estimate of the period since the landslide occurred.

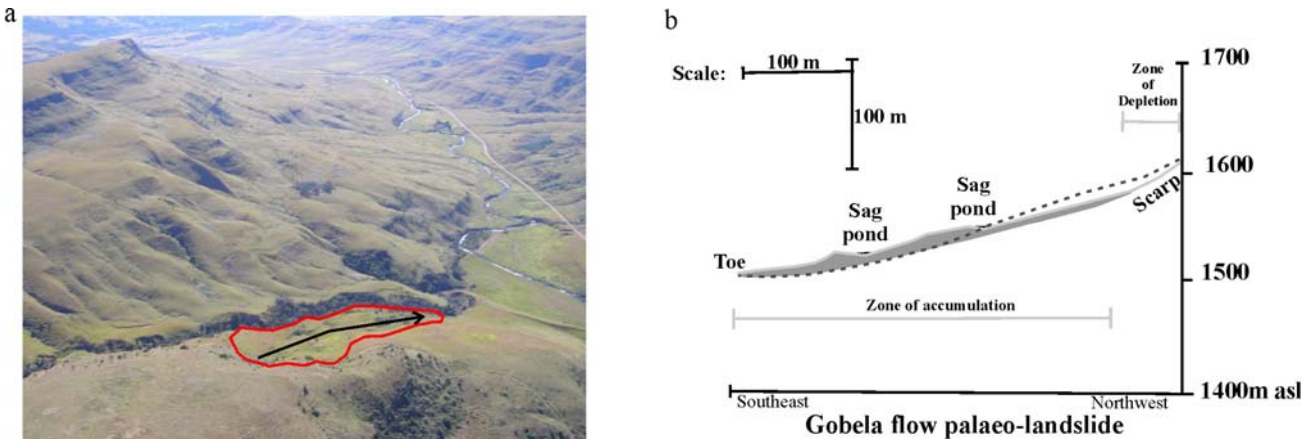


Figure 18a, b. (a) Aerial view of the Gobela palaeo-landslide, located in the Giant's Castle Nature Reserve. (b) Cross-section through the Gobela flow palaeo-landslide showing the geomorphic features and the geometry.



Figure 19. Sag ponds within the hummocky topography of the Gobela palaeo-landslide .

(e) Mooihoek landslide

The Mooihoek landslide is part of a larger mass movement complex on the southeast-facing slopes of the Brandwagkop mountain (1492 m amsl) north of Babanango. This undifferentiated, very large palaeo-landslide is situated on the farm Mooihoek 394. The head of the landslide is characterised by a relatively flat surface, just below the scarp (40 m relief, 1420–1380 m amsl) and is associated with poorly drained silty clay sediments. Hummocky topography characterises the palaeo-landslide debris surface which extends over an area of approximately 1.06 km^2 and has a runout of approximately 2000 m into the Mpembeni River valley (Fig 20a). The 5 to 10 m high, transverse hummocks have been incised by streams, exposing the landslide debris, which consists of angular to rounded, cobble- to boulder-sized dolerite blocks up to 1 m in diameter with a matrix of shale debris and reddish-brown clayey sand (Fig 20b). This landslide is classified as a debris failure. Organic-rich pond infill deposits from a typical sag pond covering 25 m^2 yielded a radiocarbon age of 1150 ± 50 yr BP (Pta-9570).

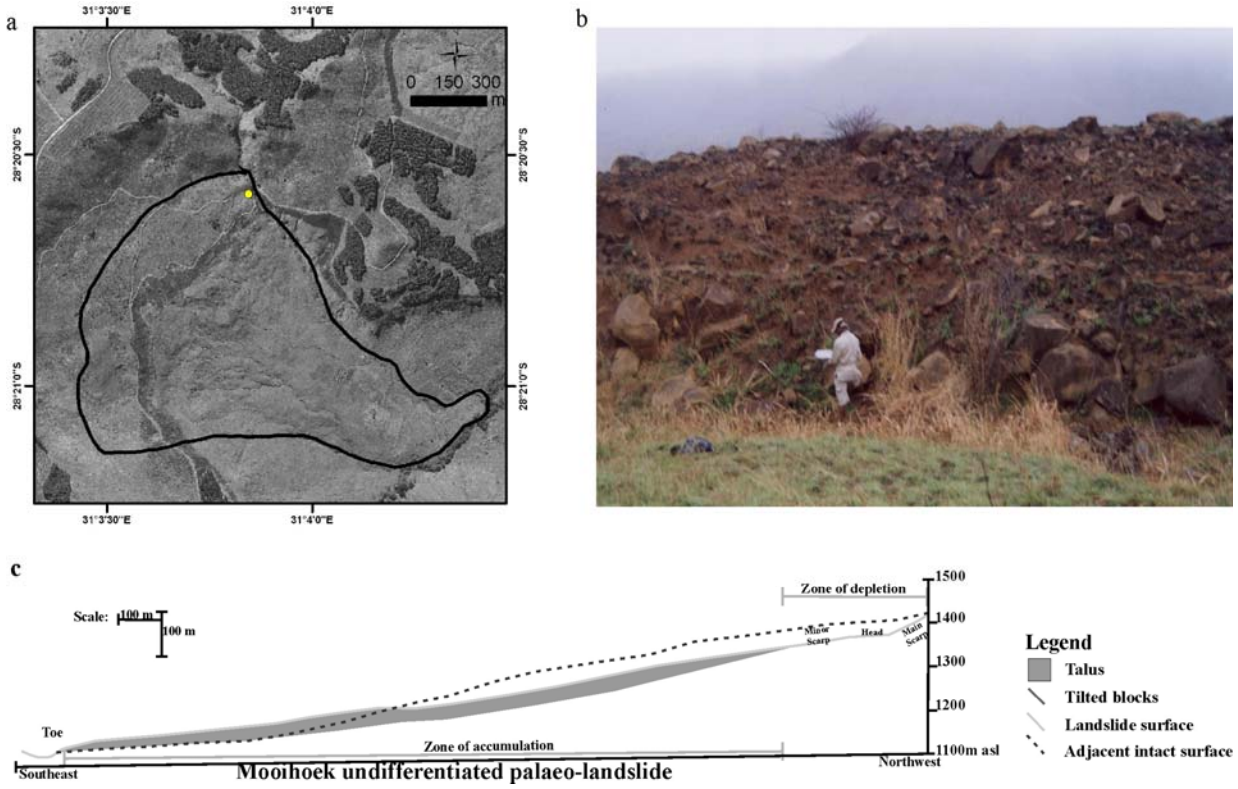


Figure 20a-c. (a) Aerial photograph of the Mooihoek palaeo-slide showing typical hummocky terrain forms. Symbol (○) refers to the locality at which the photograph shown in Figure 20b was taken. (b) Incision through a hummock exposing unsorted, angular dolerite and shale blocks in a reddish-brown clayey sand. (c) Cross-section through the Mooihoek palaeo-landslide, located north of Babanango, showing the geomorphic features and geometry.

3.7 Interpretation of landslide ages

A systematic quasi–18–year oscillation pattern recorded in rainfall from the eastern region of southern Africa (Tyson, 1986) has highlighted the variability of dry–and wet–cycle rainfall over present day southern Africa. According to Paige–Green (1989), it is during wet periods of heavy prolonged rainfall that recent landslides usually manifest themselves in the landscape such as in the summer of 1987/1988, probably the beginning of a new wet cycle. Therefore, rainfall triggered ancient landslides would most likely correspond to wetter periods in the palaeo-climatic history of this region.

A detailed record of palaeoclimate change during the late Pleistocene along the eastern margin of this part of the African subcontinent has been defined from proxy records derived from cave speleothems (Lee–Thorp et al., 2001; Holmgren et al., 2003), meteorite impact crater infill deposits (Partridge et al., 1993) or collated from numerous short–term records (Partridge et al., 1992). The Cold Air Cave speleothems from the Makapansgat valley in northeastern South Africa (Lee–Thorp et al., 2001; Holmgren et al., 2003) represent the highest resolution palaeoclimate proxy records in the summer rainfall zone of eastern South Africa. Stalagmite records from north eastern South Africa show that regional precipitation, temperatures and vegetation oscillated markedly and rapidly over the last ~6500 years on centennial and multi–decadal scales due to rapid global teleconnections (Lee–Thorp et al., 2001) and persistent millennial–scale climatic variability was superimposed on the global climatic variation over the past 25000 years (Holmgren et al., 2003). This record indicates wetter conditions in the summer rainfall areas of southern Africa during the mid Holocene warm phase with a transition toward a pronounced cool, dry episode in the past 6500 years, culminating at AD 1750.

The radiocarbon dates presented in this study suggest that the palaeo-landslides described occurred at different times during the Middle to Late Holocene (Table 8).

Table 8 Radiocarbon ages derived from organic deposits in sag ponds of palaeo-landslides in KZN.

Landslide event	**Sample designation**	**Region**	**Lab No.**	**C^{14} age (yrs BP)**	**Calibrated Date (*1 sigma range is given, with the most probable date between brackets*)**
Mount Currie	MC04/3.0-3.5 m	M-C-K	Pta-9420	2770 ± 60	923 (847) 818 BC
Mooihoek	BMH012/2.5-3.0m	CZ	Pta-9570	1150 ± 50	AD 886(963) 992
Gobela	GC57/0.5-1.0 m	U-D	Pta-9591	600 ± 50	AD 1316-1352,1390 (1406) 1421
Meander Stream	M14/1.85-2.04 m	U-D	Pta-9635	3420 ± 90	BC 1910 [1681] 1443
Knostrope	Hp4/1.75-2.00 m	L-D-V-U	Beta-229408	2980 ± 40	BC 1370-1340 (BP 3320 - 3290), BC 1320-1080 (BP 3270 -3030)

It must be emphasised that the radiocarbon dates derived from the basal sag pond infill deposits merely provide a rangefinder indication of minimum ages of the post-landslide surface topography in which organic sediment accumulated. It is possible that some sag ponds may have only developed after a secondary landslide event. When compared with the high-resolution palaeo-climatic proxy records (Fig. 21) some of the radiocarbon ages correspond with the late Mid-Holocene period when there was a high frequency of climatic variation. The correlation of individual landslide events with either relatively drier, or moist climatic phases must be approached cautiously. The lack of an obvious, strong correlation suggests that landslides across the region were triggered by the relationship between local slope threshold conditions (bedrock, structural controls, regolith cover thickness, gradient) and climatic threshold conditions. Since there is no clear correlation with rainfall or the associated relationship with elevated pore water pressure related to increased groundwater flow from springs or along dolerite intrusion contacts it is possible that large seismic events may have played a role in changing local slope threshold conditions or perhaps triggered some of these landslides.

Some of the large palaeo-landslides described occur within the Cedarville and Zululand–Lesotho Drakensberg seismic zones (Hartnady, 1990). Numerous seismic events with a magnitude >4 have

been recorded in these seismic zones (Fig 22) and some of the landslides may have been triggered by Quaternary seismic events.

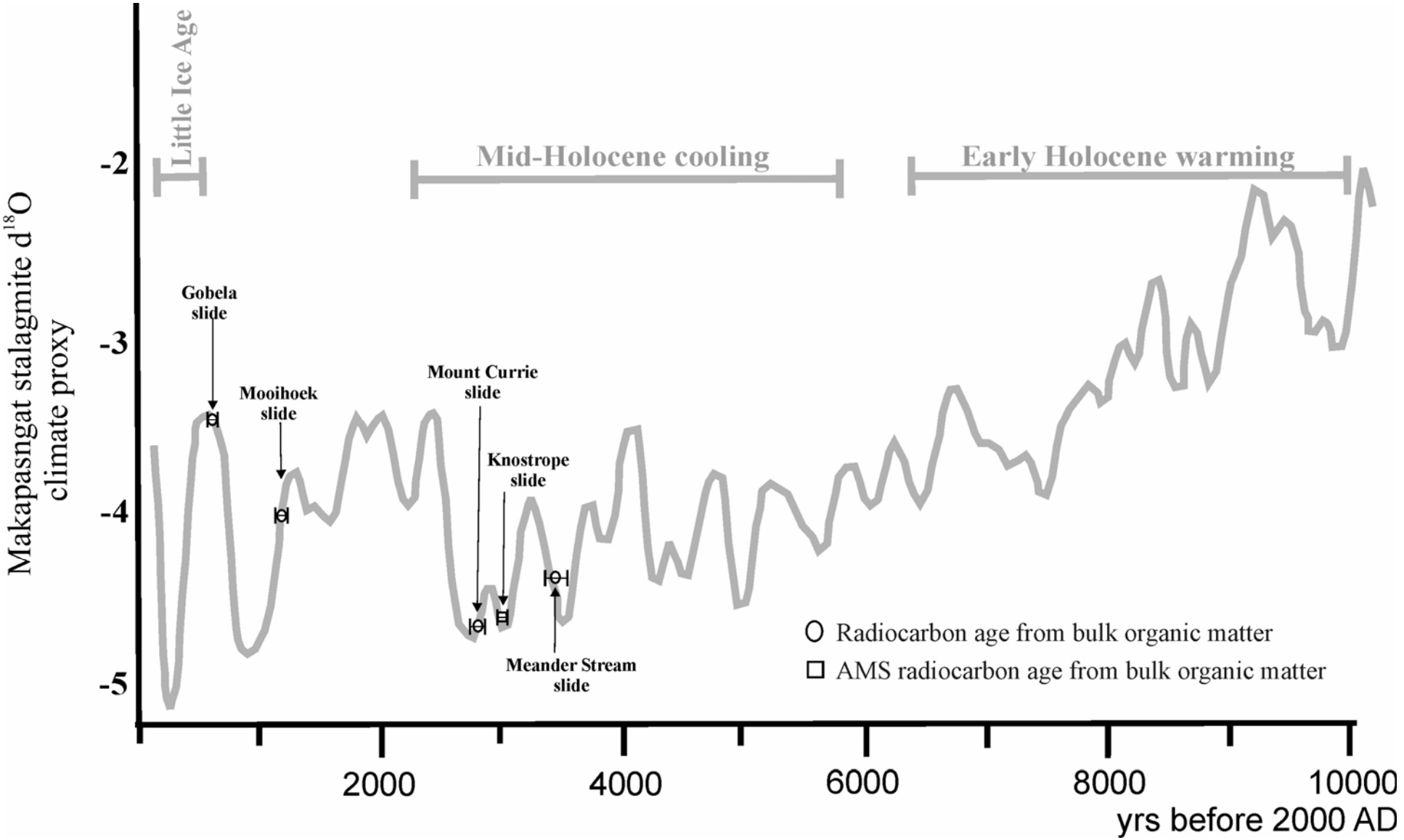


Figure 21. Age estimates of the various palaeo-landslides superimposed on the palaeo-climatic proxy record from the Cold Air Caves speleothem (Lee-Thorp et al., 2001; Holmgren et al., 2003). There is no clear correlation with warmer, relatively more humid periods.

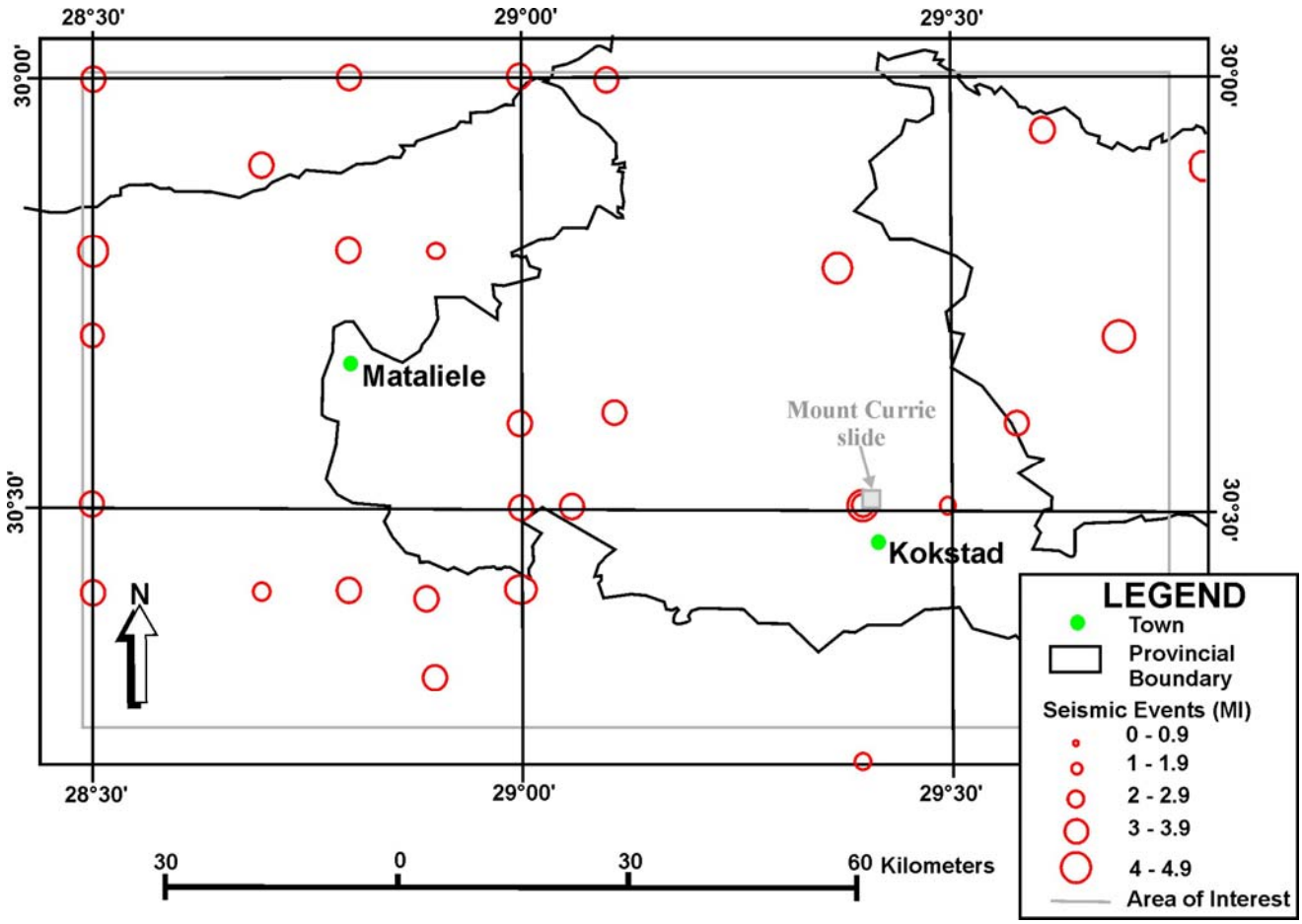


Figure 22. Seismicity map of the Matatiele-Cedarville-Kokstad region showing relatively large magnitude seismic events in the Mount Currie area (Seismology Unit, Council for Geoscience, 2005).

It is likely that large, deep seated rock- or regolith debris palaeo-landslides across the province owe their origin to the interplay between a number of triggering threshold conditions. It seems likely that these large volume mass movements were also affected by very high intensity rainfall events which could have been significantly larger than recent storms with a return periodicity of 1:50 years in this region which only triggered numerous small debris slides on hillslopes and cut- or fill embankments.

3.8 Ground truthing

Many other landslides have also been ground-truthed to confirm the aerial photographic interpretations, served in testing the modified classification system and also provided insight into

primary landslide causal factors. These landslides include the Poplars debris flow palaeo-landslide situated 1.5 km northeast of the Mount Currie slide (a), large debris palaeo-landslide in the Royal Natal National Park, situated north of the hotel (b) and the palaeo-landslides in the vicinity of Fort Mistake (c).

(a) The Poplars, Kokstad area

Figure 23 shows a debris flow palaeo-landslide situated on The Poplars farm on the east-southeast facing slopes of the Bushy Ridge. The mass movement deposit is characterised by 5 to 15 m high elongated lobes which spread laterally at the toe of the failure defining a runout zone extending 1550 m from the upper hillslope. These longitudinal lobes comprise dolerite cobble and boulder debris up to 2 m in diameter. Uniform vegetation and well-defined soil profiles are associated with the flow which covers an area of 0.5 km^2.

(b) Mahai valley, Royal National Park

The 0.69 km^2 debris flow palaeo-landslide deposit is characterised by 5 to10 m hummocks that spread laterally, giving rise to a prominent toe (Fig. 24a-c). The hummocks consist of unsorted debris in the cobble to large boulder size range set in fine-grained matrix, derived from the overlying formations. The palaeo-landslide debris has a runout of approximately 1750 m into the Mahai River valley, a tributary of the Tugela River.

(c) Fort Mistake landslides

Widespread hummocky topography characterises the steep slopes adjacent to the R23 main road in the vicinity of Fort Mistake, km from. Transverse hummocks, associated with a numerous landslides, range in height from 5 to 10 m and consist of debris comprising angular to rounded dolerite cobbles and boulders in a clayey sand matrix. Geomorphologically these landslides manifest in the landscape as shallow scars having developed throughout most of the area. Some pronounced landslides have also been identified on the farm “Waterkloof No. 2”, including two

debris flow palaeolandslides, and a debris rotational palaeo-landslide in the southeastern portion and northwestern portion respectively.

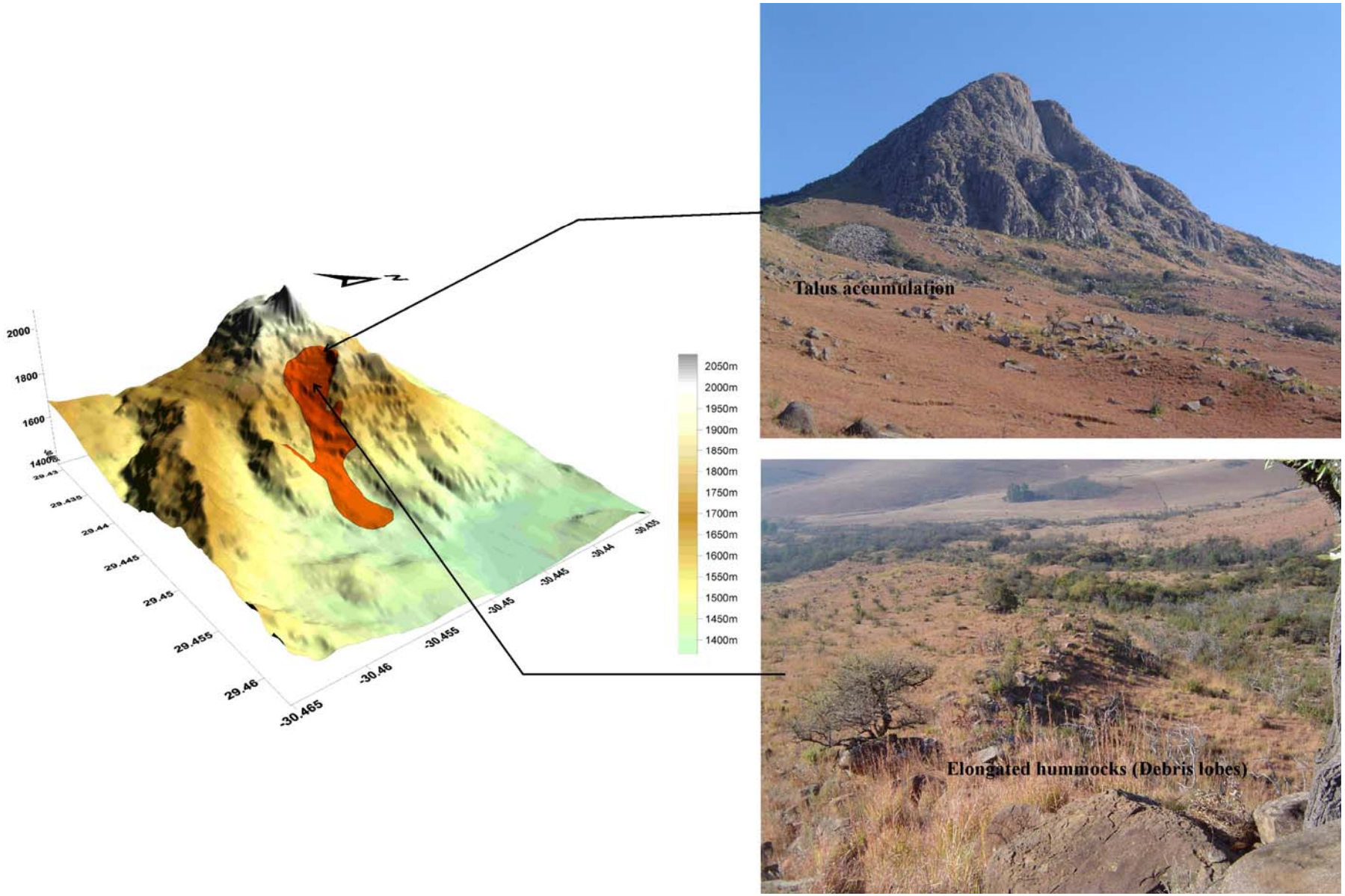


Figure 23. Digital elevation model (DEM) of the Poplars landslide based on a 20m grid interval. The landslide area includes the zones of depletion and accumulation. Vertical exaggeration x2.3. The X and Y scales are in decimal degrees.

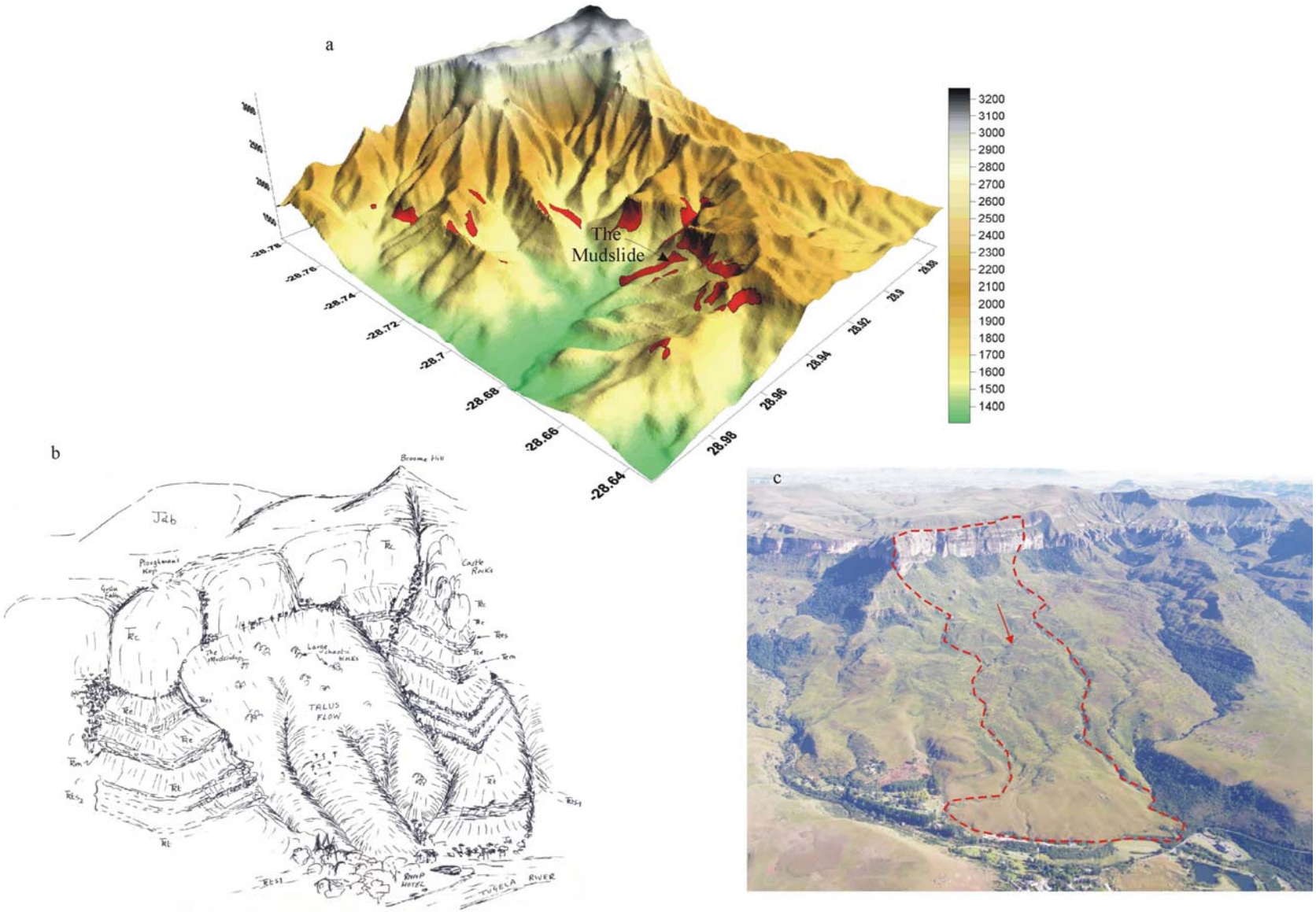


Figure 24a-c. (a) Digital elevation model (DEM) of the landslides in Royal National Park based on a 90m grid interval. Vertical exaggeration x2.5. The X and Y scales are in decimal degrees. (b) A flow debris palaeo-landslide (Mudslide) in the Royal Natal National Park, view to the northeast (Thomas, 1985). (c) Aerial view of the flow debris palaeo-landslide.

3.9 Landslide characteristics

Mass movement mapping within the various study regions highlighted the range of factors and site specific variables that influence slope failure;

- Landslides often occur in areas of steep and/or dip slopes, high relief and/or steeply dipping bedrock,
- Although large mass movements are associated with all bedrock types there are definite association with dolerite intrusions because of:
    - Differential weathering between the dolerite and sedimentary country rocks has created areas of steep topography and/or high relief.
    - Dolerite intrusions alter the dip of the adjacent country rocks locally so that bedding dips become concordant with the slope gradient.
    - The contact zone between dolerite and country rocks as well as the dense vertical jointing within the dolerites act as zones of preferential groundwater flow. Groundwater saturation may periodically increase pore pressure within the highly jointed contact zone and associated weathering profile, reduce rockmass or regolith strength.
- Long term accumulation and weathering of talus on steep slopes.
- Some palaeo-slope failures occur along zones that are presently more seismically active than the rest of the southeastern coastal hinterland (Hartnady, 1990). Other large landslide complexes may have been triggered by isolated Quaternary seismic events.
- Most recent landslide events are small slope failure triggered by extreme rainfall events and anthropogenic influences.

CHAPTER FOUR

4. LANDSLIDE SUSCEPTIBILITY MAPPING

4.1 Overview

The forces exerted by rocks, earth or other debris moving down a slope can be immense and therefore can devastate anything in its path. The initial devastation and long-term adjustments after the landslide event represent geomorphological threats responsible for significant socio-economic disruption and potential losses over extended periods. Countries such as the United States, Italy and India suffer annual landslide losses which have been estimated to range from $1 billion to $2 billion (Schuster, 1996). In South Africa, areas associated with mass movements can create a negative impact on urbanisation with annual costs of landslide impaction being estimated at about $20 million in 1989 (Paige–Green, 1989). Mass movements and their associated debris deposits are significant geomorphological threats, therefore the potential for landslides is a primary consideration in town planning and land use zonation. In South Africa mass movements exclude large areas in urban nodes from formal development and many areas of informal housing are potentially at risk. A landslide susceptibility map categorizes a region into zones of varying degrees of stability and would be a useful town planning tool for future decision making in regional and urban development projects.

4.2 Previous landslide susceptibility maps

A national–scale landslide susceptibility map was compiled by Paige–Green (1985) based on the main regional factors which included geomorphology, water, and geology (Fig 25). Paige–Green (1989) has acknowledged landslides to be significant geohazards in areas such as the eastern coastal areas of South Africa and rugged mountains surrounding Lesotho. A revised map of southern Africa was developed using GIS by combination of geological information, digital terrain

information, the water surplus provinces and seismic information (Paige–Green and Croukamp, 2004).

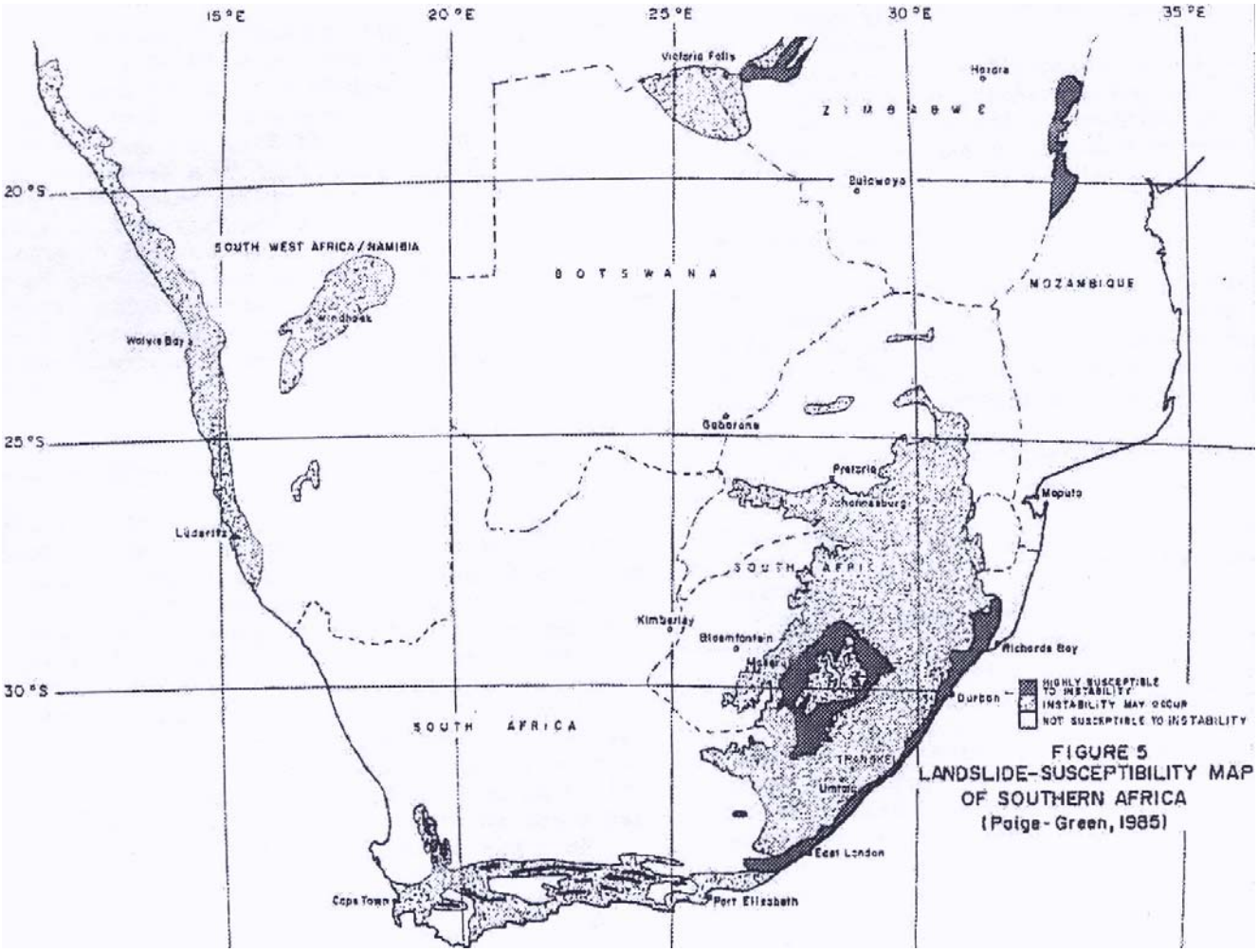


Figure 25. Landslide susceptibility map of southern Africa based on geology, geomorphology, water and historical landslide events (Paige–Green, 1985).

The investigation described here is the first provincial–scale landslide susceptibility assessment in KZN and has revealed that there are many areas that are highly susceptible to slope failure. The landslide susceptibility modeling was based on the hypothesis that slope failures in the future are more likely to occur under those conditions which led to past and present instability. The hypothesis involves an assessment of relationships between past landslide events and various instability factors. Regional landslide mapping and field knowledge combined with GIS mapping and spatial analysis capabilities formed the primary tools for the modeling of landslide susceptibility in KZN.

4.3 Landslide causal factors

Landslide occurrence is related to a variety of factors including steep rugged topography, high relief, humid climate, seismicity, lithology, geological structure, geomorphic terrain, anthropogenic activity and dip slopes etc; nevertheless, it is not always possible to include all aspects of these parameters in susceptibility assessment (Moreiras, 2005). Hence, fairly localized factors affecting slope instability such as anthropogenic activity, slopes concordant with steeply bedding planes, erosion and irregular flash flooding was not incorporated in the regional assessment. Site specific investigations conducted during the mass movement mapping phase provided some insight into the regional landslide causal factors. The following regional causal factors were initially selected (Fig 26) and are described below. These regional landslide causal factors are some of the classic independent variables used in the determination of regional susceptibility assessments (Soeters and van Westen, 1996).

4.3.1 Slope angle

Most assessments of regional landslide susceptibility employs slope angle as one of several important independent variables (Brabb et al., 1972; Carrara, 1983; Campbell and Bernknopf, 1993; Dikau and Jäger, 1994). Slope failure occurs when gravitational forces exceed the strength of the material forming the hillslope. The larger the slope angle, the larger the component of the driving forces (gravity and shearing stress) will be relative to the resisting force (friction, tensile strength). The stability of a block of material is defined by its Factor of Safety (F_s), defined in terms of the ratio between shear strength/resisting forces and driving/shear forces.

$$F_s = \text{Shear Strength/Shear Stress}$$

If the Factor of Safety becomes less than 1.0, slope instability may be expected. Mass movements also occur when the slope gradient is steeper than the natural angle of repose of the material forming that slope.

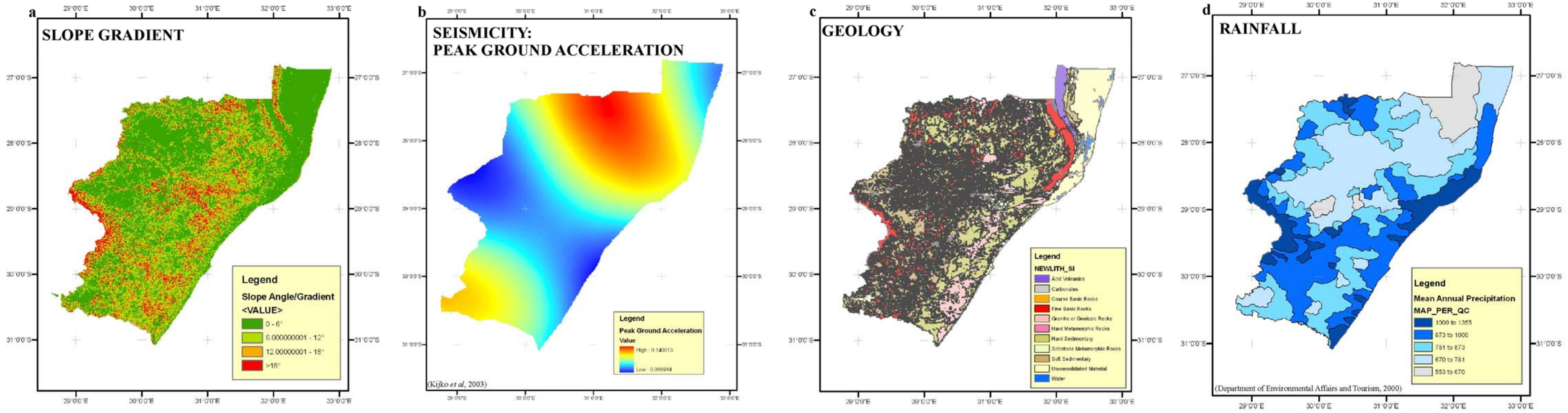


Figure 26. A compilation of the various regional landslide causal factors initially selected.

In general, the angle of repose increases as size and angularity of the particles increase and is typically 25–40 degrees for unconsolidated materials. Slopes can be over steepened by either natural causes such as stream and wave erosion undercutting the slopes or anthropogenic influences.

The 90m Shuttle Radar Topography Mission (SRTM) digital elevation model data was used to generate the slope class map (Fig 26a) of the province. Four slope class categories were delineated in accordance with the accepted industry standards for development planning prescribed by the Natal Provincial Administration (Table 9).

Table 9 The Natal Provincial Administration industry standards for development planning

Slope Angle	Slope gradient	Development Potential
0–6°	>1:10	Suitable for all types of development
6–12°	1:10–1:5	Generally suitable for residential housing and light industry
12–18°	1:5–1:3	Suitable for residential housing provided conditions suitable
>18°	>1:3	Too steep for development, high cost factor with respect to low and middle income residential housing

Slopes angles of >18° have a higher potential for instability and are deemed too steep for formal low cost housing development since potential problems would result in the alteration of the stabilizing forces acting on the slope. It must be emphasized, however, that under certain conditions the potential of instability may exist in areas with slope angles less than 18°. Generally, the steeper the slope the less stable it is hence the potential for landslides increases with higher slope angles.

4.3.2 Seismicity

Seismic activity can also trigger mass movements when the seismic waves generate vibration that may lead to failure by increasing the downward stress or by decreasing the internal strength of the hillslope sediments through particle movement. In general, earthquakes with magnitudes 4.0 or greater are often strong enough to cause landslides.

Southern Africa has passive continental margins and is regarded as being relatively stable from a geological and tectonic perspective. Generally the seismicity of Southern Africa is very moderate and of shallow character relative to world standards. According to the Earthquake catalogues of the Council for Geoscience there are two types of seismic event that occur in southern Africa, namely natural earthquakes and mine tremors. Intraplate seismicity characterizes South Africa and occasional natural seismic activity occurs sporadically within all provinces. However, certain zones of more concentrated seismicity have been recognized. According to Hartnady (1990), in KZN there are two seismically active zones (one greater, one lesser in linear extent) across the continent–ocean boundary at high angles, which is inconsistent with the isostatic stress corollary of margin parallel warping. These two seismically active zones are represented by the Cedarville seismic zone which extends from the eastern Free State to the KZN south east coast, near Port Shepstone and the Zululand–Lesotho Drakensberg seismic zone, running through northern KZN from the Zululand coast to the Drakensberg.

Although, the 1932 Zululand earthquake had its epicenter situated in the sea off Cape St Lucia the shocks felt in the greater part of KZN were of the 4^{th} and 5^{th} degrees of intensity. Higher degrees of intensity were felt in Zululand and the on shore near Cape St Lucia (Krige and Venter, 1933). The numerous Quaternary seismic events of magnitude > 4 have been known to be associated with these seismic zones. Some of the largest mass movements are located on the epicenters of recent seismic events suggesting that earthquakes may have played a triggering role in these slope failures (Fig. 24). Seismic hazard can be described as being the physical effects of an earthquake such as surface faulting, ground shaking and liquefaction. Hence, the seismic hazard map of KZN (Fig 26b) where a 10% probability of exceeding the calculated peak ground acceleration (maximum acceleration of the ground shaking during an earthquake) at least once in every 50 years was employed in this study.

4.3.3 Lithostratigraphy and rock type

Lithology is another major landslide parameter to be considered when analyzing the spatial distribution of landslide occurrence. Across the province, the Council for Geoscience (formerly the Geological Survey) 1:250 000 scale geological map series was simplified to highlight rocks with similar lithological properties and geological age (Fig 26c).

KZN, located on the east coast of South Africa is characterized by a sub humid climate and has a Weinert's climatic N–value ranging between 1 and 3 (Weinert, 1980). Decomposition in this climatic regime has produced thick residual soils and deeply weathered bedrock, particularly in areas underlain by granite, gneisses and dolerite. Although mass movements are associated with all bedrock types within the province there are definite associations with dolerite intrusions for the majority of large scale slope failures. The dolerite weathering product of corestones and deep red clay act as a sponge storing groundwater. Groundwater saturation may increase pore pressure within the weathering profile and thus reduce strength.

The moist climatic conditions of KZN also make rocks of decreased rock strength (i.e. resistance to erosion), such as the argillaceous and arenaceous sedimentary rocks of the Karoo Supergroup, highly susceptible to rapid weathering. Since the weathering products derived from the softer Karoo Supergroup rocks have a high degree of cohesion and mobility they often are prone to slope movements of the slide and flow types. In KZN the steeper slopes are often mantled by palaeo–landslide debris or thick in situ soils which exhibit instability problems particularly if the slope equilibrium is disturbed. Hence, debris slides and flows usually dominate in areas of unconsolidated material where the slope gradient is at or above the internal friction of the material. Rocks of increased rock strength are highly resistant to deep weathering such as Clarens and Molteno Formation rocks. These rocks are hard and brittle and disengagement of blocks from the near–vertical rock faces are along fracture and joint planes which pry loose by gravitational stress

and/or freeze–thaw processes, making falls the most common type of landslide in the uKhahlamba–Drakensberg region.

The layering and internal structure of rocks are also important because rocks dipping concordantly with the slope are more prone to mass movements than rocks with bedding dips in other orientations. In areas where bedding dips lie at higher angles to the regional dip and the bedding dip and direction is concordant with slope, there is a potential that the slope may fail. In KZN dip slopes are particularly important in areas of Pietermaritzburg Formation due to the tendency of shale bedrock to fail along bedding and at the bedrock/soil interface. This study includes the spatial analysis of bedding dip, dip direction and correlation with topography identified dip slope areas. This dip slope assessment identified dip slope areas characteristic of high slope instability potential and was confined to the Durban 1:50000 map sheet area (2930DD and 2931CC) (Fig. 27) since the accuracy of the analysis depends on the quality, quantity and distribution of available data.

4.3.4 Rainfall

The KZN Province experiences a humid climate. Past landslide studies in KZN have shown that during prolonged wetter periods there is a dramatic increase in frequency of slope failures occurrences which are often manifested on steep slopes hence rainfall is an important landslide triggering factor (van Schalkwyk and Thomas, 1991). The comparison of the mean annual precipitation values (Fig. 26d) with landslide polygon density yielded confirmation that rainfall is directly proportional to the landslide occurrence.

During periods of prolonged rainfall infiltrating rainwater builds up in shallow aquifers beneath a slope. Changes in moisture content of the regolith or rock under a hillslope can adversely affect the stability of that slope. An increase in pore water pressure and weight give rise to a larger gravitational force acting on the slope. The saturation of soil also reduces cohesion and friction between grains thus resulting in the reduction of the internal strength of the slope. With increased moisture clay minerals become hydrated and expand, prolonged dry periods causes shrinkage

cracks in cohesive soil slopes which facilitate the ingress of water from rain. Increased moisture can reduce friction along zones of weakness such as bedrock and soil interfaces, fractures, joints and bedding planes causing material above that particular plane to slide along the lubricated surface.

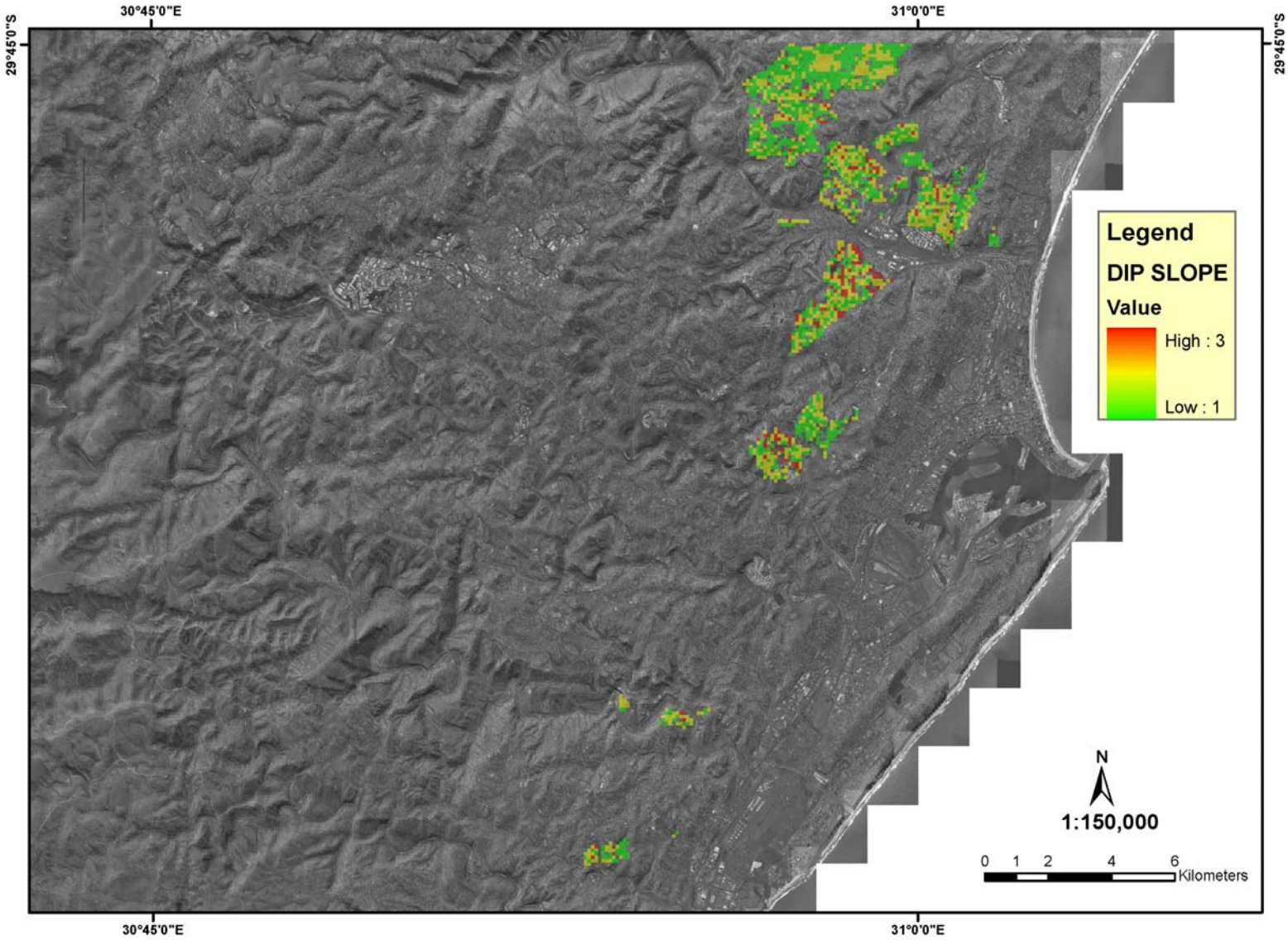


Figure 27. Map illustrating the relationship of bedding dip in shales of the Pietermaritzburg Formation with slopes in the Durban area. High values indicate concordant relationship of bedding with slope dip.

4.3.5 Dolerite intrusion contact zones

Although mass movements are associated with all bedrock types in KZN, the majority of larger slope failures have a definite association with dolerite intrusions (Fig. 26e). This association may be due to the differential weathering between the dolerite and sedimentary country rocks which creates areas of steepened topography and/or high relief. Dolerite intrusions often alter the dips of the country rocks locally so that on some slopes the bedding dip becomes concordant with the slope gradient. Contact zones between dolerite and country rocks as well as the dense vertical jointing within the dolerites generally act as zones of groundwater migration. Seasonal groundwater saturation or infiltration following extreme rainfall events may increase pore pressures within the weathering profile associated with these zones and reduce regolith or rockmass strength.

4.3.6 Lineaments

Detailed lineament, fault and dykes studies have been carried out by von Veh (1995) in the KZN area. von Veh (1995) documented three major trends in the basements and cover rocks of KZN, namely N–S and W–NW and E–NE. These linear structures (Fig 26f), commonly tracing faults, closely-spaced joints or dolerite dykes, are planes of weakness and provide storage space and pathway for groundwater migration. Groundwater saturation may increase pore pressures within these weakened planes resulting in a reduction of strength. Increased moisture can easily percolate and reduce friction along zones of weakness causing material above that particular plane to slide along the lubricated surface.

4.3.7 Terrain morphology

The landscape of the Drakensberg mountain foothills has been sculpted in response to an aggressive erosional regime that began after the fragmentation of Gondwana during the late Jurassic. Two epeirogenic uplift events during the Neogene resulted in rejuvenated drainage incision and modification of hillslope form (Partridge and Maud, 1988). Monoclinal warping and seaward tilting of the coastal regions led to thick accumulation of sediments in deeply incised river valleys.

Successive cycles of uplift and erosion have moulded the KZN landscape which is characterized by an extremely rugged topography with deeply incised river valleys and steep river gradients between the high escarpments and the flat-lying coastal plains along the Indian Ocean.

Kruger (1983) categorised South Africa into various terrain morphological regions based on slope geometry and angle, relief, drainage density and stream frequency. KZN can be broadly subdivided into all ten terrain units, ranging from steep closed mountains with high relief to broad open plains of low relief, thus highlighting the topography variance of the province. Kruger's (1983) mapping polygons (Fig 26g) were adapted for the susceptibility study as many areas in KZN are prone to slope failure due to irregular, steep topography and high relief.

4.3.8 Aspect

Slope aspect, or the slope orientation relative to the movement of the sun, is another factor that can influence slope failure. In the southern hemisphere, north–facing slopes receive more sunlight than south–facing slopes. The difference in the amount of solar radiation received may result in differences in soil temperature, moisture and soil thickness. Over long periods of weathering and erosion valley slopes can develop distinctive gradients and soil cover characteristics that distinguish the exposed north-facing slopes from the more shaded south-facing slopes. In the Ukahlamba-Drakensberg foothills within Giant's Castle Nature Reserve, Boelhouwers (1988a, b) described pronounced slope asymmetry between the shaded south-facing slopes and the opposite valley slopes.

Through the creation of different microclimates the north-facing slopes are generally hot and relatively drier with shallow soils whereas the more shaded, southerly facing slopes are often cooler and wetter with deeper, more clay-enriched soil profiles. Therefore, in the southern hemisphere, south facing slopes should theoretically have a much higher correlation with landslide occurrences as opposed to north facing slopes. The slope aspect map of KZN was determined by using spatial

analyst to process the 90m SRTM digital elevation model data where the value of the output raster data set is measured clockwise in degrees from 0 to 360 (Fig. 26h).

4.4 Landslide susceptibility methodologies

In the last two decades there has been an increasing international interest in landslide susceptibility assessments yet no standard procedure exists for the production of landslide susceptibility maps (Ercanoglu and Gokceoglu, 2004). The process of creating landslide susceptibility maps can follow several qualitative or quantitative approaches (Soeters and van Westen, 1996). The qualitative or direct mapping approach includes the landslide inventory and heuristic analyses which are generally based on personal experience or knowledge and can be considered as subjective. Some qualitative approaches, however, rank and weight the observed occurrences and may evolve to be semi–quantitative in nature. The quantitative methods such as statistical methods and deterministic approaches can be considered as more objective due to the data–dependent character of the methodologies rather than experience driven knowledge

According to Soeter and Van Westen (1996), conventional well developed landslide susceptibility methods can be classified into four broad categories: (a) landslide inventories; (b) Heuristic approaches; (c) Statistical methods; (d) Deterministic approaches.

(a) Landslide inventory is the most elementary approach giving the spatial distribution of mass movement deposits. It involves the compilation of a database of pre–existing landslides whereby the susceptibility map is derived directly from the landslide inventory map.

(b) Heuristic analysis, consists of two main types:

(i) *Geomorphic analysis* involves the determination of the hazard by drawing on individual experience, field observations and reasoning by analogy with similar sites elsewhere.

(ii) *Qualitative map combination* entails the assigning of weighting values to a series of thematic maps based on the skills and experience of the scientist which are summed at various locations and hence the area is classified into a hazard class.

(c) Statistical approach or indirect mapping, includes:

(i) *Bivariate statistical analysis* combines each factor map with the landslide distribution map and weighting values. Each parameter class is based on cross tabulation data defining their spatial correlation.

(ii) *Multivariate statistical analysis* is based on the presence or absence of landslides within a defined land unit (e.g. catchment areas, geomorphic units, or other terrain units). The analysis entails the sampling of all relevant factors either on a large–grid basis or in morphometric units. For each sampling unit, the presence or absence of landslides is also determined. The resulting matrix is then analysed using multiple regression or discriminant analysis.

(d) Deterministic approaches, requires detailed geotechnical and hydrological data and is expressed in terms of the factor of safety. This method is only applicable when the geomorphic and geological conditions are fairly homogeneous over the entire study area and is used in analysis of large scale areas.

4.5 Evaluation of methodologies

Not all methods of landslide susceptibility are equally applicable at each working scale (Soeters and van Western, 1996). An overview of the various methodologies and recommendations of their use at three most relevant scales are provided in Table 10. In contrast to Soeter and Van Westen (1996), Casagli et al., (2004) suggests that statistical methods performed best when applied at the scale of regional planning. Hence, this regional study adopted the less subjective bivariate statistical analysis.

Table 10 Overview of methodologies and recommendations of their use at three most relevant scales (Soeter and Van Westen, 1996)

Scale of use recommended					
Type of analysis	**Technique**	**Characteristics**	**Regional**	**Medium**	**Large**
Inventory	Landslide distribution analysis	Analyse distribution and classification of landslides	Yes	Yes	Yes
	Landslide activity analysis	Analyse temporal changes in landslide pattern	No	Yes	Yes
	Landslide density analysis	Calculate landslide density in terrain units	Yes	No	No
Heuristic	Geomorphological analysis	Use in–field expert opinion in zonation	Yes	Yes	Yes
	Qualitative map combination	Use expert–based weight values of parameter maps	Yes	Yes	No
Statistical	Bivariate statistical analysis	Calculate importance of contributing factor combination	No	Yes	No
	Mutivariate statistical analysis	Calculate prediction formula from data matrix	No	Yes	No
Deterministic	Safety of factor analysis	Apply hydrological and slope stability models	No	No	Yes

In the bivariate statistical analysis (ranking/weighting) values of each parameter sub-class were fundamentally based on cross tabulation data defining the spatial correlation between the landslide inventory map and individual parameter maps, thus allowing for a less subjective susceptibility analysis.

4.6 Bivariate statistical susceptibility analysis

In the bivariate statistical method, ranking values of each parameter sub-class are fundamentally based on cross tabulation data defining the spatial correlation between the landslide inventory map and individual parameter maps (Fig. 28), allowing for a less subjective susceptibility analysis. In reality certain landslide causal factors are more relevant than others so weighting values were generated for each parameter map to reflect their relative importance.

The inter–relationship (ranking/weighting) of the various sub–classes of the individual landslide causal factors was evaluated from polygon density calculations. Using GIS the polygon density was calculated by equation *PD*.

$$PD = Area\ of\ landslides\ in\ Sub\text{–}Class_a / Total\ area\ of\ Sub\text{–}Class_a$$

A subsequent multicriteria decision making method, the Analytical Hierarchy Process, was utilised for the evaluation of weighting values of the various KZN landslide causal factors. The landslide causal factors utilized in the analysis are some of the classic independent variables in the determination of regional susceptibility assessments (Soeters and van Westen, 1996).

4.6.1 Calculation of ranking values of Pertinent Sub–Classes

Inter–relationships of the various sub–classes of the individual landslide causal factors were evaluated from polygon densities calculated in a GIS. The subsequent plotting and categorisation of the polygon density graphs of slope angle, seismicity, geology, rainfall and terrain morphology supported the evaluation of ranking values (Appendix 2). Ranking values of 1 to 3 were assigned relative to the position of each sub-class on the graph (Table 11). An abitrary value of 0.01% was assigned to critical sub–classes that are known to be present in KZN but absent in the subsidiary mapping study regions (Table 11).

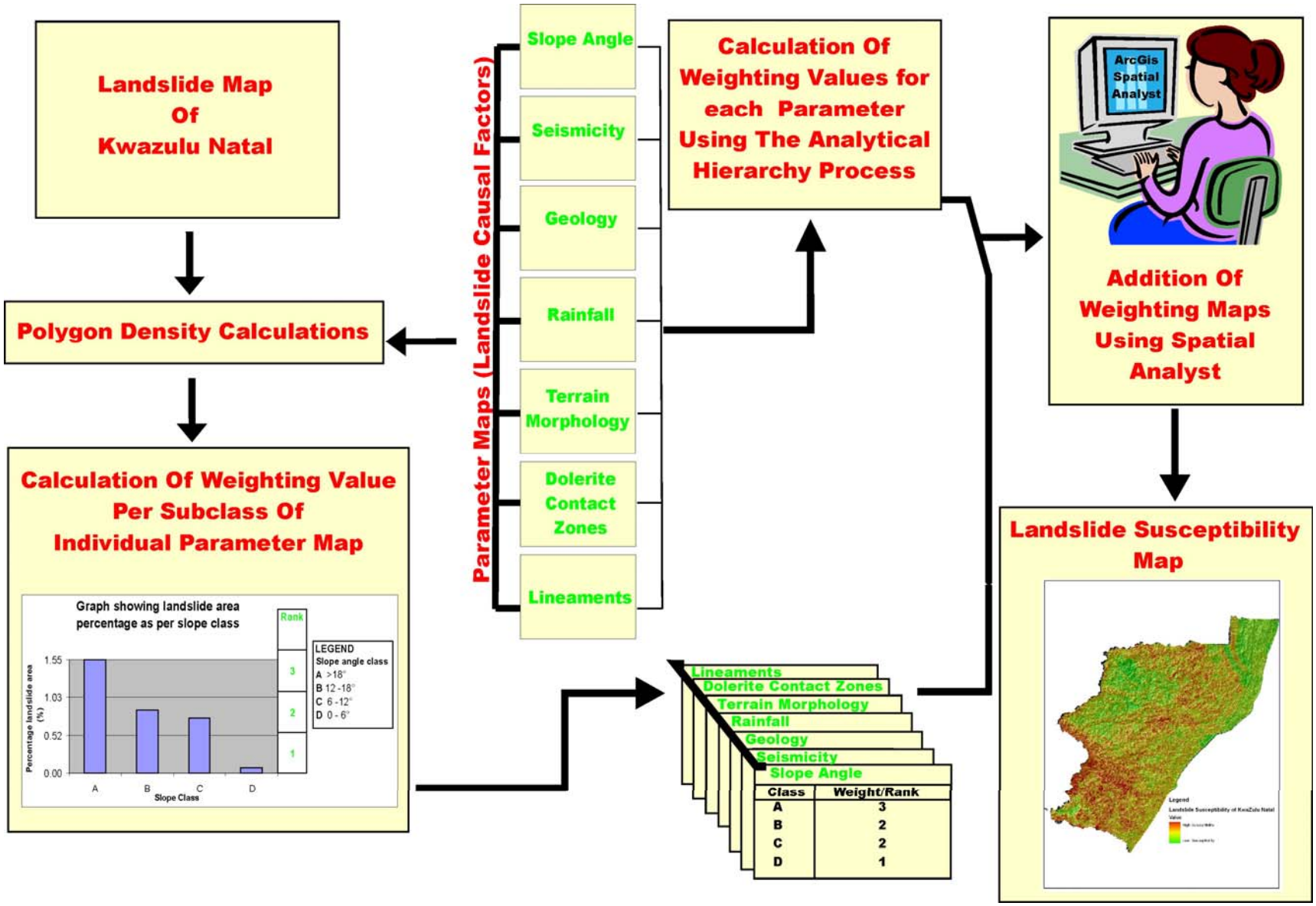


Figure 28. Flowchart showing the various critical steps in the bivariate statistical analysis (modified after Soeter and Van Westen, 1996).

Slope angle, being the most critical causal factor, has been utilised to illustrate the above explained methodology. The 90m SRTM digital elevation model data was used in the determination of the slope class map by using the Spatial Analyst extension of ArcGIS. In accordance with the accepted industry standards for development planning prescribed by the Natal Provincial Administration, the slope map was categorized into four classes (Class A–D, where class A is >18°, B is 12 – 18°, C is 6 –12° and D is 0–6°) in the decreasing order of slope angle. The graph of the nexus between four slope classes and observed landslides displays a proportional relationship between slope angle and slope failure in KZN (Fig. 29).

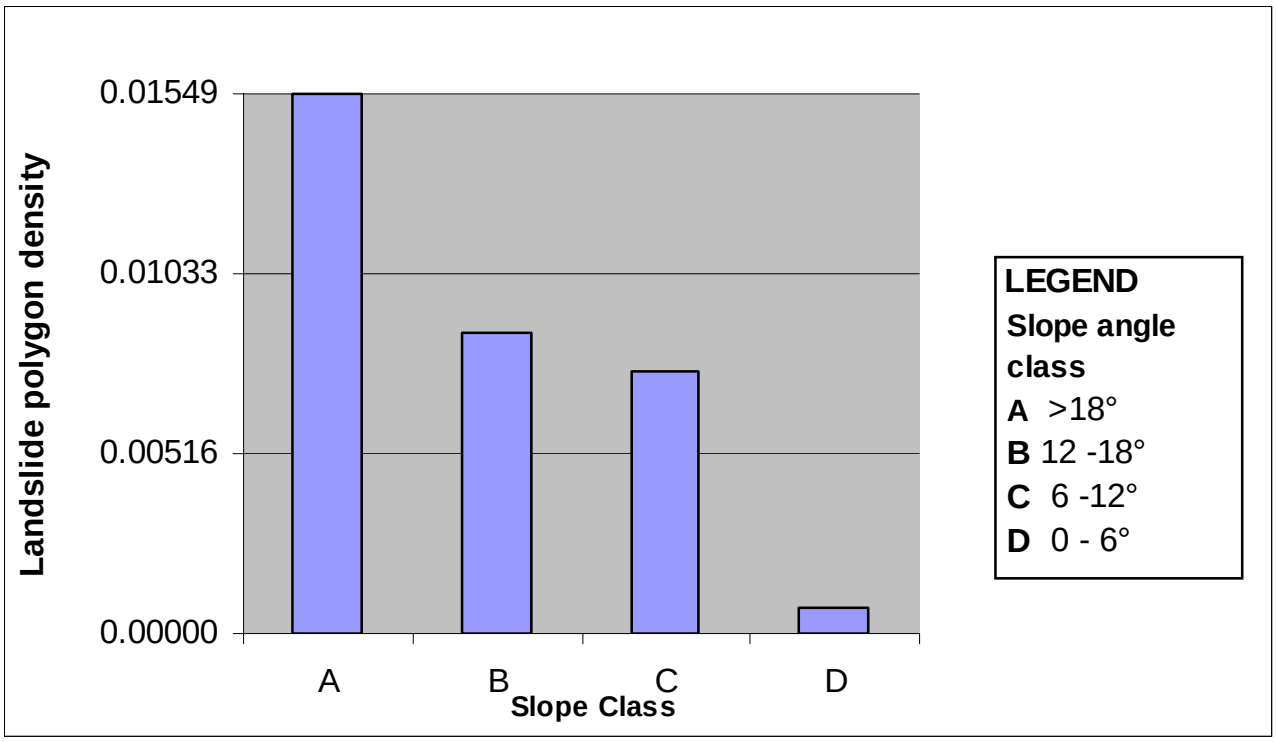


Figure 29. Graph showing landslide polygon density versus slope class**.**

Table 11 Ranking values of each sub-class

SLOPE ANGLE

Slope angle sub-class	Slope angle	Landslide area/slope sub-class area	Slope angle sub-class landslide area %	Rating Value
A	>18°	0.015489585023	1.55	**3**
B	12-18°	0.008650985105	0.87	**2**
C	6-12°	0.007502125244	0.75	**2**
D	0-6°	0.000767050499	0.08	**1**

SEISMICITY: PEAK GROUND ACCELERATION (PGA)

PGA sub-class	PGA range	Landslide area/PGA sub-class area	PGA sub-class landslide area %	Rating Value
A	>0.1150	0.005713040805	0.57	**3**
B	0.100 - 0.1150	0.006132665500	0.61	**3**
C	0.085 - 0.100	0.002970981598	0.30	**2**
D	0.07 - 0.085	0.001251106545	0.13	**1**

GEOLOGY/LITHOLOGY

Lithology sub-class	Lithological unit	Landslide area/lithology sub-class area	Lithology sub-class landslide area %	Rating Value
A	Acid volcanics	0.000000000000	0.00	**1**
B	Coarse basic rocks	0.000000000000	0.00	**1**
C	Fine basic rocks	0.001743621382	0.17	**1**
D	Granitic or gneissic rocks	0.000137459406	0.01	**1**
E	Hard metamorphic rocks	0.000000000000	0.00	**1**
F	Hard sedimentary	0.002575303466	0.26	**1**
G	Schistose metamorphic rocks	0.000000000000	0.00	**1**
H	Soft sedimentary	0.004553898084	0.46	**1**
I	Unconsolidated material	0.024563137605	2.46	**3**
J	Water	0.000000000000	0.00	**1**

RAINFALL: MEAN ANNUAL PRECIPITATION (MAP)

MAP sub-class	MAP (mm/yr)	Landslide area/MAP sub-class area	MAP sub-class area landslide area %	Rating Value
A	1000-1355	0.016713836793	1.67	**3**
B	873 – 1000	0.005075687841	0.51	**1**
C	781 – 873	0.002524031430	0.25	**1**
D	670 - 781 &	0.002091795384	0.21	**1**
***E**	*553 – 670	0.0001	0.01	**1**

*** An abitrary value of 0.01% is assigned to sub-classes that are present in KZN but absent in the subsidiary study area**

GEOMORPHOLOGY

Terrain Unit sub-class	Terrain unit	Landslide area/Terrain unit sub-class	Terrain unit sub-class landslide area %	Rating Value
A	Closed hills and mountains with moderate to high relief	0.007237603000	0.72	**3**
B	Lowlands, hill and mountains with moderate to high relief	0.001597580042	0.16	**1**
C	Open hills, lowlands and mountains with moderate to high relief	0.006793459107	0.68	**3**
D	Plains with low to moderate relief	0.000000000000	0.00	**1**
***E**	*** Table lands with moderate to high relief**	0.000100000000	0.01	**1**

*** An abitrary value of 0.01% is assigned to sub-classes that are present in KZN but absent in the subsidiary study area**

Angles greater than 18° present the highest potential for slope failure. By using the yielded value of sub–class A as a maximum value for slope failure, the y axis was equally divided into three ranking units (Fig 30). Sub–class A therefore was subsequently given the maximum ranking value of 3 and the other sub–classes were given ranking values accordingly (Fig. 30). The dolerite contact zones and lineament maps being polyline datasets were assigned ranking values according to data presence or absence where values of 3 or 0 were assigned respectively.

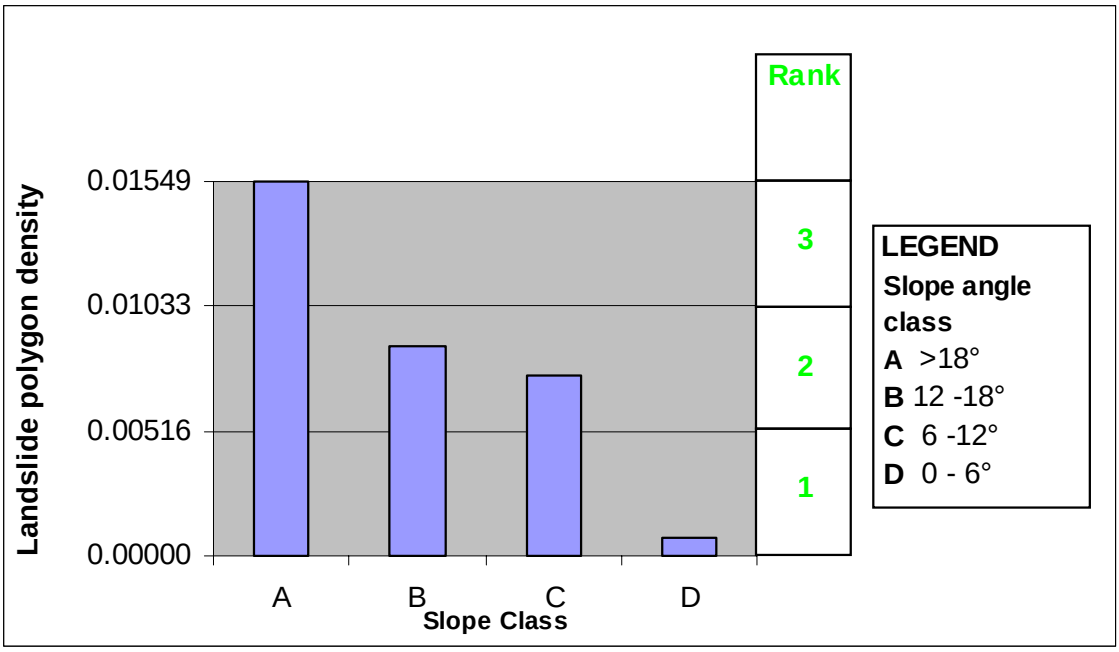


Figure 30. Graph showing ranking values per slope angle class**.**

The spatial correlation between the landslide inventory map and individual landslide causal factor (mentioned in section 4.3) maps highlighted the low impact that slope aspect has on landslide occurrence since both north and south facing slopes showed equal influence (Appendix 2f) on landslides in KZN. By considering the other seven factors, a landslide susceptibility map of province was generated.

Slope angle is the most critical landslide causal factor in KZN and is closely related to many other factors such as the rainfall, geology, geological structure, seismicity, and geomorphic terrain

4.6.2 Analytical Hierarchy Process evaluation of weighting values

In the early 1970s, Dr Thomas Saaty formulated the AHP as a generalised quantitative method for dealing with multi-criteria decision making (Saaty 1980, 1986, 1995). The main concept of fuzzy sets can be aided by the AHP to attain operational economy of application in the evaluation of suitability assessments (Weerakoon, 2002). The AHP has shown that weighting activities in multi-criteria decision making can be effectively dealt with via hierarchical and pairwise comparisons. This mathematical technique empowers humans to make decisions involving many kinds of issues including scientific assessments such as environmental management planning, land use planning, and has also been used to determine the relative weights among decision elements for GIS–based suitability and routing modeling (Robert et al., 2000).

The AHP was conducted using the following three steps:

(a) Identification of the decision elements

In order to reduce subjectivity, a group of experienced decision makers was established to identify and evaluate the relative importance of the various landslide causal factors (decision elements). From the expert scientific knowledge gained from the members of the group, the seven critical landslide causal factors for KZN were arranged according to their relative importance.

(b) Construction of an importance table

In using the pairwise comparison technique, each decision–maker (D1-D4) was required to respond to a pairwise comparison question asking the relative importance of ***factor A*** over ***factor B*** (Table 12 and Table 13). The intermediate judgment values 2, 4, 6 and 8 are used to represent shades of judgments between the five basic assessments i.e between equally, moderately, strongly, very strongly, and extremely. The number of pairwise combinations was calculated by the equation:

$$\#\text{Pairs} = 1/2N\,(N1)$$

where N is the number of decision elements

Table 12 Preference rating values

Preference Rating Value (Saaty,1893)	CCI–AHP Program Importance Scale	Significance Level (How important is *A* relative to *B*?)
9	9	Extremely more important
7	7	Very strongly more important
5	5	Strongly more important
3	3	Moderately more important
1	1 or –1	Equally important
1/3	–3	Moderately less important
1/5	–5	Strongly less important
1/7	–7	Very strongly less important
1/9	–9	Extremely less important

Table 13 The pairwise comparisons of each decision–maker

Relationship			Rating Values					
			D1	D2	D3	D4	Total	Mean rating value
Slope Angle	vs	Seismics	4	5	6	4	19	5
Slope Angle	vs	Geology	5	6	7	5	23	6
Slope Angle	vs	Rainfall	6	7	5	6	24	6
Slope Angle	vs	Terrain morphology	7	3	4	7	21	5
Slope Angle	vs	Dolerite contact zones	4	4	6	5	19	5
Slope Angle	vs	Lineaments	8	8	9	5	30	8
Seismics	vs	Geology	-1	-2	3	2	2	1
Seismics	vs	Rainfall	3	4	-1	3	9	2
Seismics	vs	Terrain morphology	3	-2	4	5	10	3
Seismics	vs	Dolerite contact zones	3	3	5	2	13	3
Seismics	vs	Lineaments	6	7	7	6	26	7
Geology	vs	Rainfall	3	4	-2	3	8	2
Geology	vs	Terrain morphology	2	1	-3	3	3	1
Geology	vs	Dolerite contact zones	-1	1	-3	1	-2	-1
Geology	vs	Lineaments	4	6	5	4	19	5
Rainfall	vs	Terrain morphology	1	-1	3	2	5	1
Rainfall	vs	Dolerite contact zones	1	-7	2	2	-2	-1
Rainfall	vs	Lineaments	4	3	5	3	15	4
Terrain morphology	vs	Dolerite contact zones	-2	2	-4	-3	-7	-2
Terrain morphology	vs	Lineaments	4	6	6	1	17	4
Dolerite contact zones	vs	Lineaments	3	6	5	4	18	5

The pair–wise comparison technique resulted in a robust and reliable method for capturing individual preferences. Average preference rating values were evaluated and utilized as the input values in the importance table/comparison matrix. If the judgment was that *B* is more important

than *A*, then the reciprocal of the relevant index value was assigned as shown in the derived landslide causal factor comparison matrix (Table 14).

Table 14 Landslide causal factor comparison matrix

	SA	S	G	R	TM	DCZ	L
SLOPE ANGLE (SA)	1	5	6	6	5	5	8
SEISMICITY (S)	1/5	1	1	2	3	3	7
GEOLOGY (G)	1/6	1/1	1	2	1	–1	5
RAINFALL (R)	1/6	1/2	½	1	1	–1	4
TERRAIN MORPHOLOGY (TM)	1/5	1/3	1/1	1/1	1	–2	4
DOLERITE CONTACT ZONES (DCZ)	1/5	1/3	1/1/1	1/1/1	1/1/2	1	5
LINEAMENTS (L)	1/8	1/7	1/5	1/4	1/4	1/5	1

Prior to computing the landslide causal factor weights (values 0 to 1) based on pairwise comparisons, the overall consistency of judgments is measured by the consistency Ratio (CR). Perfect consistency implies a value of zero for the inconsistency index. Since human decision making is often biased and inconsistent due to our subjective nature, it is considered acceptable if CR $\leq$ 0.1 (Saaty, 1986). A low value 0.048 was achieved, proving good consistency (Appendix 3).

(c) Computing the relative weights

The first step of the calculation was to evaluate the reciprocal values and complete the comparison matrix. To obtain normalized weights, the sum of each column was computed. Subsequently each value in the table was divided by its corresponding column sum. The next step was to calculate the average value of each row and the resultant values were used as the weighting values. The equation $\sum_{i=1}^{7} w_i = 1$ holds true for the weighting values obtained in the study as shown in the final step of the table Appendix 4. Since this multi-criterion method depends on relatively advanced matrix algebra for the evaluation of weighted values, cross evaluation (Step 5 of Appendix 4) of the calculated weighting values was pertinent. Cross evaluation was obtained by using a web application (www.cci–icc.gc.ca/tools/ahp/index_e.asp) based on Saaty's AHP model (Appendix 5) and analogous values were yielded

4.6.3 Model computation using the ArcGIS Spatial Analyst

The Raster Calculator of ArcGIS Spatial Analyst is the main interface for performing advanced Map Algebra. Map algebra (simple syntax similar to any algebra) is the analysis language for Spatial Analyst. The mathematical operators and functions in this software package evaluates the expression only for input cells that are spatially coincident with the output cell. Figure 31 simply illustrates how mathematical operators and functions can be used to combine data on a cell–by–cell basis to derive new information. This is a powerful GIS tool which facilitates the speed and ease for combining multiple maps, assigning weights, identifying relationships and performing suitability/susceptibility analyses.

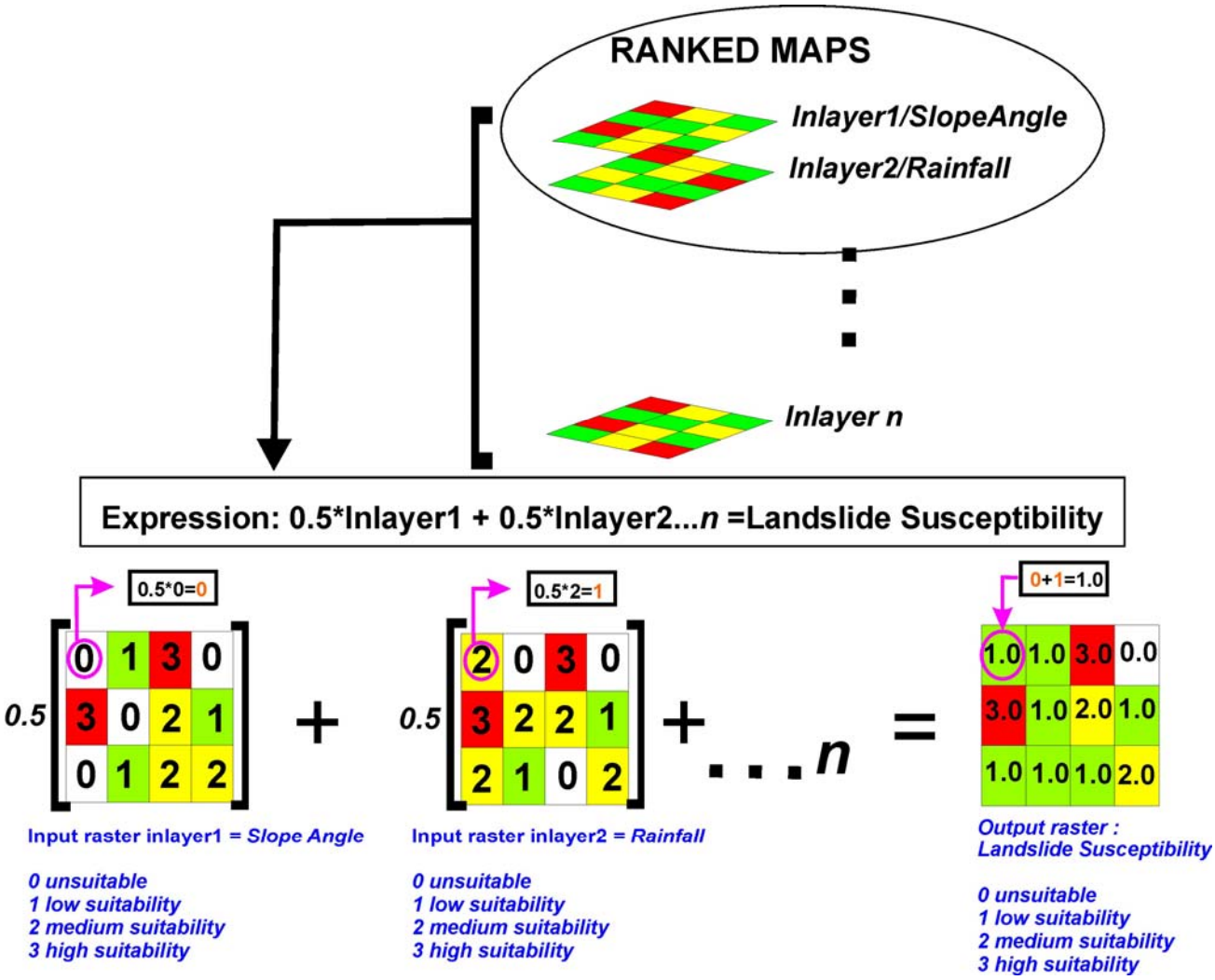


Figure 31. Illustration showing how map algebra uses mathematical operators and functions to derive new information on a cell by cell basis.

4.7. Landslide susceptibility evaluation

Data processing in the Raster Calculator of ArcGIS Spatial Analyst required all datasets to be in raster format. All landslide causal factor data was acquired in vector format i.e polygon and polyline shape files. These source files were easily converted to raster datasets using Convert of ArcGIS Spatial Analyst.

In this study the Reclassify function of Spatial Analyst was utilised as shown in Figure 32 to rank the sub-classes of individual landslide parameter map. The slope angle, seismicity, geology, rainfall and terrain morphology raster dataset/layer was reclassified on a scale of 1 to 3, with 3 being most susceptible to mass movement. Since the dolerite contact zones and lineaments layers were acquired as polylines their subsequent raster layer was reclassified to create ranked maps based on data presence or absence where values of 3 or 0 was assigned respectively.

From scientific knowledge certain landslide causal factors were more relevant than others and are reflected in the susceptibility model by the introduction of weighted parameter maps. In order to change the relative influence of individual landslide causal factors the weighting value ranging from 0 to 1 (Step 5 of Appendix 3) is multiplied to express the earth scientist's opinion on the estimated relative significance of each factor. Each grid/inlayer will have a decimal weight associated with it, and the sum of the decimal weights must be 1 as shown in Table 15.

Table 15 Weighting values of each landslide causal factor

Landslide causal factors	Weight values
Slope angle	0.45
Seismicity	0.16
Geology	0.11
Rainfall	0.08
Terrain morphology	0.08
Dolerite contact zones	0.10
Lineaments	0.03
Total (Sum)	**1.01**

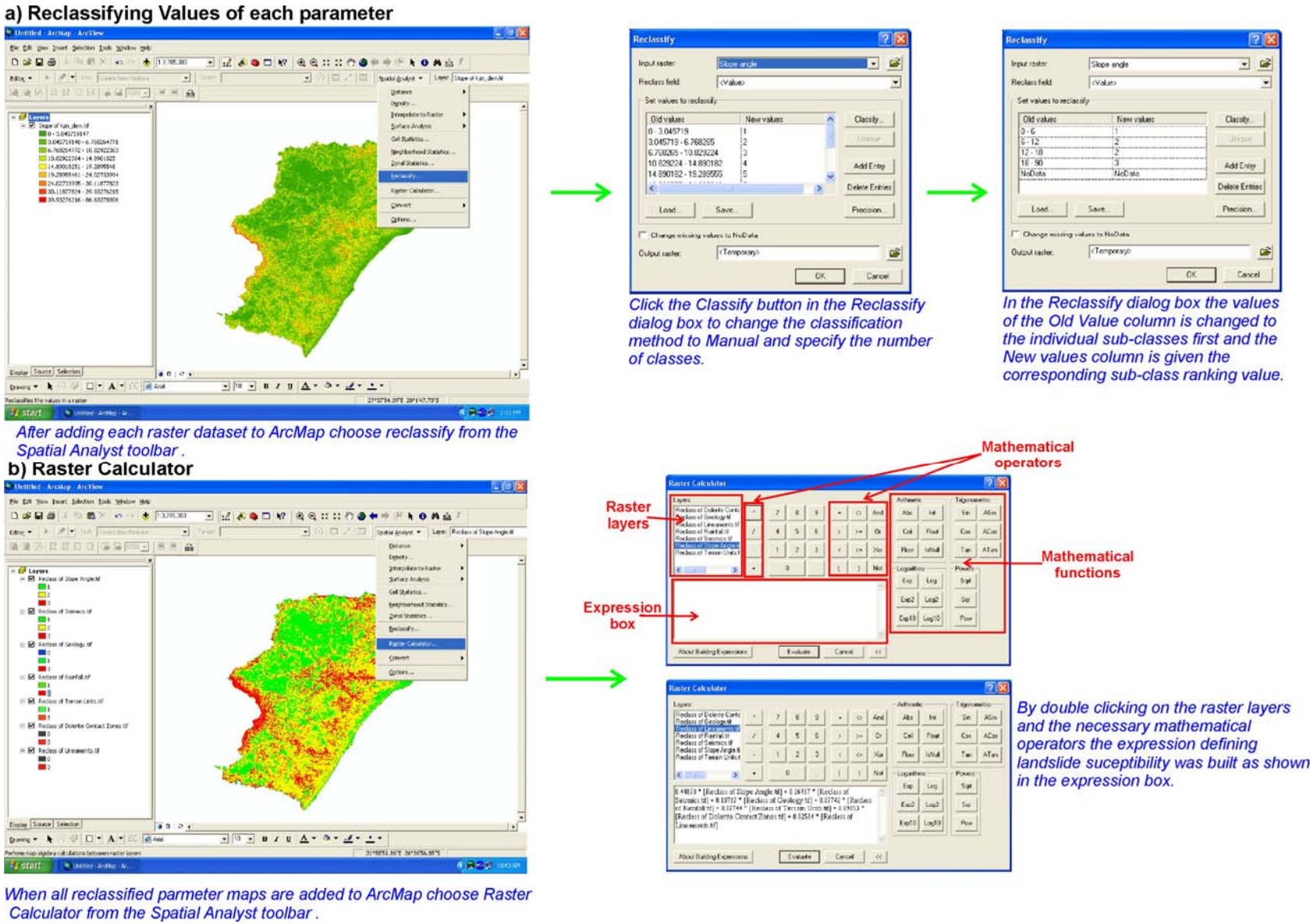


Figure 32. llustration on the utilisation of the Reclassify and Raster calculator functions of Spatial Analyst.

In implementing the relative weights in a GIS based model, the map layers are multiplied by their respective weights; the products are summed and then divided by the sum of the weights to calculate the weighted average for each map location. Hence, the landslide susceptibility coefficient (M) for each pixel will be calculated by the expression M where $X_{1...}$ X_7 are related slope angle, seismicity, geology, rainfall, terrain morphology, dolerite contact zones and lineaments respectively and $w_{1...}$ w_7 are related to respective their respective weights.

$$M = (w_1X_1 + w_2X_2 + w_3X_3 + w_4X_4 + w_5X_5 + w_6X_6 + w_7X_7)/1 \quad (1)$$

With substituting the relative weights in equation (1), the final model input equation was derived:

$$M = (0.45X_1 + 0.16X_2 + 0.11X_3 + 0.08X_4 + 0.08X_5 + 0.10X_6 + 0.03X_7)/1 \quad (2)$$

Using Map algebra the landslide susceptibility coefficient data was easily evaluated on a cell–by–cell basis in ArcGIS Spatial Analyst thus highlighting landslide susceptibility of KZN (Fig. 33).

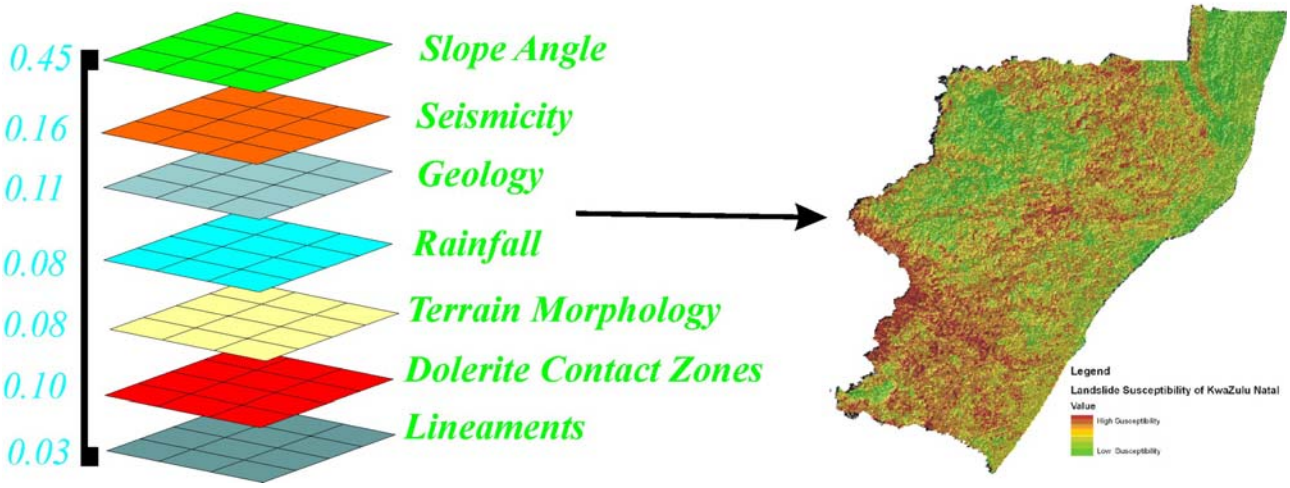


Figure 33. Illustration showing how the landslide susceptibility coefficient data was evaluated on a cell-by–cell basis.

The quality of the resultant KZN landslide susceptibility map at a regional scale was examined by overlaying the map and landslide inventory data. The verification of the map has proven favourable results.

4.8 Landslide Susceptibility Map

The landslide susceptibility zonation map highlights areas of possible future landslide occurrence and can be interpreted in relation to the potential devastation of environments or infrastructure present in the different areas. The zonation resulting from the weighting of the main landslide causal factors and ranking of their subclasses represents landslide susceptibility. This indicates the potential terrain instability but gives no indication of likely temporal occurrence or recurrence intervals. The regional KZN landslide susceptibility map is a preliminary indicator of potential slope instability and is not a design tool that can replace detailed site specific investigations. Most susceptibility maps use a colour scheme that relates to stable, moderately stable and unstable areas. The following colour scheme is used in the landslide susceptibility map of KZN, characterizing the area into various slope–stability zones.

Low Susceptibility: Within these areas there is a low potential to adversely influence slope stability. However, development in these areas must be guided by normal planning and other building regulations.

Moderate Susceptibility: Areas for which the combination of factors may adversely influence slope stability. Development may proceed based on detailed geotechnical investigations and advice. The scale and nature of proposed development should be taken into consideration. The cost of investigations and remedial and/or preventive measures are likely to be high.

High Susceptibility: Areas of high landslide potential. In general, these areas are unsuitable for site development. The cost of carrying out standard geotechnical investigations and remedial or preventive work for slope stabilization may be very high. Therefore, it is best to avoid these slopes as far as possible except for the most essential use. A thorough ground investigation report by competent persons should be required before any site development is undertaken.

4.9 Landslide Susceptibility Map Description and Verification

The accuracy of any susceptibility analysis depends greatly on the quantity and quality of data available. The KZN landslide susceptibility map (Fig. 34) highlights distinct susceptibility zones; four regions are areas of relatively low susceptibility and two zones of high susceptibility independent of the four regions (Section 3) which were targeted during the mapping phase due to their known associations with mass movement deposits. The low susceptibility zones include the generally shallow gradient areas of the Cedarville Flats, the Zululand coastal plain and the Wasbank–Buffalo–Dundee–Ingagane–Newcastle–Utrecht–Vryheid river basin plains. The two regions of high susceptibility, independent of the four regions initially recognised to have landslides associated with them are the Umkomaas River valley and Tugela River valley regions. The following section highlights the landslide mapping/inspection carried out in Umkomaas and Tugela Valley regions.

(a) Umkomaas Valley Region

The landslide verification mapping exercise highlighted the widespread spatial distribution of a range of types and sizes of slope failures in the Umkomaas valley region. Some of these landslides include the very large Dilston ancient landslide and recent toppling in vertically jointed dolerite in the vicinity of Helehele. The Dilston slide is one of the largest palaeo–landslides located in the province and occurs in a relatively dry area (Fig. 35). Covering an area of ~3.0 km^2 this palaeo-landslide occurs on the southern (right bank) valley slopes of the Umkomaas River i.e. northeast facing slopes of the Dilston Farm and is characterized by hummocky terrain. Thick colluvium (~8–10m) comprising angular to sub–rounded shale and dolerite cobble and boulders in a sandy clay matrix is associated with the slide. The slide debris is eroded and the landforms degraded which along with the dense vegetation cover and deep stream incision along its margins led to this large slope failure being classified as an undifferentiated palaeo–landslide.

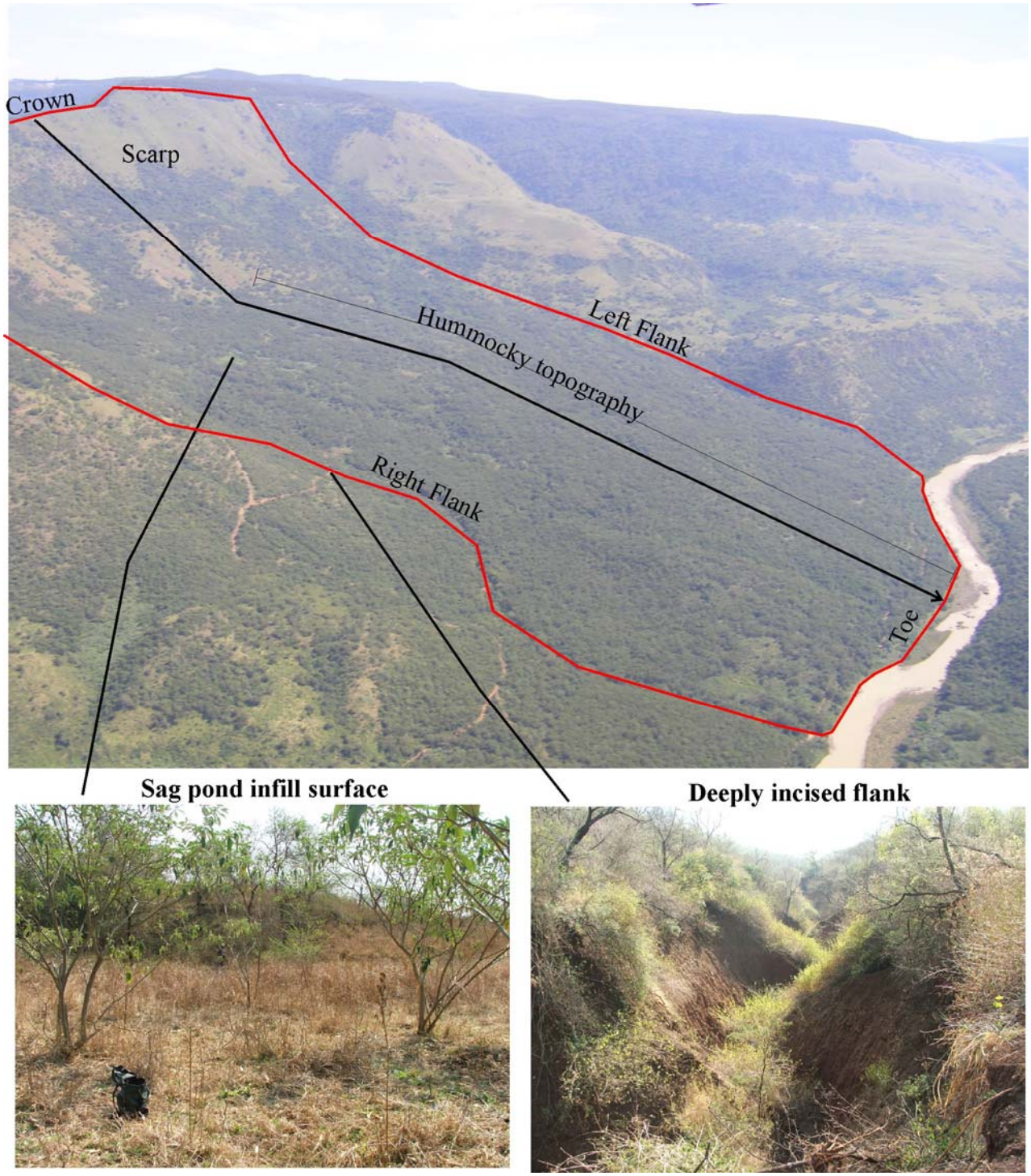


Figure 35. The large Dilston landslide is an undifferentiated palaeo-landslide with an areal extent of approximately 3.0 km^2, located in the Umkomaas valley, approximately 50 km SSW of Pietermaritzburg.

Distinctive toppling failures have been noted in the shales of the Pietermaritzburg Formation (Fig. 36) along the district road in the vicinity of Helehele. The vertical jointing in the shales act as planes of weakness along which a block/mass of material rotates forward and is eventually displaced down the steep slopes of the Ka Helehele mountain.



Figure 36. Toppling in vertically jointed shales in the vicinity of Helehele**.**

(b) Tugela Valley Region

According to Smith (1977) mass slips are commonly identified by steeply dipping sediments tilted back into the hillslope suggesting rotational movement with rock falls being a common occurrence. The aerial photographic interpretation of the region provided confirmation of the widespread landslide occurrences in this relatively drier area of the province. These aerial photographic

interpretations were plotted on the various 1: 50 000 geological field sheets indicating that landslides in this region also have a definite association with dolerite sills and dykes.

The following previously well documented landslide data of the Pietermaritzburg and Durban areas were not incorporated in the susceptibility modeling for the very purpose of map verification.

(i) Pietermaritzburg area slides

Numerous slope failures have occurred in the past and further areas of potential slope instability exist particularly due to the impact of urbanization in the Pietermaritzburg area (Fig. 37). Various types of landslides were recognised throughout the Pietermaritzburg area and these include rock falls, translational slides, rotational slides as well as undifferentiated landslides. Some of these landslides include the rock falls evident below the KwaMfazobomvu Hill in the Sinathingi area where a rock talus deposit has accumulated at the toe of the slope (Botha and Botha, 2002). In areas prone to donga erosion, shallow slumps / non–circular rotational slides along the bedrock/colluvium interface result in continual over-steepening of the donga sidewalls and are responsible for donga/gully extension. Translational slides have occurred at the interface between colluvium and dipping shale beds of the Pietermaritzburg Formation. Botha and Botha, (2002) identified a failure around donga a in the KwaMpumuza area where the failure surface was formed from a combination of curved and planar elements. Since the slide movement has partially rotational and translational components and the order of movement can not be determined the slide is classified as undifferentiated. In the Pietermaritzburg area many slopes display hummocky topography and are often latent with thick ancient landslide debris comprising coarse (up to 2 m), generally angular blocks of dolerite and rare sandstone in a variably structured matrix of red soil. These areas of ancient mass movements may become unstable particularly if slope equilibrium is altered because of urban development as displayed by the palaeo–landslide deposits below the Worlds View escarpment.

Maurenbrecher and Booth (1975), with the aid of aerial photographic interpretation, identified six palaeo–landslides across the pediment below the World's View escarpment which they classify as multiple regressive slides or pelitic rock landslide on predetermined surfaces. In the current regional study these landslide deposits below the prominent World's View escarpment have been collated and classified as a large undifferentiated palaeo–landslide since the original morphology of this geomorphic feature has been modified by degradation. Recent, non–circular, rotational slides are commonly associated with these palaeo–landslide hillslopes.

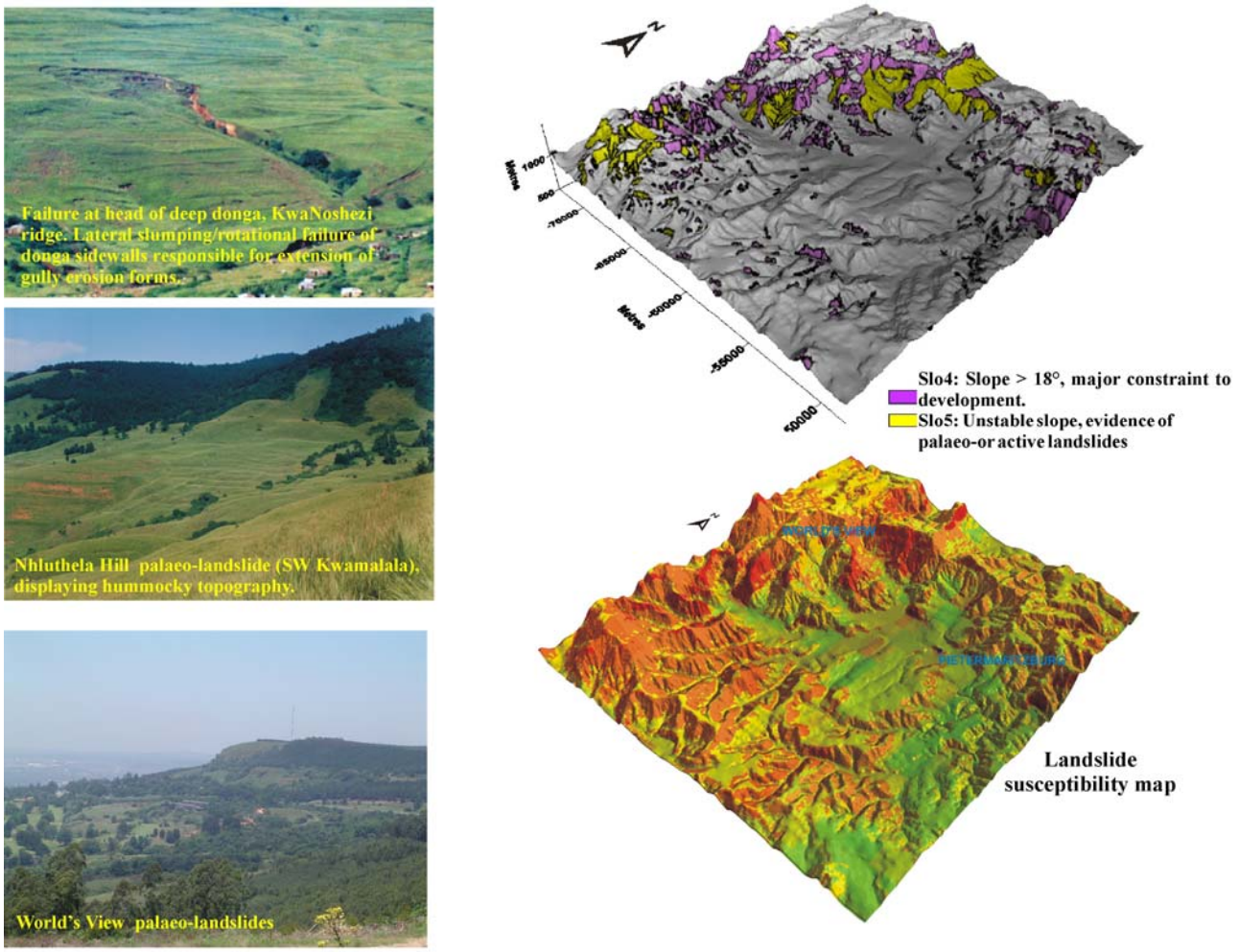


Figure 37 The landslide susceptibility map shows good visual correspondence with the slope instability identified by Richards et al., (2008) during the Pietermaritzburg geotechnical mapping programme.

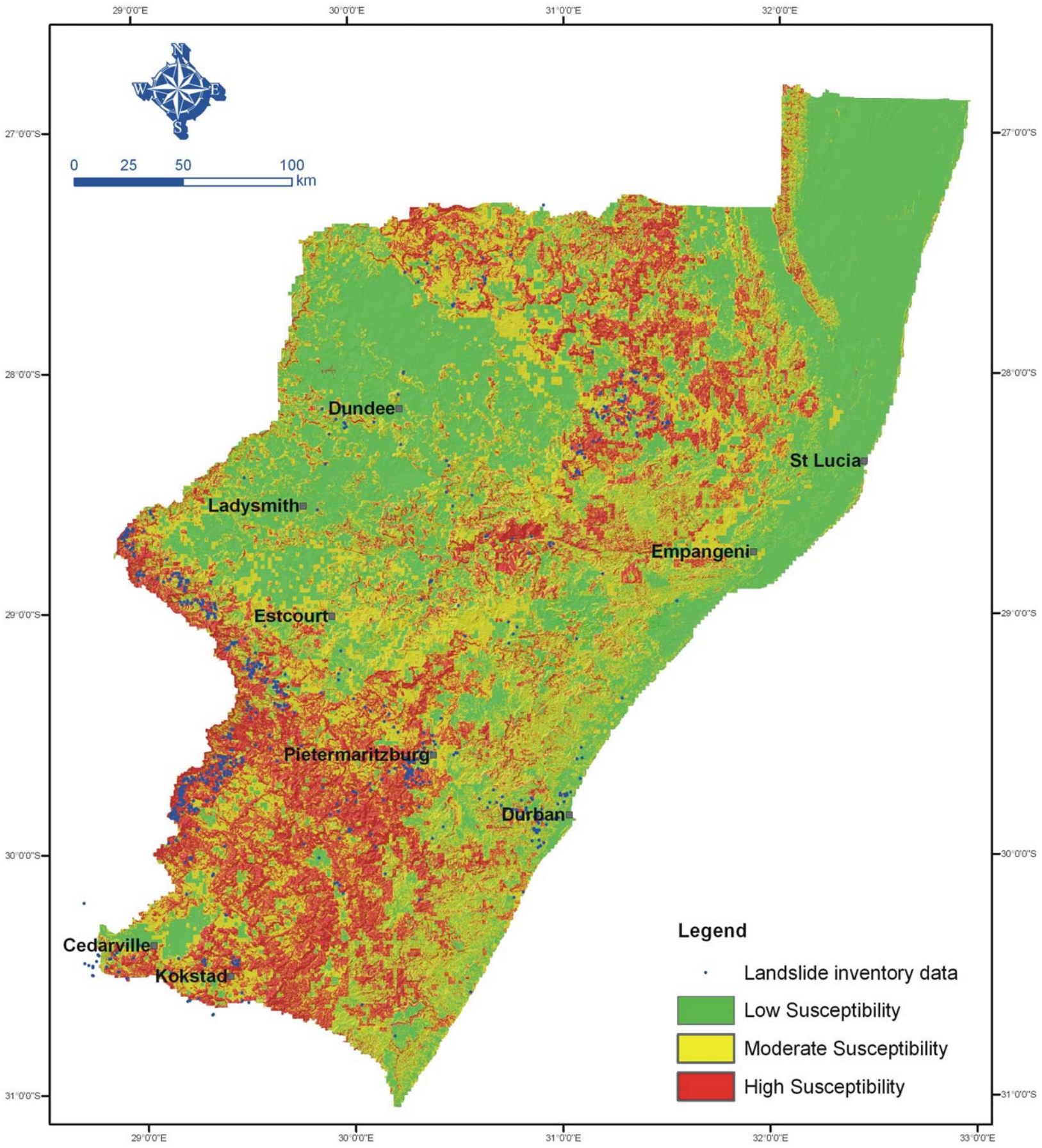
(ii) Slope failures in Durban and surrounding areas

In the Durban area slope failure often results from anthropogenic environmental changes related directly to development and/or prolonged heavy rainfall which increases pore water pressure. Slope failure deposits are widespread and these geomorphic features are associated with all bedrock types. A number of different types of landslides were recognised throughout the Durban area and these include falls, flows, translational slides, rotational slides as well as undifferentiated landslides. Rock falls are evidence of oversteepening where rock talus deposits have accumulated at the toe of some slopes as evident below the Key Ridge Hill in the Peacevale area. Translational slides are often associated with dipping beds of the Pietermaritzburg Formation and Natal Group. The Mayat Place landslide in the Clare Hills area adjacent to the N2 (29° 45' 30" S and 30° 55' 30" E), studied extensively by the firm D.L.Webb and Associates (1975) and summarized by Webb (1983), occurred in an area of Pietermaritzburg Formation bedrock where bedding of the shale bedrock dips concordantly with the hillslope. The Harinagar Drive landslide in the Shallcross area (29° 53' 21" S and 30° 52' 58" E) occurred on eastward dipping bedding planes within the sandstone bedrock of the Natal Group. Translational slides have also occurred at the interface between colluvium and dipping sandstone beds of the Natal Group, as evident by the secondary Hammarsdale landslide (29° 49' 28" S and 30° 38' 23" E). Secondary movement was initiated by the excessive ingress of water and involved the saturated colluvium sliding downslope within the scarp of a pre–historic slide which was primarily triggered by the build up of pore water pressure along the contact between Natal Group sandstones and the overlying dolerite sill. Shallow flows are also associated in areas of "Berea Red Sand", particularly on steep embankments (Fig. 38). Lateral slumping of donga sidewalls often take the form of shallow, non–circular rotational slides with movement along the bedrock/colluvium interface.



Figure 38. Shallow flows associated with the "Berea Red Sand" in the La Lucia area, north of Durban.

The overall quality of the resultant KZN landslide susceptibility map at a regional scale was examined by overlaying regional landslide inventory data (Fig 39). The overlapping of regional landslide occurrences (i.e. both recent and palaeo-landslides) with the susceptibility map yielded a strong correlation (Fig 39). This is probably because the past is the key to the present, and future landslides will most likely occur under similar conditions to those of the past.



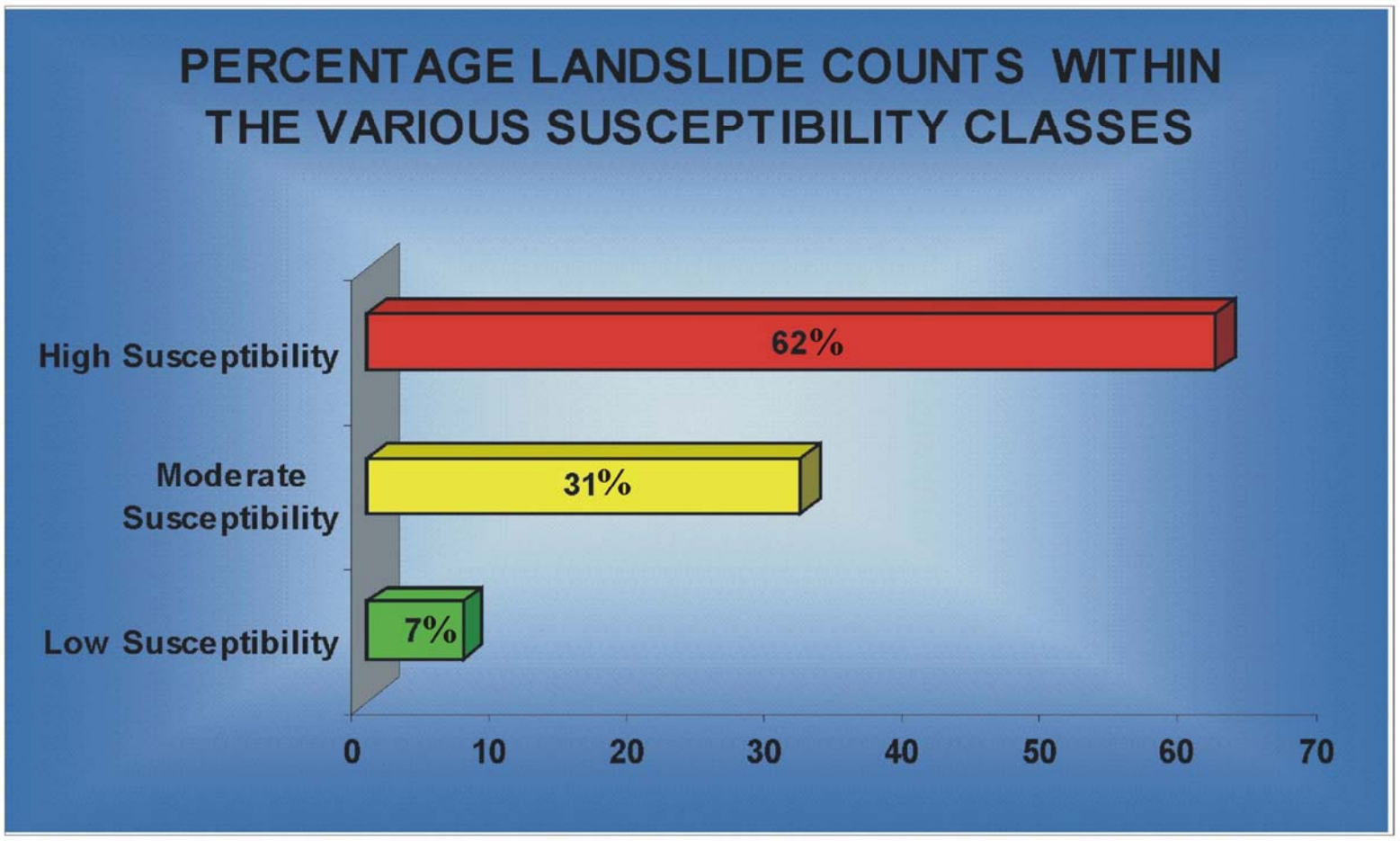


Figure 39. The landslide susceptibility map shows strong correlation with the regional slope instability inventory data.

CHAPTER FIVE

5. DISCUSSION

In KZN the majority of the large landslides are palaeo–landslides that have been subjected to differing periods of weathering and erosion. The landscape of the Ukhahlamba–Drakensberg mountain foothills has been sculpted by an aggressive erosional regime that began after the fragmentation of Gondwana during the late Jurassic. Two epeirogenic uplift events during the Neogene rejuvenated drainage incision and modification of hillslope form (Partridge and Maud, 1988). Widespread hillwash sediments and fine colluvial deposits that mantle many hillslopes in the region preserve a record of periodic gully cut-and-fill events spanning the last glacial cycle (~130 ka) (Botha et al., 1994; Botha, 1996). Mass movement events on upper hillslopes provided much of the unconsolidated material that was weathered, eroded and subsequently transported onto lower slopes as fine colluvial and ephemeral stream sediments during this period forming the Masotcheni Formation deposits. This demonstrates the antiquity of the steep hillslopes and escarpments defining the broad river basins of central and western KZN. During the past ~130,000 years there was little change to hillslope form apart from periodic incision and net aggradation of the veneer of hillslope deposits. The presence of these colluvial mantles in surrounding areas serves as a means of relative-dating of landslide affected slopes. The large palaeo–landslides described in the study are generally well preserved terrain morphological features and represent Holocene landscape features.

Detailed records of palaeoclimate change during the late Pleistocene along the eastern margin of this part of the African subcontinent has been defined from proxy records derived from cave speleothems (Lee–Thorp et al., 2001; Holmgren et al., 2003), meteorite impact crater infill deposits (Partridge et al., 1993) or collated from numerous short–term records (Partridge et al., 1992). It is evident from the less continuous record of palaeosols preserved within the colluvial deposits on hillslopes that long–periods of hillslope stability were interrupted by gully erosion events and colluviation during the period of environmental cooling and desiccation following the Last

Interglacial climatic optimum (Botha, 1996; Botha et al., 1994). It is possible that on some steep hillslopes deep, composite weathering profiles developed within dolerite bedrock were preserved relatively intact during much of this period

The hillslope context of most large landslides reflects the result of differential weathering and erosion during the Pleistocene between the Permo-Triassic sedimentary country rocks and intrusive Jurassic dolerite sills and dykes. The fractured contact zone between dolerite and country rock and the dense pattern of vertical cooling joints within the dolerite represent zones of groundwater migration and preferential weathering. Clay-enriched regolith forms within the negatively weathered fracture zones and clay films line some joint planes. Groundwater saturation after high intensity storm rainfall can lead to a significant increase in pore pressures within the deep weathering profiles associated with these zones. The combined effects of high relief, steep slopes and weathered joint patterns can reduce the rock mass and regolith strength locally resulting in the strong association between landslides and the intersection of the dolerite intrusion contacts by the landsurface.

In most cases the large palaeo-landslides are stable and pose little threat to infrastructure. However, notable exceptions such as the Rickivy slide on World's View escarpment in Pietermaritzburg (Maurenbrecher, 1973; Maud, 1985) show that secondary failures of *in situ* weathered debris in gully eroded landslide runout topography do occur. These are probably related to soil piping caused by the disrupted vadose zone groundwater flow, localized collapse of cavities and sinkhole formation, or creep of the soil mass over groundwater lubricated bedrock unconformity surface. These processes extend the impact of the landslide risk over longer timeframes. Although no detailed investigations have focused on the numerous small landslides that resulted from recent high intensity rainfall events it is vital that these smaller-scale slope failures be recognized as those most likely to create significant damage to infrastructure. Since the triggering mechanism for these landslides is commonly has a result of anthropogenic influences, the smaller-scale, recent slope

failures are most disruptive in urban areas. When evaluating landslide risk the focus must shift to urban areas or close to linear infrastructure where associations with small scale, recent landslides occur most frequently.

CHAPTER SIX

6. CONCLUSION

The various landslide deposits identified across a range of climatic and topographic settings have revealed that the landslide classification system based on international best practice is suitable in the context of KZN, although some modification was necessary. The high number, huge size and wide extent of palaeo-landslide deposits mapped, is a revelation in the context of eastern South Africa, despite some being very large features, have not been recognised or mapped by geologists conducting regional mapping. The regional comprehensive landslide inventory highlights the fact that these Quaternary disequilibrium geomorphic features are more widespread than is commonly appreciated. The widespread hummocky topography in areas of steep slopes and high relief suggests that mass movement derived from slope failure is a significant geomorphic mechanism responsible for hillslope evolution in KZN**.** Majority of the large landslides described are palaeo-landslides that have been subjected to weathering and erosion over periods of up to several thousand years since the displacement occurred.

The series of radiocarbon dated palaeo-landslides across KZN represent the first published attempt to provide a geochronological framework for significant slope instability events in the province. The range of radiocarbon age estimates for landslide events during the middle to late Holocene, a period of rapid climatic fluctuation, suggests that either local site threshold factors or possibly seismic events triggered the large slope failures. The association of some of the largest palaeo-landslides with seismically active zones where numerous seismic events with a magnitude of >4 have been recorded, could provide a link with a high energy triggering mechanism that exacerbated local slope threshold conditions.

The landslide susceptibility modeling resulted in the first provincial scale landslide susceptibility map in South Africa. The KZN landslide susceptibility map does not consider human activity hence the susceptibility to slope instability of those areas considered as moderate susceptibility

zones may be increased by human activity. A good spatial validation of the landslide susceptibility map was possible considering the regional landslide inventory data. The landslide susceptibility map will become a useful town planning tool for future decision making in regional development projects. However, it must be emphasized that the regional KZN landslide susceptibility map is a preliminary indicator of the likelihood of slope instability and is not a design tool that can replace detailed site specific investigations.

The modified landslide classification system and susceptibility modeling technique used was eminently suitable for the KZN Province and was based on international best practice. The application of the methodology used in this research can be used in other areas of South Africa and is equally applicable in the broader African context.

REFERENCES

Anderson, J.M. and Anderson, H.M. (1985). Palaeoflora of Southern Africa. Prodromus of South African Megafloras: Devonian to Lower Cretaceous. A.A Balkema, Rotterdam, 423pp.

Baltzer, A. (1875). Uber einen neurlichen Felssturz am Rossberg, nebst einigen allgemeinen bemberkungen uber derartige Erscheinungen in den Alpen. *Neues Jahrbuch für Mineralogie*, pp. 15-26.

Bell, F.G. and Maud, R.R. (1996a). Landslides associated with the Pietermaritzburg Formation in the Greater Durban area of Natal, South Africa: Some Case Histories. *Environmental and Engineering Geoscience*, vol.II, pp. 557-573

Bell, F.G. and Maud, R.R. (1996b). Examples of landslides associated with the Natal Group and Pietermaritzburg Formation in the Greater Durban area of Natal, South Africa. *Bulletin of the International Association of Engineering Geology*, vol. 53, pp. 11-20.

Bell, F.G. and Maud, R.R. (2000). Landslides associated with the colluvial soils overlying the Natal Group in the greater Durban region of Natal, South Africa. *Environmental Geology*, vol. 39, pp. 1029–1038.

Beckedahl, H.R., Hanvey, P.M and Dardis, G.F. (1988). Geomorphology of the Esikhaleni mass complex, Transkei, South Africa: preliminary observations. In: Dardis, G.F. and Moon, B.P. (Eds): Geomorphological Studies in Southern Africa, Balkema, Rotterdam, pp. 457-471.

Beukes, N.J. (1970) Stratigraphy and sedimentology of the Cave Sandstone Stage, Karoo System, In: 2nd International Gondwana Symposium. Proceedings and papers. Council for Scientific and Industrial Research, Pretoria, pp. 321-342.

Blong, R.J. (1973a). Relationships between morphometric attributes of landslides. *Zeitschrift für Geomorphologie*, Supplement Band, vol. 18, pp. 66-77.

Bijker, H.J. (2001). A hydrological-slope stability model for shallow landslide prediction in the Injisuthi Valley, KwaZulu-Natal Drakensberg. *Unpublished Masters Dissertation*, University of Pretoria, Pretoria.

Blong, R.J (1973b). A numerical classification of selected landslides of the debris slide-avalanche-flow type. *Engineering Geology* , vol. 7, pp. 99-114.

Boelhouwers, J.C. (1988a). Geomorphological mapping of a part of the Gaint's Castle Game Reserve, Natal Drakensberg, Unpublished Masters Thesis, University of Natal, Pietermaritzburg.

Boelhouwers, J.C. (1988b). An interpretation of valley asymmetry in the Natal Drakensberg, South Africa. *South African Journal of Science*, vol. 84, pp. 913 - 916.

Botha, G.A. (1996). Cyclical colluvial accretion on bedrock pediments in northern Natal, South Africa. *Zeitschrift fur Geomorphologie*, Supplement Band, vol. 103, pp. 85-102.

Botha, G.A., Wintle, A.G. and Vogel, J.C. (1994). Episodic Late Quaternary palaeogully erosion in northern KwaZulu-Natal, South Africa. *Catena*, vol. 23, pp. 327-340.

Botha, R.C.N. and Botha, G.A. (2002). *Geology of the Pietermaritzburg area.* Explanation, Sheet 2930 CB Pietermaritzburg, Scale 1:50 000. Council for Geoscience, South Africa.

Brabb, E.E., Pampeyan. E.H., and Bonilla, M.G. (1972). Landslide susceptibility in San Mateo County, California: U.S. Geological Survey Miscellaneous Field Studies Map MF-360, scale 1:62,500.

Bray, J.D., Sancio, R.B., Kammerer, A.M., Merry, S., Rodriguez-Marek, A., Khazai, B., Chang, S., Bastani, A., Collins, B., Hausler, E., Dreger, D., Perkins, W.J., and Nykamp, M. {2001). In: Highland, L.M 2003. An Account of Preliminary Landslide Damage and Losses Resulting from the February 28, 2001, Nisqually, Washington, Earthquake.
Online at http://pubs.usgs.gov/of/2003/ofr-03-211/NisquallyFinal.html. *Accessed on*: May 2008.

Brown, R.W., Rust, D.J., Summerfield M.A., Gleadow, A.J.W. and. De Wit, M.C.J. (1990). An Early Cretaceous phase of accelerated erosion on the southwestern margin of Africa: Evidence from apatite fission track analysis and the offshore sedimentary record. *Nuclear Tracks and Radiation Measurements*, vol. 17, pp. 339–351.

Brown, R.W., Gallagher, K., Gleadow, A.J.W., Summerfield, M.A. (2000). Morphotectonic evolution of the South Atlantic margins of Africa and South America. In: M.A. Summerfield (ed), Geomormorphology and Global Tectonics. John Wiley & Sons, Chichester, pp. 255-281.

Brunsden, D. (1979). Mass movements. In: *Progress in Geomorphology*. (C.E. Embleton and J. B. Thornes, Eds), Arnold, pp. 130-186.

Burke, K. (1996). The African Plate. *South African Journal of Geology*, vol 99, pp. 341-409.

Cairncross, B., Beukes, N.J., Muntingh, D.J., Rehfeld, U. (1998). Late. Permian deltaic successions from the Karoo Supergroup, South Africa: Fresh water or marine deposits? *Abstract***:** 15th International Sedimentological Congress.**,** *International Association of Sedimentologists,* p. 224.

Campbell, R.H. and Bernknopf, R.L. (1993). Time-dependent landslide probability mapping: American Society of Civil Engineers, Proceedings of the 1993 Conference, Hydraulic Engineering '93; July, 1993, San Francisco, pp. 1902-1907.

Carrara, A. (1983). Multivariate models for landslide hazard evaluation. *Mathematical Geology*, vol. 15, no.3, pp. 403-426.

Casagli, N., Catani, F., Puglisi, C., Delmonaco, G., Ermini L., and Margottini, C. (2004). An Inventory–Based Approach to Landslide Susceptibility Assessment and its Application to the Virginio River Basin, Italy. *Environmental and Engineering Geoscience*, vol. 10, no.3, pp. 203–216.

Coates, D.R. (1977). Landslide perspectives. In: Landslides (D. R. Coates, Ed.) *Geological Society of America*, pp. 3-28.

Crozier, M.J. (1973). Techniques for the morphometric analysis of landslips. *Zeitschrift für Geomorphologie. Dynamique*, vol 17, pp. 78-101.

Cruden, D.M. (1991). A Simple Definition of a Landslide. *Bulletin of the International Association of Engineering Geology*, vol 43, pp. 27–29.

Cruden, D.M. (2003). The First Classification of Landslides? *Environmental & Engineering Geosciences*, vol. IX, pp. 197-200.

Cruden, D.M. and Varnes, D.J. (1996). Landslide types and Processes. In Landslides investigation and Mitigation. *Transportation Research Board*, US National Research Council, Turner, A.K. And Schuster, R.L. (Eds). *Special Report,* vol. 247, pp. 36-75.

Dana, J.D. (1862). Manual of geology; treating of the principles of the science with special reference to American Geological History for the use of Colleges, Academies, and Schools of Science. Philadelphia, T. Bliss. p. 798.

Department of Environmental Affairs and Tourism. (2000). The Environmental Potential Atlas for KwaZulu-Natal:Mean Annual Precipitation.
Online at http://www.environment.gov.za/Enviro-Info/prov/kn/knrain.jpg. *Accessed on*: September 2006.

de Wit, M.J., Jeffery, M., Bergh, H., Nicolaysen, L. (1988). Geological Map of Sectors of Gondwana Reconstructed to their Dispositions at 150 Ma, Scale 1:10 000 000. *American Association of Petroleum Geology*, Tulsa, Oklahoma, USA.

Dikau, R. and Jäger, S. (1994). Landslide hazard modelling in Germany and New Mexico. In McGregor, D. and Thompson, D., ed., Geomorphology and Land Management in a Changing Environment. Wiley. Chichester, pp. 53-67.

Dixey, F. (1938). Some observations on the physiographic development of central and southern Africa. *Transactions of the Geological Society of South Africa,* vol. 41, pp. 113-171.

Dixey, F. (1942). Erosion cycles in central and southern Africa. *Transactions of the Geological Society of South Africa,* vol. 45, pp. 151-181.

Dixey, F. (1945). A contribution to the geomorphology of the Natal Drakensberg. *Transactions of the Geological Society of South Africa,* vol. 48, pp. 125-133.

Doucoure, M. and de Wit, M.J. (2003). Old inherited origin for the present near-bimodal topography of Africa. *Journal of African Earth Sciences*, vol. 36, pp. 371-388.

Ercanoglu, M. and Gokceoglu, C. (2004). Use of fuzzy relations to produce landslide susceptibility map of a landslide prone area (West Black Sea Region, Turkey), *Engineering Geology*, vol. 75, pp. 229-250.

Eriksson, P.G. (1981). A palaeoenvironmental analysis of the Clarens Formation in. the Natal Drakensberg. *Transactions of the Geological Society of South Africa,* vol. 84, pp. 7–17.

Ermini, L., Catani, F., and Casagli, N. (2005). Artificial Neural Networks applied to landslide susceptibility assessment. *Geomorphology*, vol. 66, pp. 327–343.

Erskine, C.F. (1973). Landslides in the vicinity of the Fort Randall reservoir, S.
Dakota. *U. S. Geoogical. Survey Professional Paper*, vol. 675, p. 64.

Fleming, A., Summerfield, M.A., Stone, J.O., Fifield, L.K., Cresswell, R.G. (1999). Denudation rates for the southern Drakensberg escarpment, SE Africa, derived from in-situ-produced cosmogenic ^{36}Cl: initial results. *Journal of the Geological Society*, London, vol. 56, pp. 209-212

Garland, G. and Olivier, M.J. (1993). Predicting landslides from rainfall in a humid, sub-tropical region, *Geomorphology*, vol. 8, pp. 165-173.

Gold, D.J.C. (1996). The Pongola Supergroup. *In*: Johnson, M.R., Anhaeusser, C.R. and Thomas, R.J. (Eds.), *The Geology of South Africa.* The Geological Society of South Africa, Johannesburg/Council for Geoscience, Pretoria, pp. 135-147.

Hansen, M.J. (1984). Strategies for classification of landslides. In: D. Brunsden & D.B. Prior (Eds), *Slope Instability*. J.Wiley & Sons, pp. 1-25.

Hartnady, C.J. (1990). Seismicity and plate boundary evolution in southeastern Africa. *South African Journal of Geology*, vol. 93, pp. 473-484.

Heim, A. (1882). Ueber Bergsturze. *Neujahrsblatt der Zürcherischen Naturforschenden Gesellschaft*, Blatt 84, p. 31.

Holmgren, K., Lee-Thorp, J.A., Cooper, G.R.J., Lundblad, K., Partridge, T.C., Scott, L., Sithaldeen, R., Talma, S. and Tyson, P. (2003). Persistent millenial-scale climatic variability over the past 25,000 years in Southern Africa. *Quaternary Science Reviews*, vol. 22, pp. 2311-2326.

Howe, E. (1909). Landslides in the San Juan Mts, Colorado: including a consideration of their causes and classification. *U.S. Geological. Survey Professional Paper*, vol. 67, p. 58.

Hunter, I. (2007). Extensive flooding and damage to coastal infrastructure along the KwaZulu-Natal coast.
Online at : http://ports.co.za/shippingworld/article_2007_03_21_3337.html. Accessed on: June 2008.

Hutchinson, J.N. (1968). Mass movement. In: *Encyclopaedia of Earth Sciences*, (R.W. Fairbridge, Ed.) Reinhold, New York, pp. 688-695.

International Federation of the Red Cross and Red Crescent Societies, (2007). Philppines: Landslides and Floods. Appeal No. MDRPH001.
Online at http://www.ifrc.org/cgi/pdf_appeals.pl?06/MDRPH00107.pdf. Accessed on: June 2008.

Janisch, E.P. (1931). Notes on the central part of the Zoutspanberge Range and on the origin of Lake Funduzi, *Transactions of the Geological Society of South Africa*, vol. 34, pp. 151–162.

Johnson, M.R., Van Vuuren, C.J., Visser, J.N.J., Cole, D.I., De V. Wickens, H., Christie, A.D.M., Roberts, D.L. and Brandl, G. (2006). Sedimentary rocks of the Karoo Supergroup. *In*: Johnson, M.R., Anhaeusser, C.R. and Thomas, R.J. (Eds.), *The Geology of South Africa.* The Geological Society of South Africa, Johannesburg/Council for Geoscience, Pretoria, pp. 461-499.

Kijko, A., Graham, G., Bejaichund, M., Roblin, D and Brandt, M.D.C. (2003). Probabilistic seismic hazard maps for South Africa. Council for Geoscience, (Unpublished).

King, L.C. (1941). The monoclinal coast of Natal, South Africa. *Journal of Geomorphology*, vol. 3, pp. 144-153.

King, L.C. (1944). Geomorphology of the Natal Drakensberg. *Transactions of the Geological Society of South Africa*, vol. 47, pp. 255-282.

King, L.C. and King, L.A. (1959), A reappraisal of the Natal monocline, *South African Geographical Journal*, vol. 41, pp. 15–30.

King, L.C. (1972). The Natal monocline, explaining the origin and scenery of Natal, South Africa. Geology Department, University of Natal, Durban, 113 pp.

King, L. C. (1982). The Natal Monocline (2nd ed.). University of Natal Press, Pietermaritzburg, 134pp.

Krige L.J. and Venter (1933). The Zululand earthquake of the 31st December, 1932. *Transactions of the Geological Society of South Africa*, vol. 33, pp. 101-112.

Kruger, G.P. (1983). Terrain morphological map of Southern Africa 1: 2 500 000. Department of Agriculture, Pretoria.

Ladd, G.E. (1935). Landslides, subsidences and rockfalls. *Bulletin of the American Railway Engineering Association,* vol. 37, pp. 1091-1162.

Lang, A., Moya, J., Corominas, J., Schrott, L. and Dikau, R. (1999). Classic and new dating methods for assessing the temporal occurrence of mass movements. *Geomorphology*, vol. 30, no.1-2, pp. 33-52.

Lee-Thorp, J.A., Holmgren, K., Lauritzen, S.E., Linge, H., Momberg, A., Partridge, T.C., Stevenson, C., and Tyson, P.D. (2001). Rapid climate shifts in the southern African interior throughout the mid to late Holocene. *Geophysical Research Letters*, 28/23, pp. 4507-4510.

Marshall, C.G.A. (1994). The stratigraphy of the Natal Group. Unpublished Masters Thesis, University of Natal, Pietermaritzburg, 291pp.

Marshall, C.G.A. and Von Bronn, V. (1999). The stratigraphy and orgin of the Natal Group. *South African Journal of Geology*, vol. 102, pp. 15 - 25.

Marshall, C.G.A. (2003a). Lithostratigraphy of the Durban Formation (Natal Group), including the Ulundi, Eshowe, Melmoth, Kranskloof, Situndu and Dassenhoek Members. Lithostratigraphic Series, South African Committee for Stratigraphy., vol. 36, 28pp.

Marshall, C.G.A. (2003b). Lithostratigraphy of the Mariannhill Formation (Natal Group), including the Tulini, Newspaper and Westville Members. Lithostratigraphic Series, South African Committee for Stratigraphy., vol. 37, 17pp.

Maud, R.R. (1985). Instability of road embankment on N3 freeway, Rickivy, Pietermaritzburg. In: Brink, A.B.A. (Ed), *Engineering Geology of Southern Africa*, vol. 4, Post-Gondwana deposits, pp. 165-166.

Maurenbrecher, P.M. (1973). Instability of a road embankment at Rickivy, Pietermaritzburg. *The Civil Engineer in South Africa*, pp. 218-224.

Maurenbrecher, P.M. and Booth, A.R. (1975). Some slope stability problems in soils derived from the Ecca Shales of Natal, South Africa. *Engineering Geology*, vol. 9, pp. 99–121.

McCalpin, J. (1989). Prehistoric earthquake-induced landslides along the Awatere Fault, South Island, New Zealand; *Association of Engineering Geologists* 32nd Annual Meeting, Abstracts and Program, Vail, CO, p. 94.

Moreiras, S.M. (2005). Landslide susceptibility zonation in Rio Mendoza Valley, Argentina; *Geomorphology*, vol. 66, pp. 345-357.

Olivier, M., Garland, G., Jermy, C. and Sumner, P.D. (1993). Rainfall-landslide relationships in Durban-A preliminary assessment, *Geookodynamik,* vol. 14, no.1-2, pp. 85-93.

Paige-Green, P. (1985). The development of a regional landslide susceptibility map of southern Africa. *Proceedings Annual Transportation Convention*, FB, Paper FB4. Pretoria.

Paige-Green, P. (1989). Landslides: extent and economic significance in southern Africa. In: Brabb, E.E. & B.L. Harrod (Eds.): *Landslides: Extent and Economic Significance*: Balkema, Rotterdam, pp. 261-269.

Paige-Green, P. and Croukamp, L. 2004. A revised landslide susceptibility map of southern Africa. Geoscience Africa 2004, University of the Witwatersrand, Johannesburg, 12–16 July 2004.

Partridge, T.C., Avery, D.M., Botha, G.A., Brink, J.S., Deacon, J., Herbert, R.S., Maud, R.R., Scholtz, A., Scott, L., Talma, A.S. and Vogel, J.C. (1992). Late Pleistocene and Holocene climatic change in Southern Africa. *South African Journal of Science*, vol. 86, pp. 302–306.

Partridge, T. C., Kerr, S.J., Metcalfe, S.E., Scott, L., Talma, A.S and Volgen, J.C. (1993). The Pretoria Saltpan: a 200,000 year Southern African lacustrine sequence. *Palaeogeography, Palaeoclimatology, Palaeoecology,* vol. 101, pp. 317–337.

Partridge, T. C. and Maud, R.R. (1987). Geomorphic evolution of southern Africa since the Mesozoic. *South African Journal of Geology*, vol. 90, pp. 179 - 208.

Partridge, T.C., Maud, R.R. (1988). The geomorphic evolution of Southern Africa: A comparative review. *Geomorphological Studies in Southern Africa*, pp. 5-15.

Partridge, T.C and Maud, R.R. (2000). Macro-scale geomorphic evolution of southern Africa, In: The Cenozoic of Southern Africa (Partridge, T.C. and Maud, R.R., editors), Oxford University Press, New York, pp. 3–18.

Penck, A. (1908). Der Drakensberg und der Quatlambabruch. *Z. d. K. Preussische Akademie der Wissenschaften*, vol. 11, pp. 15-30.

Petley, D. and Rosser, N. (2007). The impact of landslides – 2007:Poster.
Online at http://www.dur.ac.uk/resources/TheImpactofLandslides-2007poster.pdf. Accessed on: June 2008.

Popov, I. V. (1946). A scheme for the natural classification of landslides. Doklady *USSR Academy of Sciences*, vol. 54, pp. 157-59.

Randall W.J. (2005), Landslide Hazards at La Conchita, California, USGS Open-
File Report 2005-1067.
Online at http://pubs.usgs.gov/of/2005/1067/. Accessed on: June 2008.

Reiche, P. (1937). The Toreva Block; a distinctive landscape type. *Journal of Geol*ogy, vol. 45, pp. 538-548.

Reynolds, S.H. (1932). Landslips. *Proceedings of the Bristol Naturalists' Society*, vol. 7, pp. 352-357.

Richards, N.P. (2008). Explanation of the engineering geological and geotechnical conditions for the 1:50 000 scale map sheet 2930 DD & 2931 CC Durban. Council for Geoscience.

Robert, M.I., Glen, S.M., Kathleen, M.H. (2000). Integrating the Analytical Hierarchy Process with GIS to capture expert knowledge for Land Capability Assessment. *4th International Conference on Integrating GIS and Environmental Modeling (GIS/EM4)*: Problems, Prospects and Research Needs.Banff, Alberta, Canada, September 2 – 8.

Saaty, T.L. (1980). The Analytical Hierarchy Process, *McGraw–Hill, New York*.

Saaty, T. L. (1986). Axiomatic foundation of the analytic hierarchy process. *Management Sciences*, vol. 32, pp. 841-855.

Saaty, T.L. (1995). Decision Making for Leaders: The Analytical Hierachy Process for Decisions in a Complex world. *RWS Publications, Pittsburgh*

Savarenskii, P.F. (1937). *Inzhenernaya geologiya*, Moskva.

Schaub, T. (2004). Downloaded Arcscript: FeatureDensity.zip, Avenue, ArcView GIS.
Online at http://arcscript.esri.com/details.asp?dbid=12441. Accessed on: September 2006.

Schulze, B.R. (1972). South Africa. In: Climates of Africa, Griffiths, J.F. (ed.), Elsevier, Amsterdam, pp. 501-586.

Schuster, R.L.. (1996). Socioeconomic significance of landslides. In Landslides investigation and Mitigation. *Transportation Research Board*, US National Research Council, Turner, A.K. And Schuster, R.L. (Eds). *Special Report,* vol. 247, pp. 13-35.

Sharpe, C.F.S. (1938). Landslides and Related Phenomena. *Columbia University Press, New York*, 137.

Singh R.G, Botha G.A, and McCarthy T. (2007). Landslide susceptibility mapping in eastern South Africa. XVII congress of the International Union for Quaternary Research, (Abstract) Quarternary International Volume 167-168, Cairns Convention Centre, Queensland, Australia, 28 July to 3 August 2007. pp. 387-388.

Singh R.G, Botha G.A, McCarthy T and Richards, N.P. (2008). Holocene landslides in KwaZulu-Natal , South Africa. South African Journal of Geology, pp. 39-52.

Skempton, A.W. and Hutchinson J.N. (1969). Stability of natural slopes and embankment foundations. In *Proceedings of the 7th International Conference on Soil Mechanics and Foundation Engineering*, Mexico City, State of the Art Volume, pp. 291-340.

Smith, N.J.P. (1977). The Phanerozoic rocks of Sheets 2830DA, DC & DD. Geological Survey, (Unpublished).

Smith, R.M.H. (1990). A review of stratigraphy and sedimentary environments of the Karoo Basin of South Africa. *Journal of African Earth Science*, vol. 10, pp. 117–137.

Smith, R.M.H., Erikkson, P.G. anf Botha, W.J. (1993). A review of stratigraphy and sedimentary environments of the Karoo-aged basins of southern Africa. *Journal of African Earth Science*, vol. 16, pp. 143–169.

Soeters, R and van Western, C.J. (1996). Slope instability recognition, analysis, and zonation. In Landslides investigation and Mitigation. *Transportation Research Board*, US National Research Council, Turner, A.K. And Schuster, R.L. (Eds). *Special Report,* 247, pp. 129-177.

South African Weather Service (2007).
Online at http://www.weathersa.co.za/. *Accessed on*: November 2007.

Stout, M.L. (1969) Radiocarbon Dating Of Landslides In Southern California And Engineering Geology Implications. In United States Contributions to Quaternary Research (S.A. Schumm and W.C. Bradley, Eds). *Geological Society of America*, Special Paper, 123, pp. 167-179.

Stout, M.L. (1977). Radiocarbon dating of landslides in southern California: *California Geology*, vol. 30, pp. 99-105.

Suess. E. (1904). The face of the Earth. Clarendon Press, Oxford, 1, 604pp.

Sumner, P.D. (1993). A landslide complex near Sani Pass, Natal Drakensberg, South Africa, *Geookodynamik*, vol. 14, no.1-2, pp. 93-103.

Sumner P.D. (1997). Case studies in the Gaint's Castle Game Reserve, *SoSAG/SAAG/SAPG* field guide for the international conference on environment and development in Africa: an Agenda and solutions for the 21st century, 4–6July.

Sumner, P.D and Meiklejohn, K.I. (2000): Landscape evolution in a changing environment, In Fox, R and Rowntree, K (eds.), The Geography of South Africa in a changing world, *Oxford University Press, Cape Town*.

Talma, A.S. and Vogel, J.C. (1993). A simplified approach to calibrating 14C dates. *Radiocarbon*, vol. 35, pp. 317-322.

Tankard A.J., Jackson M.P.A., Eriksson K.A., Hobday D.K., Hunter D.R. and Minter W.E.L. (1982), Crustal Evolution of Southern Africa: 3.8 billion years of earth history, *Springer–Verlag, New York.*

Taverner-Smith, R., Cooper, J.A.J. and Rayner, R.J. (1988). The depostional environment in the Volksrust Formation (Permian) in the Mhlatuze River, Zululand, *South African Journal of Geology*, vol. 91, pp. 198 - 206.

Tennant, W.J. and van Heerdan, J. (!994). The influence of orography and local sea-surface temperature anomalies on the development of the 1987 Natal floods: a general circulation model study. *South African Journal of Science*, vol. 90, pp. 45-49.

Terzaghi, K. (1950). Mechanisms of landslides. *Geological Society of America,* Berkey Volume, pp. 83-123.

Thomas, R.J. (1989). A tale to two tectonic terranes. *South African Journal of Geology*, vol. 91, pp. 275 - 291

Thomas, R.J. (1985). Report on the geology of areas 2828 DB (Witsieshoek) and 2828 DD (Mont-Aux-Sources) an addendum to the report on the geology of areas 2829 CB, CC and CD. Geological Survey, (Unpublished).

Thomas, M.A. & van Schalkwyk, A. (1993). Geological hazards associated with intense rain and flooding in Natal. *Journal of African Earth Science*, vol. 16, pp. 193–204.

Tyson, P.D. (1969Atmospheric circulation and precipitation over South Africa, Department of Geography and Environmental Studies, *Occasional Report*, 2, University of Witwatersrand, Johannesburg, 22pp.

Tyson, P.D. (1986). Climatic change and variability in southern Africa, Cape Town: *Oxford University Press.*

United States Search and Rescue Task Force, (2000).
Online at http://www.ussartf.org/landslides.htm. *Accessed on*: June 2008.

van Schalkwyk, A and Thomas, M.A. (1991). Slope failures associated with the floods of September 1987 and February 1988 in Natal and Kwa-Zulu, Republic of South Africa. *Geotechnics in the African Environment*, Blight et al. (Eds), pp. 57-63.

Varnes, D.J. (1958). Landslides types and processes. In: Landslides and Engineering Practice (E.B. Eckel, Ed.), *Highway Research.Board, Special Report*, 29, pp. 20-47

Varnes, D.J. (1978). Chapter 2, Slope movement types and processes. In: R.L. Schuster & R.J. Krizek (Eds), Landslides, analysis and control. National Research Council, *Transport Research Board, Special Report*, 176, pp. 11-33.

Visser, J.N.J. (1990). The age of the late Palaeozoic glacigene deposits in Southern Africa. *South African Journal of Geology*, vol. 93, pp. 366 - 375.

Visser, J.N.J. and Botha, B.J.V. (1980). Meander channel, point bar, crevasse splay and aeolian deposits from the Elliot Formation in Barkley Pass, northeastern Cape. *Transactions of the Geological Society of South Africa*, vol. 83, pp. 55–62.

von Veh, M.W. (1995). A structural geological analysis of satellite lineaments and fault and dyke traces in the KwaZulu-Natal province, Report: Department of Water Affairs and Forestry, University of Natal. pp. 1-56.

Ward, W.H. (1945). The stability of natural slopes. *Geographical Journal*, vol. 105, pp. 170-197.

Webb, D.L. (1983). Slope failure on shale of the Pietermaritzburg Shale Formation, Mayat Place, Durban. In: Brink, A.B.A. 1983 *Engineering geology of Southern Africa: Volume 3. The Karoo Sequence.* Building Publications, Pretoria, pp. 107–111.

Webb, D.L. & Associates (1975). Report to the City Engineer, The stability of Mayat Place. Report Ref. 3092.

Weerakoon, K.G.P.K (2002). Integration of GIS based suitability analysis and multi criteria evaluation for urban land use planning; contribution from the analytic hierarchy process. In: Proceedings of the Third Asian Conference on Remote Sensing. Asian Association on Remote Sensing, Nepal.
Online at http://www.gisdevelopment.net/aars/acrs/2002/urb/. Accessed on: December 2007.

Weinert, H.H. (1980). The natural road construction material of southern Africa. Academia, Cape Town.

Whitmore, G., Uken, R., Meth, D. et al., (1999). KwaZulu-Natal: 3500 million years of Geological History, University of Natal.

Wilson, M.G.C. (1992). A Brief report on the landslide, near Nhlwati, in the Molletshe tribal authority area, KwaZulu. STK Mineral Development Division. Report Ref. 3086.

WP/WLI (International Geotechnical Societies' UNESCO Working Party on World Landslide Inventory). (1990). A suggested method for describing the activity of a landslide. *Bulletin International Association of Engineering Geology*, vol. 47, pp. 53–57.

WP/WLI (International Geotechnical Societies' UNESCO Working Party on World Landslide Inventory), (1991). A suggested method for a landslide summary. *Bulletin International Association for Engineering Geology*, vol. 43, pp. 101-110.

WP/WLI (International Geotechnical Societies' UNESCO Working Party on World Landslide Inventory), (1993a). A suggested method for describing the activity of a landslide. *Bulletin International Association for Engineering Geology*, vol. 47, pp. 53-57.

WP/WLI (International Geotechnical Societies' UNESCO Working Party on World Landslide Inventory), (1993b}. Multilingual Landslide Glossary. BiTech Publishers Ltd, Richmond, British Columbia, Canada, 59pp.

Zaruba, Q. and Mencl, V. (1969). Landslides and their Control. Academia & Elsevier, Prague, 205 pp.

Zaruba, Q. and Mencl, V. (1982). Landslides and Their Control, 2nd ed. Elsevier, Amsterdam, Netherlands, 324 pp.

APPENDIX 1: LANDSLIDE INVENTORY

LANDSLIDE ID	LANDSLIDE NAME	LONGITUDE	LATITUDE	MAP SHEET	PREDOMINANT MATERIAL	TYPE OF MOVEMENT	AGE DESCRIPTION	AREA (m^2)
Abel1	Ethekweni_53	30.87972	-29.98972	2930DD & 2931CC	Debris	Translational	Recent-landslide	500.00000000
Abel2	Ethekweni_51	30.89111	-29.98278	2930DD & 2931CC	Debris	Rotational	Recent-landslide	500.00000000
Abel3	Ethekweni_50	30.88556	-29.95917	2930DD & 2931CC	Debris	Translational	Recent-landslide	500.00000000
BM01	Hammarsdale	30.63958	-29.82432	2930DC	Debris	Translational	Recent-landslide	400000.00000000
CW98	Ethekweni_46	31.08577	-29.57595	2931CA	Debris	Undifferentiated	Recent-landslide	500.00000000
CW99	Ethekweni_2	31.06582	-29.62346	2931CA	Debris	Undifferentiated	Recent-landslide	500.00000000
DBN1	Ethekweni_5	30.89144	-29.98246	2930DD & 2931CC	Earth	Rotational	Recent-landslide	50000.00000000
DBN2	Ethekweni_4	30.88571	-29.95941	2930DD & 2931CC	Earth	Translational	Recent-landslide	500.00000000
DBN3	Ethekweni_3	30.88130	-29.98790	2930DD & 2931CC	Rock	Translational	Recent-landslide	50000.00000000
DBN4	Ethekweni_68	30.89650	-29.83130	2930DD & 2931CC	Debris	Flow	Recent-landslide	5.00000000
DBN5	Ethekweni_36	30.80050	-29.79320	2930DD & 2931CC	Debris	Flow	Recent-landslide	5.00000000
DBN6	Ethekweni_Harinagar	30.88274	-29.88901	2930DD & 2931CC	Rock	Translational	Recent-landslide	5.00000000
KZN 0001	Buildfontein	29.42060	-30.43678	3029AD	Debris	Undifferentiated	Palaeo-landslide	1584590.38700000
KZN 0002	Mount Currie	29.43192	-30.46783	3029AD	Debris	Undifferentiated	Palaeo-landslide	1822210.77600000
KZN 0003	Highwater	28.90750	-30.51620	3028DB	Debris	Undifferentiated	Palaeo-landslide	368162.13500000
KZN 0004	Strydberg	29.12002	-30.49739	3029AC/3029CA	Debris	Undifferentiated	Palaeo-landslide	627801.93900000
KZN 0005	Pufadders Hoek 1	29.20798	-30.61536	3029CA	Debris	Undifferentiated	Palaeo-landslide	494010.40000000
KZN 0006	Pufadders Hoek 2	29.19863	-30.61804	3029CA		Undifferentiated	Landslide	187740.24700000
KZN 0007	Mooimeisiesfontein 1	29.43943	-30.46338	3029AD	Rock	Fall	Recent-landslide	3136.51600000
KZN 0008	Mooimeisiesfontein 2	29.44133	-30.46943	3029AD	Debris	Flow	Palaeo-landslide	90305.39100000
KZN 0009	Melkfontein	29.07189	-30.49761	3029AC		Undifferentiated	Landslide	52494.14400000
KZN 0010	The Poplars	29.44558	-30.44910	3029AD	Debris	Flow	Palaeo-landslide	501115.57400000
KZN 0011	Weltevrede	29.28424	-30.46560	3029AD		Undifferentiated	Landslide	63991.62600000
KZN 0012	Rooi Poort 1	29.28249	-30.44232	3029AD		Undifferentiated	Landslide	45524.61600000
KZN 0013	Rooi Poort 2	29.28063	-30.44433	3029AD		Undifferentiated	Landslide	9501.50100000
KZN 0014	Rooi Poort 3	29.28111	-30.44626	3029AD		Undifferentiated	Landslide	22216.65500000
KZN 0015	Rooi Poort 4	29.28200	-30.45227	3029AD		Undifferentiated	Landslide	31728.94700000
KZN 0016	Tiger Hoek	29.27105	-30.45122	3029AD		Undifferentiated	Landslide	34937.03000000
KZN 0017	Mooi Fontein 1	29.38912	-30.26178	3029AD		Undifferentiated	Landslide	20620.67700000
KZN 0018	Mooi Fontein 2	29.38628	-30.26069	3029AD		Undifferentiated	Landslide	16285.34100000
KZN 0019	Mooimeisiesfontein 3	29.43087	-30.45095	3029AD		Undifferentiated	Landslide	31909.66200000
KZN 0020	Location_8 Lupindo 1	28.72661	-30.45934	3028BC		Undifferentiated	Landslide	27516.89300000
KZN 0021	Location_8 Lupindo 2	28.70736	-30.45220	3028BC		Undifferentiated	Landslide	115724.42700000
KZN 0022	Location_8 Lupindo 3	28.74519	-30.46952	3028BC		Undifferentiated	Landslide	36818.88500000
KZN 0023	Location_8 Lupindo 4	28.74527	-30.46640	3028BC		Undifferentiated	Landslide	176945.49400000
KZN 0024	Location_8 Lupindo 5	28.74647	-30.46350	3028BC		Undifferentiated	Landslide	52753.21200000
KZN 0025	Pakkies	29.25063	-30.60664	3029CA/CB		Undifferentiated	Landslide	25340.15700000
KZN 0026	Usherwood West	29.45988	-30.62003	3029CA		Undifferentiated	Landslide	34362.29700000
KZN 0027	Location_9 Brooksnek	29.49028	-30.62673	3029CA		Undifferentiated	Landslide	141771.98300000
KZN 0028	Location_20 Nkanji 1	29.31693	-30.67743	3029CA		Undifferentiated	Landslide	27189.39000000
KZN 0029	Location_20 Nkanji 2	29.32003	-30.67345	3029CA		Undifferentiated	Landslide	24534.97900000
KZN 0030	Kenilworth	28.85141	-30.41911	3028BD		Undifferentiated	Landslide	226711.34800000
KZN 0031	Location_6 Mgubo 1	28.77745	-30.42077	3028BD		Undifferentiated	Landslide	34097.48900000
KZN 0032	Location_6 Mgubo 2	28.77250	-30.41595	3028BD		Undifferentiated	Landslide	40530.45500000
KZN 0033	Location_6 Mgubo 3	28.77175	-30.41802	3028BD		Undifferentiated	Landslide	70095.17400000
KZN 0034	Location_8 Lupindo 6	28.76425	-30.44361	3028BD		Undifferentiated	Landslide	52568.50100000
KZN 0035	Ribbles Dale	28.81172	-30.46699	3028BD		Undifferentiated	Landslide	23315.04600000
KZN 0036	Entre Monts	28.86149	-30.40844	3028BD		Undifferentiated	Landslide	48617.11700000
KZN 0037	Drumreaske	28.94019	-30.43373	3028BD		Undifferentiated	Landslide	335248.80900000
KZN 0038	Weltevreden 1	28.83242	-30.43453	3028BD		Undifferentiated	Landslide	11637.40700000
KZN 0039	Weltevreden 2	28.82674	-30.43538	3028BD		Undifferentiated	Landslide	83321.76300000
KZN 0040	Ogden Vale	28.86778	-30.49041	3028BD		Undifferentiated	Landslide	100208.52200000
KZN 0041	Lange Kuil	28.87026	-30.48953	3028BD		Undifferentiated	Landslide	51194.82900000
KZN 0042	Location_10 Matendel1	28.74669	-30.50341	3028DA		Undifferentiated	Landslide	39534.85100000
KZN 0043	Location_10 Matendel2	28.74297	-30.50162	3028DA		Undifferentiated	Landslide	22033.99700000
KZN 0044	Sibi Location_4	28.70967	-30.20379	3028BB		Undifferentiated	Landslide	99870.38500000
KZN 0045	Glen Donall 43_1	29.22056	-30.01940	3029AA		Undifferentiated	Landslide	6869.13000000
KZN 0046	Glen Donall 43_5	29.22342	-30.01960	3029AA		Undifferentiated	Landslide	19132.03900000
KZN 0047	Glen Donall 43_4	29.22652	-30.01972	3029AA		Undifferentiated	Landslide	2136.88900000
KZN 0048	Glen Donall 43_2	29.22407	-30.02659	3029AA		Undifferentiated	Landslide	51843.73100000
KZN 0049	Glen Donall 43_3	29.21967	-30.02245	3029AA		Undifferentiated	Landslide	53187.28900000
KZN 0050	CLKN Edward 77	29.20010	-30.17264	3029AA		Undifferentiated	Landslide	5506.01400000
KZN 0051	Ettercairn 39	29.19571	-30.03833	3029AB		Undifferentiated	Landslide	14393.76700000
KZN 0052	Windhoek 1	29.41358	-30.45581	3029AD		Undifferentiated	Landslide	1020368.97000000
KZN 0053	Windhoek 2	29.41983	-30.46329	3029AD		Undifferentiated	Landslide	2517350.63400000
KZN 0054	Sisonke_1	29.33113	-30.09079		Debris	Translational	Recent-landslide	10000.00000000
KZN 0055	Sisonke_2	29.32545	-30.09850		Debris	Translational	Recent-landslide	100.00000000
KZN 0056	Wachtenbietjieshoek	30.63539	-27.64137	2730AD	Debris	Undifferentiated	Palaeo-landslide	525876.26400000
KZN 0057	Schurveberghoek_1	30.63542	-27.62718	2730AD	Debris	Flow	Palaeo-landslide	139259.75600000
KZN 0058	Mooihoek	30.62578	-27.61521	2730AD	Debris	Rotational	Palaeo-landslide	176777.26500000
KZN 0059	Klipfontein 31	30.57227	-27.66415	2730AD	Debris	Rotational	Recent-landslide	39546.57600000
KZN 0060	Schurveberghoek_2	30.63679	-27.62248	2730AD	Debris	Undifferentiated	Palaeo-landslide	240297.60300000
KZN 0061	Twisthoek 84	30.62516	-27.53790	2730AD		Undifferentiated	Landslide	89955.55000000
KZN 0062	Mbulwana	29.84225	-28.58144	2829DB	Debris	Flow	Palaeo-landslide	778946.72400000
KZN 0063	Dwars Rivier 1170	29.97346	-28.24012	2829BB		Undifferentiated	Landslide	223415.34700000
KZN 0064	Bosch Kloof 1073	29.98351	-28.23312	2829BB		Undifferentiated	Landslide	542967.23700000
KZN 0065	Waterkloof No.2_3	29.97843	-28.22132	2829BB	Debris	Flow	Palaeo-landslide	288317.19900000

KZN 0066	Waterkloof No.2_2]	29.97253	-28.21725	2829BB	Debris	Flow	Palaeo-landslide	392911.40000000
KZN 0067	Waterkloof No.2_1	29.93509	-28.20218	2829BB	Debris	Undifferentiated	Palaeo-landslide	558111.53200000
KZN 0068	Quaggas Kerk	29.97116	-28.18593	2829BB	Debris	Rotational	Palaeo-landslide	259844.88100000
KZN 0069	One Tree Hill 3301	29.96536	-28.15070	2829BB		Undifferentiated	Landslide	194211.18600000
KZN 0070	Mooiplaats 2163	29.86968	-28.15959	2829BB		Undifferentiated	Landslide	136087.39400000
KZN 0071	Langverwacht 13301	30.23811	-28.30952	2830AC		Undifferentiated	Landslide	498913.04400000
KZN 0072	Rthinus Drift 11	30.75540	-27.52480	2730DB		Undifferentiated	Landslide	241559.09000000
KZN 0073	Schaap plaats 5689	29.88282	-28.38866	2829DB	Debris	Flow	Palaeo-landslide	706403.57800000
KZN 0074	Beeses Fontein 2421	29.90140	-28.26550	2829DB		Undifferentiated	Landslide	811853.32800000
KZN 0075	Bosch Hoek 183	30.36659	-27.55746	2730CB	Debris	Rotational	Palaeo-landslide	217495.68500000
KZN 0076	Uitzicht 1113	30.37962	-27.51399	2730CB		Undifferentiated	Landslide	73436.17500000
KZN 0077	Vaalbank 104	30.41255	-27.57474	2730CB		Undifferentiated	Landslide	7330.82600000
KZN 0078	Utrecht townlands	30.32246	-27.63598	2730CB	Rock	Fall	Recent-landslide	49011.73700000
KZN 0079	Zwartkop 91	30.26110	-27.59566	2730CB	Debris	Rotational	Palaeo-landslide	1117347.88800000
KZN 0080	Weltevreden 182_3	30.48158	-27.73270	2730CB		Undifferentiated	Landslide	193831.19500000
KZN 0081	Weltevreden 182_2	30.48537	-27.73635	2730CB		Undifferentiated	Landslide	51936.16100000
KZN 0082	Weltevreden 182_1	30.49144	-27.72626	2730CB		Undifferentiated	Landslide	56052.94400000
KZN 0083	Burnside 3237	30.11306	-28.21653	2830AA		Undifferentiated	Landslide	273726.47500000
KZN 0084	Morgenstond 3347	30.22736	-28.10236	2830AA	Debris	Undifferentiated	Palaeo-landslide	582613.34000000
KZN 0085	Melrose11667	30.25334	-28.00727	2830AA/2830AB		Undifferentiated	Landslide	283698.41300000
KZN 0086	Stanmore 2412	30.25229	-28.01353	2830AA/2830AB		Undifferentiated	Landslide	374376.58500000
KZN 0087	Koostrofe 3316/Knostrope	30.45312	-28.37784	2830AD	Debris	Undifferentiated	Palaeo-landslide	1422666.49200000
KZN 0088	Baviaanskloof 5031	30.46278	-28.39907	2830AD	Debris	Undifferentiated	Palaeo-landslide	658113.67500000
KZN 0089	Cobham Staatsbos10	29.38652	-29.52214	2929CB	Rock	Fall	Recent-landslide	69032.18100000
KZN 0090	Cobham Staatsbos 2	29.41184	-29.52209	2929CB	Rock	Fall	Recent-landslide	280484.92200000
KZN 0091	Cobham Staatsbos 1	29.41085	-29.50760	2929CB	Rock	Fall	Recent-landslide	30984.82300000
KZN 0092	Twin Streams of Cobham 2	29.41832	-29.50983	2929CB	Rock	Fall	Recent-landslide	470835.79100000
KZN 0093	Twin Streams of Cobham 1	29.42077	-29.52703	2929CB	Rock	Fall	Recent-landslide	258486.39900000
KZN 0094	Cobham Staatsbos 4	29.42304	-29.57685	2929CB		Undifferentiated	Landslide	16811.36300000
KZN 0095	Cobham Staatsbos 5	29.42958	-29.57740	2929CB		Undifferentiated	Landslide	14766.42000000
KZN 0096	Cobham Staatsbos17	29.35869	-29.60262	2929CB	Rock	Fall	Recent-landslide	156943.91200000
KZN 0097	Cobham Staatsbos18	29.37040	-29.60458	2929CB	Rock	Fall	Recent-landslide	204710.08500000
KZN 0098	Cobham Staatsbos13	29.37791	-29.60682	2929CB	Rock	Fall	Recent-landslide	141122.97900000
KZN 0099	Cobham Staatsbos14	29.38211	-29.60795	2929CB	Rock	Fall	Recent-landslide	247617.38900000
KZN 0100	Cobham Staatsbos15	29.38841	-29.60682	2929CB	Rock	Fall	Recent-landslide	134114.52600000
KZN 0101	Cobham Staatsbos16	29.40198	-29.61054	2929CB	Rock	Fall	Recent-landslide	45178.56200000
KZN 0102	Cobham Staatsbos8	29.42128	-29.60747	2929CB		Undifferentiated	Landslide	60533.07500000
KZN 0103	Cobham Staatsbos7	29.44502	-29.61803	2929CB	Rock	Fall	Recent-landslide	496727.31800000
KZN 0104	Cobham Staatsbos19	29.47185	-29.61025	2929CB	Rock	Fall	Recent-landslide	475731.16300000
KZN 0105	Cobham Staatsbos12	29.47448	-29.61678	2929CB	Rock	Fall	Recent-landslide	13886.30800000
KZN 0106	Cobham Staatsbos11	29.47820	-29.61996	2929CB	Rock	Fall	Recent-landslide	56563.24100000
KZN 0107	Cobham Staatsbos9	29.47061	-29.63107	2929CB	Rock	Fall	Recent-landslide	1957512.52500000
KZN 0108	Cobham Staatsbos6	29.44791	-29.63452	2929CB	Rock	Fall	Recent-landslide	346664.50600000
KZN 0109	Good Hope	29.43597	-29.64537	2929CB		Undifferentiated	Landslide	152639.87800000
KZN 0110	Makhakhe of Cobham Staa1	29.42362	-29.63239	2929CB		Undifferentiated	Landslide	290450.06600000
KZN 0111	Makhakhe of Cobham Staa2	29.41863	-29.62943	2929CB		Undifferentiated	Landslide	52114.82100000
KZN 0112	Cobham Staatsbos 3	29.38422	-29.62103	2929CB	Rock	Fall	Recent-landslide	1354248.80000000
KZN 0113	Cobham Statefores43	29.33969	-29.60656	2929CB	Rock	Fall	Recent-landslide	11227.31400000
KZN 0114	Cobham Statefores40	29.39068	-29.62839	2929CB	Rock	Fall	Recent-landslide	75812.96200000
KZN 0115	Cobham Statefores39	29.38529	-29.63305	2929CB	Rock	Fall	Recent-landslide	170864.28800000
KZN 0116	Cobham Statefores29	29.36516	-29.63425	2929CB	Rock	Fall	Recent-landslide	60537.13100000
KZN 0117	Cobham Statefores28	29.36606	-29.63740	2929CB	Rock	Fall	Recent-landslide	61202.28500000
KZN 0118	Cobham Statefores27	29.37381	-29.64088	2929CB	Rock	Fall	Recent-landslide	289444.22300000
KZN 0119	Cobham Statefores26	29.37525	-29.64583	2929CB	Rock	Fall	Recent-landslide	126971.42100000
KZN 0120	Cobham Statefores25	29.37351	-29.64938	2929CB	Rock	Fall	Recent-landslide	69125.73000000
KZN 0121	Cobham Statefores24	29.37654	-29.65312	2929CB	Rock	Fall	Recent-landslide	138338.25500000
KZN 0122	Cobham Statefores23	29.36880	-29.65645	2929CB	Rock	Fall	Recent-landslide	139946.79200000
KZN 0123	Cobham Statefores22	29.32739	-29.64461	2929CB	Rock	Fall	Recent-landslide	16437.41700000
KZN 0124	Cobham Statefores21	29.32911	-29.64529	2929CB	Rock	Fall	Recent-landslide	14141.01300000
KZN 0125	Cobham Statefores20	29.33066	-29.64883	2929CB	Rock	Fall	Recent-landslide	35021.98400000
KZN 0126	Cobham Statefores19	29.33440	-29.64598	2929CB	Rock	Fall	Recent-landslide	14144.25800000
KZN 0127	Cobham Statefores18	29.40382	-29.66199	2929CB	Rock	Fall	Recent-landslide	1301164.34400000
KZN 0128	Cobham Statefores17	29.41576	-29.66753	2929CB	Rock	Fall	Recent-landslide	538228.06500000
KZN 0129	Cobham Statefores16	29.41904	-29.67901	2929CB	Rock	Fall	Recent-landslide	49529.64300000
KZN 0130	Cobham Statefores15	29.38985	-29.68255	2929CB		Undifferentiated	Landslide	45617.40100000
KZN 0131	Cobham Statefores14	29.38792	-29.67409	2929CB	Rock	Fall	Recent-landslide	504936.29300000
KZN 0132	Cobham Statefores13	29.38855	-29.66457	2929CB	Rock	Fall	Recent-landslide	185152.93300000
KZN 0133	Cobham Statefores12	29.31726	-29.66356	2929CB	Rock	Fall	Recent-landslide	56378.29600000
KZN 0134	Cobham Statefores11	29.30496	-29.67164	2929CB	Rock	Fall	Recent-landslide	92606.48000000
KZN 0135	Cobham Statefores10	29.35062	-29.67097	2929CB		Undifferentiated	Landslide	124868.88500000
KZN 0136	Cobham Statefores9	29.33527	-29.67888	2929CB	Rock	Fall	Recent-landslide	111297.30900000
KZN 0137	Cobham Statefores8	29.33151	-29.67996	2929CB	Rock	Fall	Recent-landslide	101938.91600000
KZN 0138	Cobham Statefores7	29.37377	-29.69247	2929CB	Rock	Fall	Recent-landslide	136761.35300000
KZN 0139	Cobham Statefores6	29.37071	-29.68788	2929CB	Rock	Fall	Recent-landslide	109860.73800000
KZN 0140	Cobham Statefores5	29.36165	-29.69024	2929CB	Rock	Fall	Recent-landslide	307439.88500000
KZN 0141	Cobham Statefores4	29.27630	-29.67660	2929CB	Rock	Fall	Recent-landslide	121068.58400000
KZN 0142	Cobham Statefores3	29.28277	-29.69052	2929CB		Undifferentiated	Landslide	66939.64500000
KZN 0143	Cobham Statefores36	29.26987	-29.69917	2929CB		Undifferentiated	Landslide	27861.84300000
KZN 0144	Cobham Stateforest44	29.28997	-29.69927	2929CB	Rock	Fall	Recent-landslide	894850.41400000

KZN 0145	Cobham Statefores42	29.30673	-29.69702	2929CB	Rock	Fall	Recent-landslide	540402.79400000
KZN 0146	Cobham Statefores30	29.30779	-29.70963	2929CB	Rock	Fall	Recent-landslide	333292.47600000
KZN 0147	Cobham Statefores38	29.30093	-29.71195	2929CB	Rock	Fall	Recent-landslide	94064.95200000
KZN 0148	Cobham Statefores41	29.33559	-29.73569	2929CB	Rock	Fall	Recent-landslide	452677.08500000
KZN 0149	Cobham Statefores37	29.34447	-29.73505	2929CB	Rock	Fall	Recent-landslide	96706.91100000
KZN 0150	Cobham Statefores1	29.35139	-29.73751	2929CB	Rock	Fall	Recent-landslide	96623.36100000
KZN 0151	Cobham Statefores35	29.35191	-29.74181	2929CB	Rock	Fall	Recent-landslide	66422.93300000
KZN 0152	Cobham Statefores34	29.35698	-29.72357	2929CB	Rock	Fall	Recent-landslide	44777.03600000
KZN 0153	Cobham Statefores33	29.35693	-29.71821	2929CB	Rock	Fall	Recent-landslide	19987.88000000
KZN 0154	Cobham Statefores32	29.37340	-29.71247	2929CB		Undifferentiated	Landslide	59347.15400000
KZN 0155	Cobham Statefores31	29.35027	-29.70715	2929CB		Undifferentiated	Landslide	82322.54900000
KZN 0156	Cobham Statefores2	29.40523	-29.67618	2929CB	Rock	Fall	Recent-landslide	810882.01400000
KZN 0157	Garden Castle Statefor4	29.24742	-29.69636	2929CA	Rock	Fall	Recent-landslide	223078.16200000
KZN 0158	Garden Castle Statefor1	29.23238	-29.70926	2929CA	Rock	Fall	Recent-landslide	64845.80500000
KZN 0159	Garden Castle Statefor5	29.21864	-29.70289	2929CA	Rock	Fall	Recent-landslide	1158645.30300000
KZN 0160	Garden Castle Statefor19	29.21503	-29.69422	2929CA	Rock	Fall	Recent-landslide	109449.39500000
KZN 0161	Garden Castle Statefor15	29.20964	-29.69344	2929CA	Rock	Fall	Recent-landslide	78984.01400000
KZN 0162	Garden Castle Statefor18	29.20694	-29.69077	2929CA	Rock	Fall	Recent-landslide	32548.08100000
KZN 0163	Garden Castle Statefor14	29.20000	-29.69104	2929CA	Rock	Fall	Recent-landslide	9490.96900000
KZN 0164	Garden Castle Statefor17	29.19689	-29.69719	2929CA	Rock	Fall	Recent-landslide	15959.88200000
KZN 0165	Garden Castle Statefor2	29.18954	-29.70315	2929CA	Rock	Fall	Recent-landslide	22425.56500000
KZN 0166	Garden Castle Statefor3	29.20345	-29.72273	2929CA	Rock	Fall	Recent-landslide	32938.96200000
KZN 0167	Garden Castle Statefor12	29.17673	-29.73346	2929CA	Rock	Fall	Recent-landslide	77975.03300000
KZN 0167	Garden Castle Statefor16	29.19772	-29.72721	2929CA	Rock	Fall	Recent-landslide	26476.55300000
KZN 0168	Garden Castle Statefor13	29.18526	-29.72590	2929CA	Rock	Fall	Recent-landslide	26666.79000000
KZN 0170	Garden Castle Statefor11	29.17456	-29.74346	2929CA	Rock	Fall	Recent-landslide	50712.72400000
KZN 0171	Garden Castle Statefor10	29.17924	-29.74241	2929CA	Rock	Fall	Recent-landslide	15377.59900000
KZN 0172	Garden Castle Statefor9	29.18730	-29.73882	2929CA	Rock	Fall	Recent-landslide	731249.60600000
KZN 0173	Garden Castle Statefor8	29.19439	-29.74414	2929CA	Rock	Fall	Recent-landslide	421518.75900000
KZN 0174	Garden Castle Statefor7	29.23938	-29.69135	2929CA	Rock	Fall	Recent-landslide	526396.58000000
KZN 0175	Garden Castle Statefor6	29.23289	-29.68579	2929CA	Rock	Fall	Recent-landslide	578697.26900000
KZN 0176	State Land 1	29.42618	-29.48710	2929AD	Rock	Fall	Recent-landslide	30784.71600000
KZN 0177	State Land 2	29.42880	-29.48874	2929AD	Rock	Fall	Recent-landslide	31760.74800000
KZN 0178	Giant's Castle Game Re8	29.53236	-29.25196	2929BC	Rock	Fall	Recent-landslide	102549.50400000
KZN 0179	Giant's Castle Game Re9	29.51554	-29.26803	2929BC	Rock	Fall	Recent-landslide	41256.90300000
KZN 0180	Giant's Castle Game Re10	29.52376	-29.27473	2929BC	Rock	Fall	Recent-landslide	47409.61300000
KZN 0181	Giant's Castle Game Re11	29.52186	-29.27751	2929BC	Rock	Fall	Recent-landslide	108880.02000000
KZN 0182	Wilhelminas Rust 7427	29.59737	-29.28187	2929BC	Rock	Fall	Recent-landslide	161292.48300000
KZN 0183	Normanby 7428_2	29.59003	-29.29023	2929BC	Rock	Fall	Recent-landslide	112513.08100000
KZN 0184	Normanby 7428_1	29.58721	-29.29633	2929BC	Rock	Fall	Recent-landslide	200348.89300000
KZN 0185	Assvogel Krantz 7426_1	29.62804	-29.29012	2929BC	Rock	Fall	Recent-landslide	166775.69100000
KZN 0186	Assvogel Krantz 7426_2	29.63682	-29.29323	2929BC	Rock	Fall	Recent-landslide	287049.83000000
KZN 0187	Swarraton No 2 8337	29.64841	-29.29424	2929BC	Rock	Fall	Recent-landslide	331599.97800000
KZN 0188	Silverhill 10547	29.64139	-29.31269	2929BC	Rock	Fall	Recent-landslide	985208.07800000
KZN 0189	Cleopatra 7439_2	29.66125	-29.32751	2929BC	Rock	Fall	Recent-landslide	485052.82800000
KZN 0190	Cleopatra 7439_1	29.65714	-29.33568	2929BC	Rock	Fall	Recent-landslide	252017.73300000
KZN 0191	Cascade 9776_2	29.64408	-29.33598	2929BC	Rock	Fall	Recent-landslide	280167.89400000
KZN 0192	Cascade 9776_1	29.64449	-29.33202	2929BC	Rock	Fall	Recent-landslide	142299.90200000
KZN 0193	West Karmel 13591_1	29.67989	-29.34848	2929BC	Rock	Fall	Recent-landslide	319373.13100000
KZN 0194	West Karmel 13591_2	29.68773	-29.34704	2929BC	Rock	Fall	Recent-landslide	62699.24800000
KZN 0195	Game Pass E 5596	29.63075	-29.38291	2929BC	Rock	Fall	Recent-landslide	395547.57700000
KZN 0196	Kamberg Nature Reser2	29.67793	-29.39417	2929BC	Rock	Fall	Recent-landslide	1471409.64300000
KZN 0197	Kamberg Nature Reser5	29.69079	-29.39271	2929BC	Rock	Fall	Recent-landslide	747415.16500000
KZN 0198	Kamberg Nature Reser3	29.66994	-29.41140	2929BC	Rock	Fall	Recent-landslide	15386.84000000
KZN 0199	Allendale 9846	29.72550	-29.42329	2929BC		Undifferentiated	Landslide	32192.88300000
KZN 0200	Chalgrove 9100	29.54412	-29.42054	2929BC	Rock	Fall	Recent-landslide	100773.88100000
KZN 0201	Mkhomazi State Forest3	29.52107	-29.40417	2929BC	Rock	Fall	Recent-landslide	125935.55700000
KZN 0202	Mkhomazi State Forest2	29.50697	-29.39388	2929BC		Undifferentiated	Landslide	75072.71400000
KZN 0203	Mkhomazi State Forest1	29.50250	-29.37857	2929BC	Rock	Fall	Recent-landslide	187000.94100000
KZN 0204	Giant's Castle Nature Re	29.53397	-29.24855	2929BA	Rock	Fall	Recent-landslide	78376.59600000
KZN 0205	Giant's Castle Nature R1	29.53070	-29.23923	2929BA	Debris	Rotational	Recent-landslide	25.37400000
KZN 0206	Giant's Castle Nature R3	29.51475	-29.24221	2929BA	Rock	Fall	Recent-landslide	118789.30100000
KZN 0207	Giant's Castle Nature R4	29.50681	-29.24081	2929BA	Rock	Fall	Recent-landslide	54449.43200000
KZN 0208	Giant's Castle Nature R2	29.50380	-29.23728	2929BA	Rock	Fall	Recent-landslide	218386.77400000
KZN 0209	Giant's Castle Nature R7	29.50541	-29.22163	2929BA	Rock	Fall	Recent-landslide	76604.85600000
KZN 0210	Giant's Castle Nature R8	29.54618	-29.22498	2929BA		Undifferentiated	Landslide	55978.88100000
KZN 0211	Giant's Castle Nature R9	29.50673	-29.21827	2929BA	Rock	Fall	Recent-landslide	42329.58900000
KZN 0212	Giant's Castle Nature R6	29.52739	-29.21741	2929BA	Rock	Fall	Recent-landslide	89041.64900000
KZN 0213	Giant's Castle Nature R5	29.53472	-29.21632	2929BA	Rock	Fall	Recent-landslide	111181.76400000
KZN 0214	Foxtail	29.50937	-29.20483	2929BA	Rock	Fall	Recent-landslide	72574.04600000
KZN 0215	Hastings 7087	29.58787	-29.23355	2929BA	Rock	Fall	Recent-landslide	311178.39100000
KZN 0216	Cathkin Peak Forest Re11	29.32194	-29.00646	2929AB	Rock	Fall	Recent-landslide	426713.14100000
KZN 0217	Cathkin Peak Forest Re3	29.32458	-29.01512	2929AB	Rock	Fall	Recent-landslide	80083.21700000
KZN 0218	Cathkin Peak Forest Re8	29.31912	-29.01613	2929AB	Rock	Fall	Recent-landslide	64674.55300000
KZN 0219	Cathkin Peak Forest Re4	29.32099	-29.02072	2929AB	Rock	Fall	Recent-landslide	70797.87200000
KZN 0220	Cathkin Peak Forest Re2	29.32383	-29.02053	2929AB	Rock	Fall	Recent-landslide	105523.47100000
KZN 0221	Cathkin Peak Forest Re6	29.32187	-29.02589	2929AB	Rock	Fall	Recent-landslide	26570.03200000
KZN 0222	Cathkin Peak Forest Re7	29.33615	-29.00675	2929AB	Rock	Fall	Recent-landslide	70240.70000000
KZN 0223	Cathkin Peak Forest Re13	29.35201	-29.00790	2929AB	Rock	Fall	Recent-landslide	37208.05900000

KZN 0224	Cathkin Peak Forest Re12	29.35424	-29.01911	2929AB	Rock	Fall	Recent-landslide	33053.63900000
KZN 0225	Cathkin Peak Forest Re1	29.35491	-29.02227	2929AB	Rock	Fall	Recent-landslide	27739.47200000
KZN 0226	Cathkin Peak Forest Re14	29.35597	-29.02414	2929AB	Rock	Fall	Recent-landslide	8585.04600000
KZN 0227	Cathkin Peak Forest Re9	29.49553	-29.11417	2929AB	Rock	Fall	Recent-landslide	666973.29200000
KZN 0228	Giant's Castle Game Re5	29.45721	-29.12626	2929AB	Rock	Fall	Recent-landslide	40126.00500000
KZN 0229	Giant's Castle Game Re4	29.44754	-29.12801	2929AB	Rock	Fall	Recent-landslide	116816.39300000
KZN 0230	Giant's Castle Game Re1	29.44424	-29.13530	2929AB	Rock	Fall	Recent-landslide	156725.14700000
KZN 0231	Cathkin Peak Forest Re10	29.43173	-29.13391	2929AB	Rock	Fall	Recent-landslide	297268.92200000
KZN 0232	Cathkin Peak Forest Re5	29.42047	-29.14874	2929AB	Rock	Fall	Recent-landslide	67158.80600000
KZN 0233	Giant's Castle Game Re2	29.41304	-29.15060	2929AB	Rock	Fall	Recent-landslide	26444.70000000
KZN 0234	Giant's Castle Game Re6	29.41428	-29.15619	2929AB	Rock	Fall	Recent-landslide	58730.43900000
KZN 0235	Giant's Castle Game Re3	29.48531	-29.23643	2929AB	Rock	Fall	Recent-landslide	77392.10800000
KZN 0236	Giant's Castle Game Re7	29.48477	-29.23520	2929AB	Rock	Fall	Recent-landslide	74864.71000000
KZN 0237	Cathedral Peak Forest R2	29.31713	-28.99241	2829CD	Rock	Fall	Recent-landslide	192756.64700000
KZN 0238	Cathedral Peak Forest R1	29.29698	-28.98776	2829CD	Rock	Fall	Recent-landslide	1214508.88300000
KZN 0239	Solarcliffs N 454_1	29.28386	-28.96204	2829CD	Rock	Fall	Recent-landslide	424641.63700000
KZN 0240	Solarcliffs N 454_2	29.28917	-28.96919	2829CD	Rock	Fall	Recent-landslide	930710.72400000
KZN 0241	Brotherton 11078_2	29.26182	-28.94762	2829CD	Rock	Fall	Recent-landslide	108822.15800000
KZN 0242	Brotherton 11078_1	29.27220	-28.94972	2829CD	Rock	Fall	Recent-landslide	213290.16700000
KZN 0243	Upper Tugela Native Loc1	29.29773	-28.94762	2829CD	Rock	Fall	Recent-landslide	28057.38900000
KZN 0244	Upper Tugela Native Loc2	29.29808	-28.95179	2829CD	Rock	Fall	Recent-landslide	414561.71900000
KZN 0245	The Glens	29.32978	-28.96119	2829CD	Rock	Fall	Recent-landslide	62340.14500000
KZN 0246	The Glens	29.33595	-28.97836	2829CD	Rock	Fall	Recent-landslide	130810.56800000
KZN 0247	The Odorus 14825_4	29.35444	-28.96211	2829CD	Rock	Fall	Recent-landslide	89420.66700000
KZN 0248	The Odorus 14825_5	29.35242	-28.96737	2829CD	Rock	Fall	Recent-landslide	182728.59200000
KZN 0249	The Odorus 14825_3	29.35573	-28.97264	2829CD	Rock	Fall	Recent-landslide	265119.18200000
KZN 0250	The Odorus 14825_1	29.35618	-28.98139	2829CD	Rock	Fall	Recent-landslide	301595.79700000
KZN 0251	The Odorus 14825_2	29.35991	-28.98663	2829CD	Rock	Fall	Recent-landslide	124976.44600000
KZN 0252	Upper Tugela Locat 47_2	29.33770	-28.87204	2829CD		Undifferentiated	Landslide	62760.91400000
KZN 0253	The Climb	29.29802	-28.96357	2829CD	Rock	Fall	Recent-landslide	746440.73700000
KZN 0254	Upper Tugela Locat 4_29	28.99586	-28.86342	2828DD	Rock	Fall	Recent-landslide	23716.00000000
KZN 0255	Upper Tugela Locat 4_33	28.98846	-28.83903	2828DD	Rock	Fall	Recent-landslide	26997.87600000
KZN 0256	Upper Tugela Locat 4_5	28.98796	-28.83691	2828DD	Rock	Fall	Recent-landslide	53294.91800000
KZN 0257	Upper Tugela Locat 4_8	29.13086	-28.77690	2829CC	Debris	Flow	Palaeo-landslide	318344.82000000
KZN 0258	Upper Tugela Locat 4_1	29.00481	-28.82484	2829CC	Rock	Fall	Recent-landslide	20145.26400000
KZN 0259	Upper Tugela Locat 4_2	29.00313	-28.82706	2829CC	Rock	Fall	Recent-landslide	69767.02100000
KZN 0260	Upper Tugela Locat 4_3	29.00194	-28.84152	2829CC	Rock	Fall	Recent-landslide	65470.90100000
KZN 0261	Upper Tugela Locat 4_9	29.01514	-28.83999	2829CC	Rock	Fall	Recent-landslide	328078.17900000
KZN 0262	Upper Tugela Locat 4_6	29.02366	-28.84119	2829CC	Rock	Fall	Recent-landslide	89769.64500000
KZN 0263	Upper Tugela Locat 4_7	29.08487	-28.85811	2829CC		Undifferentiated	Landslide	146139.79900000
KZN 0264	Upper Tugela Locat 4_32	29.11463	-28.86993	2829CC	Rock	Fall	Recent-landslide	47203.32500000
KZN 0265	Upper Tugela Locat 4_31	29.14567	-28.86020	2829CC	Rock	Fall	Recent-landslide	120806.31100000
KZN 0266	Upper Tugela Locat 4_28	29.15612	-28.84430	2829CC	Rock	Fall	Recent-landslide	139536.45900000
KZN 0267	Upper Tugela Locat 4_26	29.16701	-28.83631	2829CC	Rock	Fall	Recent-landslide	549568.90700000
KZN 0268	Upper Tugela Locat 4_25	29.17442	-28.83441	2829CC	Rock	Fall	Recent-landslide	319878.91200000
KZN 0269	Upper Tugela Locat 4_24	29.18497	-28.83507	2829CC	Rock	Fall	Recent-landslide	209711.25200000
KZN 0270	Upper Tugela Locat 4_23	29.18881	-28.83893	2829CC		Undifferentiated	Landslide	129811.15900000
KZN 0271	Upper Tugela Locat 4_22	29.18605	-28.85010	2829CC	Rock	Fall	Recent-landslide	61665.55900000
KZN 0272	Upper Tugela Locat 4_21	29.18648	-28.85352	2829CC	Rock	Fall	Recent-landslide	45650.40400000
KZN 0273	Upper Tugela Locat 4_20	29.19842	-28.85798	2829CC		Undifferentiated	Landslide	86630.82700000
KZN 0274	Upper Tugela Locat 4_19	29.20519	-28.85649	2829CC	Rock	Fall	Recent-landslide	82971.28300000
KZN 0275	Upper Tugela Locat 4_18	29.19730	-28.86976	2829CC	Rock	Fall	Recent-landslide	109250.06300000
KZN 0276	Upper Tugela Locat 4_17	29.19084	-28.87653	2829CC	Rock	Fall	Recent-landslide	188520.76800000
KZN 0277	Upper Tugela Locat 4_16	29.18749	-28.89016	2829CC	Rock	Fall	Recent-landslide	21690.93300000
KZN 0278	Upper Tugela Locat 4_15	29.19210	-28.88508	2829CC	Rock	Fall	Recent-landslide	166153.70600000
KZN 0279	Upper Tugela Locat 4_14	29.22275	-28.86565	2829CC	Rock	Fall	Recent-landslide	37787.71100000
KZN 0280	Upper Tugela Locat 4_13	29.22769	-28.86423	2829CC	Rock	Fall	Recent-landslide	73079.16700000
KZN 0281	Upper Tugela Locat 4_12	29.23084	-28.86533	2829CC	Rock	Fall	Recent-landslide	53560.87300000
KZN 0282	Upper Tugela Locat 4_30	29.22247	-28.87716	2829CC	Rock	Fall	Recent-landslide	1613107.19000000
KZN 0283	Upper Tugela Locat 4_10	29.21462	-28.89368	2829CC	Rock	Fall	Recent-landslide	702262.88700000
KZN 0284	Upper Tugela Locat 4_27	29.21311	-28.90387	2829CC	Rock	Fall	Recent-landslide	334135.13600000
KZN 0285	Upper Tugela Locat 4_11	29.21444	-28.91075	2829CC	Rock	Fall	Recent-landslide	88322.29400000
KZN 0286	Cathedral Peak Researc5	29.22507	-28.94992	2829CC	Rock	Fall	Recent-landslide	45207.97800000
KZN 0287	Cathedral Peak Researc1	29.22755	-28.95221	2829CC	Rock	Fall	Recent-landslide	30981.06000000
KZN 0288	Cathedral Peak Researc2	29.22371	-28.96251	2829CC	Rock	Fall	Recent-landslide	29397.51600000
KZN 0289	Cathedral Peak Researc3	29.24081	-28.96050	2829CC	Rock	Fall	Recent-landslide	353375.37600000
KZN 0290	Cathedral Peak Researc4	29.24562	-28.95970	2829CC	Rock	Fall	Recent-landslide	483728.94200000
KZN 0291	Mafifiyela Nature Reser2	29.19345	-28.95471	2829CC	Rock	Fall	Recent-landslide	308991.83400000
KZN 0292	Upper Tugela Locat 4_4	29.23039	-28.86966	2829CC	Rock	Fall	Recent-landslide	91902.79600000
KZN 0293	Mafifiyela Nature Reser1	29.19920	-28.96660	2829CC	Rock	Fall	Recent-landslide	82337.86500000
KZN 0294	Mafifiyela Nature Reser2	29.21005	-28.95437	2829CC	Rock	Fall	Recent-landslide	277261.31000000
KZN 0295	FP 8574	29.33757	-29.77330	2929CD		Undifferentiated	Landslide	122304.37500000
KZN 0296	Wintershoek 14562_1	29.30823	-29.78426	2929CD	Rock	Fall	Recent-landslide	400346.31700000
KZN 0297	Wintershoek 14562_2	29.30252	-29.78846	2929CD	Rock	Fall	Recent-landslide	115637.94500000
KZN 0298	Zeiss 14580_2	29.25310	-29.81597	2929CD	Rock	Fall	Recent-landslide	61285.56400000
KZN 0299	Wild 14578	29.26229	-29.82067	2929CD	Rock	Fall	Recent-landslide	386372.43800000
KZN 0300	FP 263 9796	29.25977	-29.90275	2929CD	Rock	Fall	Recent-landslide	209879.77800000
KZN 0301	State Land 41	29.18364	-29.74750	2929CA & 2929CC	Rock	Fall	Recent-landslide	226450.91800000
KZN 0302	State Land 3	29.18023	-29.75108	2929CA & 2929CC	Rock	Fall	Recent-landslide	214964.09000000

KZN 0303	State Land 39	29.17216	-29.75746	2929CC	Rock	Fall	Recent-landslide	158535.19800000
KZN 0304	State Land 31	29.17615	-29.76360	2929CC	Rock	Fall	Recent-landslide	69185.80100000
KZN 0305	State Land 29	29.17862	-29.76286	2929CC	Rock	Fall	Recent-landslide	135833.27400000
KZN 0306	State Land 7	29.18624	-29.75517	2929CC	Rock	Fall	Recent-landslide	81274.49700000
KZN 0307	State Land 6	29.18942	-29.75871	2929CC	Rock	Fall	Recent-landslide	90817.45700000
KZN 0308	State Land 5	29.18523	-29.76126	2929CC	Rock	Fall	Recent-landslide	148433.41500000
KZN 0309	FP 254 8426	29.23868	-29.78510	2929CC	Rock	Fall	Recent-landslide	143664.94700000
KZN 0310	State Land 27	29.18201	-29.77709	2929CC	Rock	Fall	Recent-landslide	166931.69500000
KZN 0311	State Land 28	29.17411	-29.78055	2929CC	Rock	Fall	Recent-landslide	144586.88400000
KZN 0312	State Land 23	29.17849	-29.77849	2929CC	Rock	Fall	Recent-landslide	274913.29000000
KZN 0313	State Land 40	29.18777	-29.78129	2929CC	Rock	Fall	Recent-landslide	60737.56300000
KZN 0314	State Land 38	29.19037	-29.78233	2929CC	Rock	Fall	Recent-landslide	138105.90400000
KZN 0315	State Land 34	29.19331	-29.78331	2929CC	Rock	Fall	Recent-landslide	82104.76100000
KZN 0316	State Land 37	29.18999	-29.79216	2929CC	Rock	Fall	Recent-landslide	151225.32500000
KZN 0317	State Land 36	29.19375	-29.79473	2929CC	Rock	Fall	Recent-landslide	101512.36900000
KZN 0318	State Land 35	29.18961	-29.80027	2929CC	Rock	Fall	Recent-landslide	111374.15200000
KZN 0319	State Land 26	29.18447	-29.80299	2929CC	Rock	Fall	Recent-landslide	77762.95800000
KZN 0320	State Land 33	29.17971	-29.80255	2929CC	Rock	Fall	Recent-landslide	89652.20900000
KZN 0321	State Land 32	29.17396	-29.80024	2929CC	Rock	Fall	Recent-landslide	145869.38400000
KZN 0322	State Land 30	29.16201	-29.79955	2929CC	Rock	Fall	Recent-landslide	138912.64100000
KZN 0323	Verdant Vale 1	29.21679	-29.80143	2929CC	Rock	Fall	Recent-landslide	56245.95000000
KZN 0324	FP 316 9035_1	29.22851	-29.80760	2929CC	Rock	Fall	Recent-landslide	30466.96300000
KZN 0325	Verdant Vale 2	29.21745	-29.81534	2929CC	Rock	Fall	Recent-landslide	34898.46300000
KZN 0326	FP 316 9035_2	29.22956	-29.81265	2929CC	Rock	Fall	Recent-landslide	159563.30800000
KZN 0327	Zeiss 14580_1	29.24033	-29.82322	2929CC	Rock	Fall	Recent-landslide	88557.26300000
KZN 0328	Zeiss 14580_3	29.24585	-29.81951	2929CC	Rock	Fall	Recent-landslide	546597.66700000
KZN 0329	Stroughton 14579	29.24652	-29.83033	2929CC	Rock	Fall	Recent-landslide	103776.60300000
KZN 0330	Silver Streams 12095	29.22101	-29.82898	2929CC		Undifferentiated	Landslide	162685.48600000
KZN 0331	Stornoway	29.18590	-29.83120	2929CC	Rock	Fall	Recent-landslide	141994.65000000
KZN 0332	State Land 25	29.14971	-29.81368	2929CC	Rock	Fall	Recent-landslide	95168.95700000
KZN 0333	State Land 24	29.15005	-29.81762	2929CC	Rock	Fall	Recent-landslide	66529.23800000
KZN 0334	State Land 4	29.14687	-29.82010	2929CC	Rock	Fall	Recent-landslide	101082.92000000
KZN 0335	State Land 22	29.15150	-29.82344	2929CC	Rock	Fall	Recent-landslide	97470.36300000
KZN 0336	State Land 21	29.14295	-29.82938	2929CC	Rock	Fall	Recent-landslide	10871.63500000
KZN 0337	State Land 20	29.13845	-29.83448	2929CC	Rock	Fall	Recent-landslide	13481.97300000
KZN 0338	State Land 19	29.14835	-29.82997	2929CC	Rock	Fall	Recent-landslide	24470.21700000
KZN 0339	State Land 18	29.15537	-29.82994	2929CC	Rock	Fall	Recent-landslide	421348.81600000
KZN 0340	State Land 17	29.14265	-29.83335	2929CC	Rock	Fall	Recent-landslide	285954.54600000
KZN 0341	State Land 16	29.13309	-29.83405	2929CC	Rock	Fall	Recent-landslide	48848.63500000
KZN 0342	State Land 15	29.13379	-29.83632	2929CC	Rock	Fall	Recent-landslide	127446.98400000
KZN 0343	State Land 14	29.14173	-29.84142	2929CC		Undifferentiated	Landslide	27719.49800000
KZN 0344	State Land 13	29.13742	-29.84405	2929CC		Undifferentiated	Landslide	53844.65800000
KZN 0345	State Land 12	29.12788	-29.85002	2929CC	Rock	Fall	Recent-landslide	75150.44200000
KZN 0346	State Land 11	29.13041	-29.85424	2929CC	Rock	Fall	Recent-landslide	36165.52900000
KZN 0347	State Land 10	29.13399	-29.85620	2929CC	Rock	Fall	Recent-landslide	150934.41700000
KZN 0348	State Land 9	29.13959	-29.85535	2929CC	Rock	Fall	Recent-landslide	120062.60600000
KZN 0349	State Land 8	29.15292	-29.84325	2929CC	Rock	Fall	Recent-landslide	42616.41500000
KZN 0350	Caledonia 7	29.15124	-29.85659	2929CC	Rock	Fall	Recent-landslide	53337.18500000
KZN 0351	Caledonia 8	29.15452	-29.85693	2929CC	Rock	Fall	Recent-landslide	12385.86800000
KZN 0352	Caledonia 4	29.15982	-29.85661	2929CC		Undifferentiated	Landslide	31725.14100000
KZN 0353	Caledonia 3	29.16378	-29.85482	2929CC		Undifferentiated	Landslide	9450.47200000
KZN 0354	Caledonia 2	29.16244	-29.86538	2929CC		Undifferentiated	Landslide	43480.25100000
KZN 0355	Caledonia 1	29.16077	-29.84963	2929CC	Rock	Fall	Recent-landslide	436844.51900000
KZN 0356	Caledonia 5	29.16267	-29.85301	2929CC	Rock	Fall	Recent-landslide	87591.34100000
KZN 0357	Watershed 3	29.19688	-29.92978	2929CC		Undifferentiated	Landslide	9722.79400000
KZN 0358	Eagles Nest 2_2	29.15611	-29.94762	2929CC	Rock	Fall	Recent-landslide	94194.41500000
KZN 0359	Eagles Nest 2_1	29.15383	-29.94414	2929CC	Rock	Fall	Recent-landslide	64636.54000000
KZN 0360	Thule	29.11853	-29.95912	2929CC		Undifferentiated	Landslide	43144.09000000
KZN 0361	Caledonia 6	29.16783	-29.84849	2929CC		Undifferentiated	Landslide	10813.69900000
KZN 0362	Trilby 9061	28.97539	-28.65023	2828DB	Rock	Fall	Recent-landslide	34676.34900000
KZN 0363	Royal Natal Nat Park14	28.97414	-28.65312	2828DB	Rock	Fall	Recent-landslide	139595.44600000
KZN 0364	Royal Natal Nat Park13	28.96943	-28.65850	2828DB	Rock	Fall	Recent-landslide	13585.75700000
KZN 0365	Royal Natal Nat Park12	28.95288	-28.65144	2828DB	Rock	Fall	Recent-landslide	39219.47300000
KZN 0366	The Cavern 9708	28.94571	-28.64760	2828DB	Rock	Fall	Recent-landslide	240922.04300000
KZN 0367	Royal Natal Nat Park11	28.95050	-28.65445	2828DB	Rock	Fall	Recent-landslide	126751.93500000
KZN 0368	Royal Natal Nat Park10	28.95453	-28.65735	2828DB	Rock	Fall	Recent-landslide	55298.49600000
KZN 0369	Royal Natal Nat Park9	28.94844	-28.65938	2828DB	Rock	Fall	Recent-landslide	770652.66900000
KZN 0370	Royal Natal Nat Park4	28.93024	-28.67707	2828DB	Rock	Fall	Recent-landslide	31380.26300000
KZN 0371	Royal Natal Nat Park2	28.94395	-28.67462	2828DB		Undifferentiated	Landslide	43331.30300000
KZN 0372	Royal Natal Nat Park16	28.94768	-28.67669	2828DB		Undifferentiated	Landslide	34519.66200000
KZN 0373	Royal Natal Nat Park6	28.93534	-28.67341	2828DB	Rock	Fall	Recent-landslide	398622.61500000
KZN 0374	Royal Natal Nat Park15	28.93743	-28.66695	2828DB	Rock	Fall	Recent-landslide	58733.02500000
KZN 0375	Royal Natal Nat Park1	28.94433	-28.68113	2828DB	Debris	Flow	Palaeo-landslide	695818.02800000
KZN 0376	Royal Natal Nat Park3	28.91946	-28.68948	2828DB	Rock	Fall	Recent-landslide	350009.41600000
KZN 0377	Royal Natal Nat Park5	28.92289	-28.68313	2828DB	Rock	Fall	Recent-landslide	863595.77800000
KZN 0378	Royal Natal Nat Park7	28.93471	-28.69880	2828DB	Rock	Fall	Recent-landslide	344574.71900000
KZN 0379	Tendele	28.93851	-28.71973	2828DB	Debris	Rotational	Palaeo-landslide	598610.84100000
KZN 0380	Royal Natal Nat Park8	28.94718	-28.72008	2828DB	Rock	Fall	Recent-landslide	201948.90800000
KZN 0381	Upper Tugela Locat 47_7	28.97383	-28.70889	2828DB	Rock	Fall	Recent-landslide	68462.65100000

KZN 0382	Upper Tugela Locat 47_4	28.97384	-28.72585	2828DB	Rock	Fall	Recent-landslide	500635.25200000
KZN 0383	Upper Tugela Locat 47_5	28.96735	-28.73002	2828DB	Rock	Fall	Recent-landslide	141439.51400000
KZN 0384	Upper Tugela Locat 47_1	28.95852	-28.73718	2828DB	Rock	Fall	Recent-landslide	72163.95300000
KZN 0385	Upper Tugela Locat 47_3	28.97810	-28.76329	2828DD		Undifferentiated	Landslide	13771.52000000
KZN 0386	Upper Tugela Locat 47_6	28.97531	-28.75163	2828DB	Rock	Fall	Recent-landslide	323349.24500000
KZN 0387	Trilby 9061_Upper Tugela	29.02660	-28.66053	2829CA	Rock	Fall	Recent-landslide	98591.71900000
KZN 0388	Geluk 377	31.13623	-27.92827	2731CC		Undifferentiated	Landslide	305275.71400000
KZN 0389	Mooihoek 238_1	31.13351	-28.17407	2831AA	Debris	Undifferentiated	Palaeo-landslide	703209.01800000
KZN 0391	Mooihoek 238_2	31.14050	-28.16411	2831AA	Debris	Undifferentiated	Palaeo-landslide	569513.68500000
KZN 0392	Welverdien 66	31.07606	-28.43568	2831AC	Debris	Undifferentiated	Palaeo-landslide	702885.12000000
KZN 0393	Hartskamp 160	31.04992	-28.44315	2831AC	Debris	Undifferentiated	Palaeo-landslide	428515.51900000
KZN 0394	Rooipoort 60_1	31.06062	-28.42544	2831AC	Debris	Undifferentiated	Palaeo-landslide	360336.48000000
KZN 0395	Rooipoort 60_2	31.06393	-28.41923	2831AC	Debris	Undifferentiated	Palaeo-landslide	439666.15300000
KZN 0396	Mooihoek 394_1	31.06547	-28.34755	2831AC	Debris	Undifferentiated	Palaeo-landslide	1062769.04500000
KZN 0397	Mooihoek 394_2	31.07621	-28.34088	2831AC	Debris	Undifferentiated	Palaeo-landslide	977087.43700000
KZN 0398	Welverdiend 451	31.08582	-28.33779	2831AC	Debris	Undifferentiated	Palaeo-landslide	376371.47600000
KZN 0400	Boschhoek 489	31.27864	-28.02473	2831AB		Undifferentiated	Landslide	692857.09300000
KZN 0401	Success 296_1	31.17393	-28.10064	2831AA		Undifferentiated	Landslide	279849.83600000
KZN 0402	Success 296_2	31.17680	-28.09494	2831AA		Undifferentiated	Landslide	339549.01400000
KZN 0403	Welgevonden 29	31.26922	-28.05919	2831AB		Undifferentiated	Landslide	401545.34000000
KZN 0404	Weltevrede 41_1	31.26013	-28.12663	2831AB		Undifferentiated	Landslide	521065.61300000
KZN 0405	Weltevrede 41_2	31.29020	-28.12235	2831AB		Undifferentiated	Landslide	281304.22300000
KZN 0406	Stedham 13089_1	31.29037	-28.10919	2831AB		Undifferentiated	Landslide	522839.01100000
KZN 0407	Vreestniet 481_1	31.19187	-28.15266	2831AA		Undifferentiated	Landslide	762419.97600000
KZN 0408	Weltevrede 41_3	31.27431	-28.13146	2831AB		Undifferentiated	Landslide	243829.98300000
KZN 0409	Weltevrede 41_4	31.28115	-28.13302	2831AB		Undifferentiated	Landslide	318500.26700000
KZN 0410	Vreestniet 481_2	31.20138	-28.16305	2831AA		Undifferentiated	Landslide	148195.26400000
KZN 0411	Vreestniet 481_3	31.20544	-28.15683	2831AA		Undifferentiated	Landslide	220035.72600000
KZN 0412	No. 20 7638_5	31.41698	-28.14057	2831AB		Undifferentiated	Landslide	761317.92900000
KZN 0413	Mooihoek 238_3	31.15513	-28.18096	2831AA	Debris	Undifferentiated	Palaeo-landslide	405278.66800000
KZN 0414	Groot Geluk 201_1	31.19247	-28.19436	2831AA	Debris	Undifferentiated	Palaeo-landslide	2338281.43000000
KZN 0415	No. 20 7638_1	31.30806	-28.18114	2831AB		Undifferentiated	Landslide	534536.88700000
KZN 0416	Barend 14630	31.21091	-28.18481	2831AA	Debris	Undifferentiated	Palaeo-landslide	610036.30800000
KZN 0417	Groot Geluk 201_3	31.16328	-28.19717	2831AA	Debris	Undifferentiated	Palaeo-landslide	202225.94800000
KZN 0418	Mooihoek 238_4	31.15857	-28.19085	2831AA	Debris	Undifferentiated	Palaeo-landslide	488243.72600000
KZN 0419	No. 20 7638_2	31.33195	-28.17999	2831AB		Undifferentiated	Landslide	481248.07000000
KZN 0420	No. 20 7638_8	31.42693	-28.20175	2831AB		Undifferentiated	Landslide	366772.43200000
KZN 0421	No. 20 7638_6	31.39874	-28.19492	2831AB		Undifferentiated	Landslide	671473.59700000
KZN 0422	Townlands Mahlabathni_1	31.48480	-28.22347	2831AB		Undifferentiated	Landslide	378652.71700000
KZN 0423	Groot Geluk 201_2	31.18477	-28.20286	2831AA	Debris	Undifferentiated	Palaeo-landslide	333705.89400000
KZN 0424	Lottery 531_1	31.27546	-28.22365	2831AB		Undifferentiated	Landslide	456646.71400000
KZN 0425	Eensgevonden 551	31.25622	-28.21179	2831AB		Undifferentiated	Landslide	290459.80800000
KZN 0426	No. 20 7638_17	31.34584	-28.26342	2831AD		Undifferentiated	Landslide	214835.03100000
KZN 0427	No. 20 7638_16	31.47965	-28.24154	2831AB		Undifferentiated	Landslide	201469.53300000
KZN 0428	Townlands Mahlabathni_2	31.46596	-28.22352	2831AB		Undifferentiated	Landslide	140519.44500000
KZN 0429	Langgewacht 449_1	31.14168	-28.30045	2831AC		Undifferentiated	Landslide	720831.65200000
KZN 0430	Langgewacht 449_2	31.16902	-28.29189	2831AC		Undifferentiated	Landslide	135639.26700000
KZN 0431	No. 20 7638_18	31.34762	-28.27767	2831AD		Undifferentiated	Landslide	109722.69900000
KZN 0432	Bond Lijst 536_1	31.03970	-28.32786	2831AC		Undifferentiated	Landslide	532140.14800000
KZN 0433	Bond Lijst 536_2	31.07591	-28.31577	2831AC		Undifferentiated	Landslide	222576.15400000
KZN 0434	Uitzicht 293	31.00763	-28.40932	2831AC		Undifferentiated	Landslide	526177.99500000
KZN 0435	Weltevreden 302_1	31.10105	-28.36689	2831AC		Undifferentiated	Landslide	572343.55000000
KZN 0436	Weltevreden 302_1	31.08861	-28.34984	2831AC		Undifferentiated	Landslide	448929.64800000
KZN 0437	Rooipoort 60_3	31.07425	-28.42865	2831AC		Undifferentiated	Landslide	432716.01000000
KZN 0438	No. 20 7638_4	31.44438	-28.02917	2831AB		Undifferentiated	Landslide	530036.98200000
KZN 0439	Stedham 13089_2	31.33170	-28.01322	2831AB		Undifferentiated	Landslide	148577.29600000
KZN 0440	No. 20 7638_3	31.35305	-28.01386	2831AB		Undifferentiated	Landslide	2340484.27500000
KZN 0441	Oude Werf 426	31.24745	-28.08815	2831AA		Undifferentiated	Landslide	67048.48900000
KZN 0442	Stedham 13089_3	31.32309	-28.04195	2831AB		Undifferentiated	Landslide	110020.42900000
KZN 0443	No. 20 7638_7	31.33938	-28.01174	2831AB		Undifferentiated	Landslide	28432.58100000
KZN 0444	Boschhoek 489_2	31.32706	-28.00610	2831AB		Undifferentiated	Landslide	154871.59700000
KZN 0445	No. 20 7638_9	31.33964	-28.05273	2831AB		Undifferentiated	Landslide	533558.49400000
KZN 0446	No. 20 7638_10	31.38570	-28.03245	2831AB		Undifferentiated	Landslide	49561.55700000
KZN 0447	No. 20 7638_11	31.38633	-28.03650	2831AB		Undifferentiated	Landslide	143380.44200000
KZN 0448	No. 20 7638_12	31.41518	-28.17934	2831AB		Undifferentiated	Landslide	256446.41100000
KZN 0449	No. 20 7638_13	31.49582	-28.22215	2831AB		Undifferentiated	Landslide	257038.14900000
KZN 0450	No. 20 7638_14	31.48993	-28.21360	2831AB		Undifferentiated	Landslide	41692.35100000
KZN 0451	No. 20 7638_15	31.31174	-28.20834	2831AB		Undifferentiated	Landslide	102204.51100000
KZN 0452	Lottery 531_2	31.30298	-28.19940	2831AB		Undifferentiated	Landslide	72018.60900000
KZN 0453	Good Luck 270	31.27508	-28.16152	2831AB		Undifferentiated	Landslide	77585.87200000
KZN 0454	Gobela	29.55559	-29.21202	2929BA	Debris	Flow	Palaeo-landslide	31337.05300000
KZN 0455	Dunsink 11176	29.56097	-29.21799	2929BA	Rock	Fall	Recent-landslide	28224.69800000
KZN 0456	Giants castle Nature R10	29.54032	-29.22942	2929BA		Undifferentiated	Landslide	9834.21100000
KZN 0457	Giants castle Nature R11	29.54759	-29.23045	2929BA	Rock	Fall	Recent-landslide	612064.93700000
KZN 0458	Giants castle Nature R12	29.56743	-29.22478	2929BA	Rock	Fall	Recent-landslide	705386.08600000
KZN 0459	Giants castle Nature R13	29.56310	-29.23728	2929BA	Rock	Fall	Recent-landslide	323037.99300000
KZN 0460	Giants castle Nature R14	29.51251	-29.19760	2929BA	Rock	Fall	Recent-landslide	35001.27900000
KZN 0461	Giants castle Nature R15	29.53618	-29.24320	2929BA	Rock	Fall	Recent-landslide	122097.04400000
KZN 0462	Giants castle Nature R16	29.52527	-29.25321	2929BA	Debris	Undifferentiated	Palaeo-landslide	118471.81300000

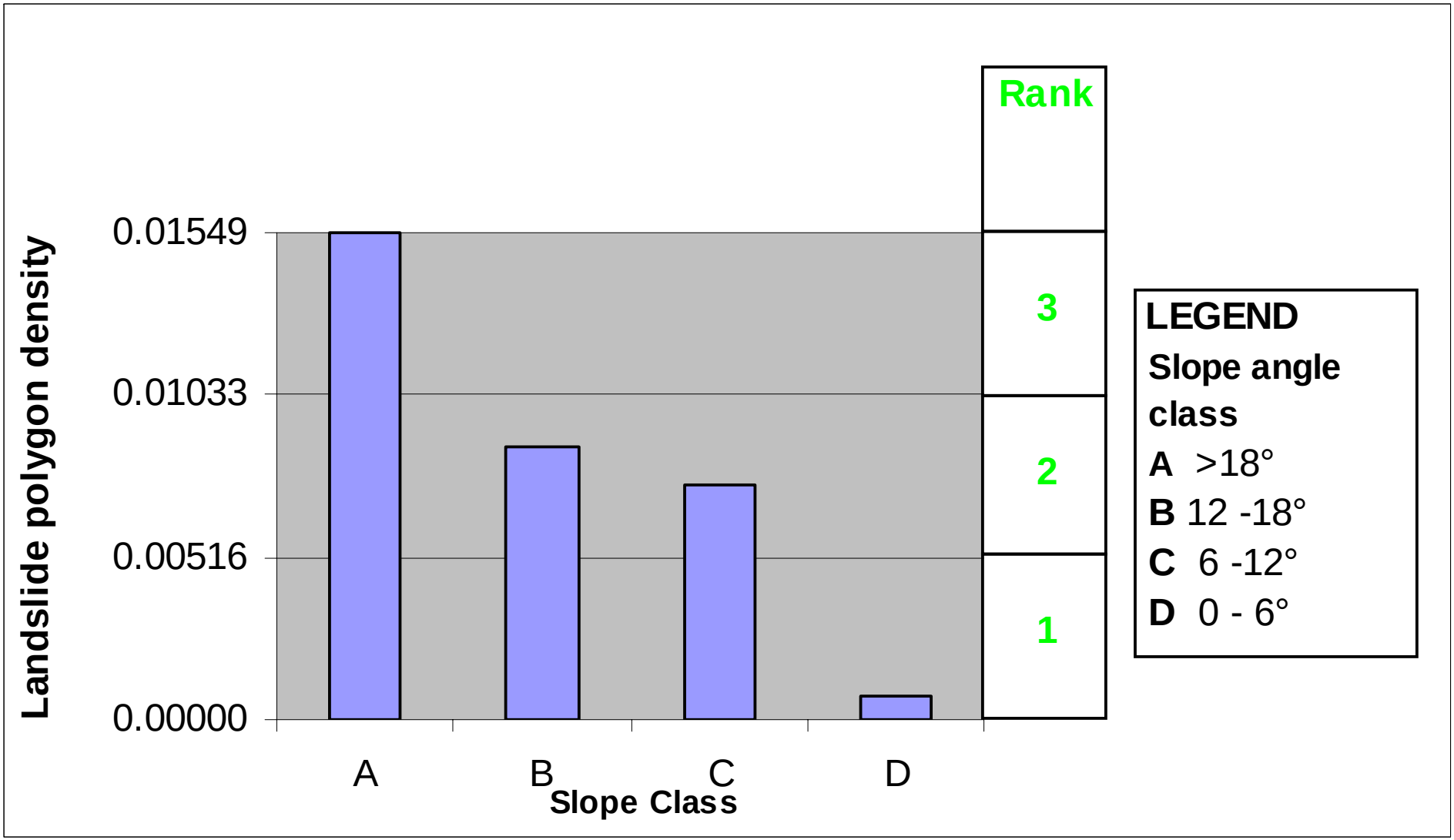
KZN 0463	Giants castle Nature R17	29.52843	-29.25284	2929BA	Debris	Undifferentiated	Palaeo-landslide	87560.01000000
KZN 0464	Giants castle Nature R18	29.53046	-29.25851	2929BC	Debris	Rotational	Recent-landslide	45.22200000
KZN 0465	Giants castle Nature R19	29.51450	-29.26638	2929BC	Debris	Rotational	Recent-landslide	22.23800000
KZN 0466	Giants castle Nature R20	29.51734	-29.26981	2929BC	Debris	Rotational	Recent-landslide	22.10900000
KZN 0467	Loteni Nature Res1	29.49867	-29.41133	2929BC	Rock	Fall	Recent-landslide	120527.11000000
KZN 0468	Loteni Nature Res1	29.51811	-29.44404	2929BC	Earth	Undifferentiated	Recent-landslide	91.44400000
KZN 0469	Giant's Castle Game Re9	29.51582	-29.26204	2929BC	Debris	Rotational	Recent-landslide	22.23900000
KZN 0470	Dart Moor 7421_1	29.62890	-29.31678	2929BC	Debris	Flow	Recent-landslide	109.07300000
KZN 0471	Dart Moor 7421_2	29.62684	-29.31657	2929BC	Debris	Rotational	Recent-landslide	127.19300000
KZN 0472	Harlech 7427_2	29.64528	-29.31843	2929BC	Debris	Rotational	Recent-landslide	140.03000000
KZN 0473	Harlech 7427_1	29.64257	-29.31761	2929BC	Debris	Rotational	Recent-landslide	24.98900000
KZN 0474	Kamberg Nature Reser3	29.67712	-29.38922	2929BC	Debris	Undifferentiated	Palaeo-landslide	94452.59200000
KZN 0475	Harlech 7427_3	29.63698	-29.31692	2929BC	Debris	Rotational	Recent-landslide	29.97900000
KZN 0476	Harlech 7427_4	29.63577	-29.31388	2929BC	Debris	Flow	Recent-landslide	78.98200000
KZN 0477	Kamberg Nature Reser4	29.65957	-29.39343	2929BC	Rock	Fall	Recent-landslide	137160.09700000
KZN 0478	Kamberg Nature Reser6	29.64712	-29.39234	2929BC	Rock	Fall	Recent-landslide	97137.84500000
KZN 0479	Kamberg Nature Reser7	29.65002	-29.39817	2929BC		Undifferentiated	Landslide	140292.27500000
KZN 0480	Dilston	30.10589	-29.98352	2930CC	Debris	Undifferentiated	Palaeo-landslide	3125176.98100000
KZN 0481	Kwa-Ncakubana_1	29.91986	-30.13274	3029BB	Rock	Fall	Recent-landslide	34372.62300000
KZN 0482	Kwa-Ncakubana_2	29.90704	-30.13601	3029BB	Rock	Fall	Recent-landslide	2007956.41200000
KZN 0483	Kendron	29.94706	-30.17803	3029BB		Undifferentiated	Landslide	891695.65700000
KZN 0484	Ncakubana	29.93225	-30.14389	3029BB	Debris	Undifferentiated	Palaeo-landslide	702998.74000000
KZN 0485	Pampa	30.31401	-30.20617	3030AB	Rock	Fall	Recent-landslide	277771.00800000
KZN 0486	Umnyesa	30.08289	-29.93076	2930CC		Undifferentiated	Landslide	1645669.59200000
KZN 0487	Maqadim_2	30.00274	-29.75335	2929DBDD_2930CACC	Rock	Fall	Recent-landslide	841097.34500000
KZN 0488	Maqadim_1	30.00214	-29.75509	2929DD_2930CC		Undifferentiated	Landslide	161496.79800000
KZN 0489	Fairlands_1	29.98829	-29.91195	2929DD	Rock	Fall	Recent-landslide	374010.32500000
KZN 0490	Voyizana	29.92972	-29.83609	2929DD		Undifferentiated	Landslide	1340271.54700000
KZN 0491	Peepdale	29.96908	-29.78922	2929DD		Undifferentiated	Landslide	999440.96500000
KZN 0492	Fairlands_2	29.98079	-29.90997	2929DD	Rock	Fall	Recent-landslide	427786.59300000
KZN 0493	Mnywanani	29.98065	-29.91946	2929DD		Undifferentiated	Landslide	912020.28600000
KZN 0494	Meander Stream	29.57069	-29.28332	2929BC	Debris	Rotational	Palaeo-landslide	122926.39800000
MT1	Ezinqoteni	30.19275	-30.77249	3030CC	Debris	Translational	Recent-landslide	5.00000000
MT10	Ingwe_1	29.83481	-30.02664	3029BB	Earth	Flow	Recent-landslide	5.00000000
MT100	Ethekweni_58	31.00351	-29.80032	2930DD & 2931CC	Debris	Rotational	Recent-landslide	50000.00000000
MT101	Ethekweni_57	30.84776	-29.78545	2930DD & 2931CC	Earth	Flow	Recent-landslide	500.00000000
MT102	Ethekweni_56	30.85404	-29.79115	2930DD & 2931CC	Earth	Flow	Recent-landslide	5.00000000
MT103	Ethekweni_55	30.82460	-29.82472	2930DD & 2931CC	Debris	Undifferentiated	Recent-landslide	50000.00000000
MT104	Ethekweni_52	30.82232	-29.83412	2930DD & 2931CC	Earth	Flow	Recent-landslide	500.00000000
MT105	Ethekweni_45	30.82713	-29.84760	2930DD & 2931CC	Earth	Flow	Recent-landslide	500.00000000
MT106	Ethekweni_35	30.87970	-29.84262	2930DD & 2931CC	Earth	Flow	Recent-landslide	500.00000000
MT107	Ethekweni_34	30.87041	-29.84632	2930DD & 2931CC	Earth	Flow	Recent-landslide	500.00000000
MT108	Ethekweni_33	30.87252	-29.85014	2930DD & 2931CC	Earth	Flow	Recent-landslide	500.00000000
MT109	Ethekweni_32	30.87472	-29.85410	2930DD & 2931CC	Earth	Flow	Recent-landslide	500.00000000
MT11	Greater Kokstad_1	29.38425	-29.97576	2929CD	Debris	Rotational	Recent-landslide	50000.00000000
MT110	Ethekweni_31	30.86933	-29.85857	2930DD & 2931CC	Earth	Flow	Recent-landslide	500.00000000
MT111	Ethekweni_30	30.76010	-29.83089	2930DD & 2931CC	Earth	Flow	Recent-landslide	500.00000000
MT112	Ethekweni_29	30.78429	-29.84143	2930DD & 2931CC	Earth	Flow	Recent-landslide	500.00000000
MT113	Ethekweni_28	30.79535	-29.86241	2930DD & 2931CC	Earth	Flow	Recent-landslide	5.00000000
MT114	Ethekweni_27	30.83595	-29.86777	2930DD & 2931CC	Earth	Flow	Recent-landslide	50000.00000000
MT115	Ethekweni_26	30.86152	-29.86264	2930DD & 2931CC	Earth	Flow	Recent-landslide	5.00000000
MT116	Ethekweni_25	30.87763	-29.87970	2930DD & 2931CC	Earth	Flow	Recent-landslide	5.00000000
MT117	Ethekweni_24	30.89495	-29.87293	2930DD & 2931CC	Earth	Flow	Recent-landslide	500.00000000
MT118	Ethekweni_23	30.90421	-29.86976	2930DD & 2931CC	Earth	Flow	Recent-landslide	500.00000000
MT119	Ethekweni_22	30.92087	-29.89432	2930DD & 2931CC	Earth	Flow	Recent-landslide	500.00000000
MT12	Ingwe_5	29.76200	-29.97073	2929DD	Debris	Translational	Recent-landslide	500.00000000
MT120	Ethekweni_21	30.95996	-29.86978	2930DD & 2931CC	Debris	Translational	Recent-landslide	50000.00000000
MT121	Ethekweni_20	30.97722	-29.86565	2930DD & 2931CC	Debris	Undifferentiated	Recent-landslide	500.00000000
MT122	Ethekweni_19	30.85984	-29.91024	2930DD & 2931CC	Earth	Flow	Recent-landslide	500.00000000
MT123	Ethekweni_18	30.85955	-29.91256	2930DD & 2931CC	Earth	Undifferentiated	Recent-landslide	500.00000000
MT124	Ethekweni_17	30.86105	-29.91663	2930DD & 2931CC	Earth	Flow	Recent-landslide	500.00000000
MT125	Ethekweni_16	30.86812	-29.91705	2930DD & 2931CC	Earth	Undifferentiated	Recent-landslide	50000.00000000
MT126	Ethekweni_15	30.86722	-29.91993	2930DD & 2931CC	Earth	Flow	Recent-landslide	500.00000000
MT127	Ethekweni_14	30.87156	-29.91784	2930DD & 2931CC	Earth	Undifferentiated	Recent-landslide	500.00000000
MT128	Ethekweni_13	30.87808	-29.91726	2930DD & 2931CC	Earth	Undifferentiated	Recent-landslide	500.00000000
MT129	Ethekweni_12	30.88658	-29.91714	2930DD & 2931CC	Earth	Flow	Recent-landslide	500.00000000
MT13	Ingwe_6	29.93224	-29.94744	2929DD	Debris	Translational	Recent-landslide	50000.00000000
MT130	Ethekweni_11	30.87031	-29.92563	2930DD & 2931CC	Earth	Undifferentiated	Recent-landslide	500.00000000
MT131	Ethekweni_10	30.87222	-29.92738	2930DD & 2931CC	Earth	Flow	Recent-landslide	500.00000000
MT132	Ethekweni_9	30.87706	-29.92895	2930DD & 2931CC		Undifferentiated	Landslide	5.00000000
MT133	Ethekweni_6	30.85183	-29.96261	2930DD & 2931CC	Earth	Rotational	Recent-landslide	500.00000000
MT14	Richmond_1	30.37626	-29.94945	2930CD	Earth	Flow	Recent-landslide	500.00000000
MT15	Ingwe_4	29.89190	-29.84881	2929DD	Earth	Flow	Recent-landslide	50000.00000000
MT16	Ingwe_2	29.92276	-29.80647	2929DD	Earth	Flow	Recent-landslide	5.00000000
MT17	Ingwe_7	30.01337	-29.79633	2930CC	Earth	Flow	Recent-landslide	5.00000000
MT18	Ingwe_8	30.01718	-29.75982	2930CC	Earth	Flow	Recent-landslide	50000.00000000
MT19	Ingwe_3	30.08437	-29.74979	2930CA	Earth	Flow	Recent-landslide	5.00000000
MT2	uMuziwabantu	30.03453	-30.64135	3030CA	Debris	Translational	Recent-landslide	5.00000000
MT20	Ingwe_10	30.08086	-29.72159	2930CA	Earth	Flow	Recent-landslide	5.00000000

MT21	The Msunduzi_5	30.13666	-29.70561	2930CA	Earth	Flow	Recent-landslide	500.00000000
MT22	The Msunduzi_4	30.17121	-29.67274	2930CA	Earth	Flow	Recent-landslide	500.00000000
MT23	The Msunduzi_1	30.20162	-29.66079	2930CA	Earth	Flow	Recent-landslide	5.00000000
MT24	The Msunduzi_2	30.24226	-29.64834	2930CA	Earth	Flow	Recent-landslide	5.00000000
MT25	Richmond_3	30.14500	-29.79181	2930CC	Earth	Flow	Recent-landslide	500.00000000
MT26	Richmond_4	30.42748	-29.90354	2930CD	Earth	Flow	Recent-landslide	500.00000000
MT27	Richmond_2	30.23233	-29.82125	2930CC	Debris	Rotational	Recent-landslide	5.00000000
MT28	Richmond_5	30.31339	-29.81990	2930CD	Debris	Rotational	Recent-landslide	50000.00000000
MT29	Ingwe_9	29.85813	-29.73511	2929DB	Debris	Translational	Recent-landslide	50000.00000000
MT3	Greater Kokstad_2	29.45831	-30.58413	3029CB	Earth	Flow	Recent-landslide	5.00000000
MT30	KZDMA43	29.39460	-29.60514	2929CB	Earth	Flow	Recent-landslide	500.00000000
MT31	Impendle_1	29.54067	-29.55913	2929DA	Debris	Translational	Recent-landslide	500.00000000
MT32	Impendle_2	29.64137	-29.62484	2929DA	Debris	Translational	Recent-landslide	100000.10000000
MT33	Impendle_3	29.75664	-29.56417	2929DB	Debris	Translational	Recent-landslide	500.00000000
MT34	Impendle_4	29.60567	-29.51449	2929DA	Earth	Flow	Recent-landslide	500.00000000
MT35	Impendle_5	29.60792	-29.57362	2929DA	Debris	Translational	Recent-landslide	500.00000000
MT36	Ethekweni_1	30.87907	-29.86013	2930DD/2931CC	Earth	Flow	Recent-landslide	500.00000000
MT37	Ethekweni_37	30.77640	-29.83188	2930DD/2931CC	Earth	Flow	Recent-landslide	50000.00000000
MT38	Ethekweni_38	30.75180	-29.84076	2930DD/2931CC	Earth	Flow	Recent-landslide	50000.00000000
MT39	Ethekweni_39	30.72541	-29.83635	2930DC	Earth	Flow	Recent-landslide	50000.00000000
MT4	Matatiele_1	29.15790	-30.43798	3029AC	Debris	Flow	Recent-landslide	50000.00000000
MT40	Ethekweni_40	30.70526	-29.81579	2930DC	Earth	Flow	Recent-landslide	50000.00000000
MT41	Ethekweni_41	30.68351	-29.80359	2930DC	Earth	Flow	Recent-landslide	50000.00000000
MT42	Ethekweni_42	30.65107	-29.80246	2930DC	Earth	Flow	Recent-landslide	500.00000000
MT43	Ethekweni_43	30.60151	-29.78741	2930DC	Earth	Flow	Recent-landslide	500.00000000
MT44	Ethekweni_44	30.66865	-29.75085	2930DC	Rock	Translational	Recent-landslide	500.00000000
MT45	The Msunduzi_6	30.37445	-29.59444	2930CB	Earth	Flow	Recent-landslide	500.00000000
MT46	uMngeni_8	30.21690	-29.50842	2930CA	Earth	Undifferentiated	Recent-landslide	500.00000000
MT47	uMngeni_7	30.19640	-29.48687	2930AC	Earth	Flow	Recent-landslide	500.00000000
MT48	uMngeni_6	30.15081	-29.46331	2930AC	Earth	Flow	Recent-landslide	500.00000000
MT49	uMngeni_5	30.08698	-29.41967	2930AC	Earth	Flow	Recent-landslide	500.00000000
MT5	Matatiele_2	28.97150	-30.38097	3028BD	Debris	Flow	Recent-landslide	500.00000000
MT50	uMngeni_3	30.06126	-29.40219	2930AC	Earth	Flow	Recent-landslide	500.00000000
MT51	uMngeni_2	30.00619	-29.36659	2930AC	Earth	Flow	Recent-landslide	500.00000000
MT52	Mooi Mpofana_5	29.99092	-29.24596	2929BB	Earth	Flow	Recent-landslide	500.00000000
MT53	uMngeni_1	30.17335	-29.43207	2930AC	Earth	Flow	Recent-landslide	500.00000000
MT54	uMngeni_4	30.15066	-29.39710	2930AC	Earth	Undifferentiated	Recent-landslide	500.00000000
MT55	Mooi Mpofana_3	29.93686	-29.28916	2929BD	Earth	Flow	Recent-landslide	500.00000000
MT56	Mooi Mpofana_1	29.93677	-29.26316	2929BD	Debris	Undifferentiated	Recent-landslide	50000.00000000
MT57	Mooi Mpofana_7	29.85376	-29.34159	2929BD	Rock	Translational	Recent-landslide	50000.00000000
MT58	Mooi Mpofana_2	29.67581	-29.34342	2929BC	Debris	Undifferentiated	Recent-landslide	50000.00000000
MT59	Mooi Mpofana_4	29.69698	-29.31580	2929BC	Debris	Flow	Recent-landslide	50000.00000000
MT6	Hibiscus Coast	30.55619	-30.58804	3030DA	Earth	Flow	Recent-landslide	500.00000000
MT60	KZDMA22	29.63858	-29.30546	2929BC	Debris	Flow	Recent-landslide	50000.00000000
MT61	Imbabazane_2	29.68452	-29.26310	2929BC	Debris	Flow	Recent-landslide	50000.00000000
MT62	KZDMA23_1	29.57201	-29.22306	2929BA	Debris	Flow	Recent-landslide	50000.00000000
MT63	KZDMA23_2	29.54394	-29.17155	2929BA	Rock	Undifferentiated	Recent-landslide	500.00000000
MT64	KZDMA23_4	29.39999	-29.15632	2929AB	Rock	Undifferentiated	Recent-landslide	50000.00000000
MT65	KZDMA23_3	29.43255	-29.12832	2929AB	Debris	Flow	Recent-landslide	500.00000000
MT66	Imbabazane_1	29.59150	-29.06302	2929BA	Debris	Flow	Recent-landslide	500.00000000
MT67	Mooi Mpofana_6	29.94858	-29.16829	2929BB	Debris	Flow	Recent-landslide	500.00000000
MT68	The Msunduzi_3	30.39278	-29.56131	2930CB	Earth	Flow	Recent-landslide	500.00000000
MT69	uMshawati	30.42167	-29.45083	2930AD	Earth	Flow	Recent-landslide	500.00000000
MT7	Ethekweni_7	30.76521	-30.19934	3030BB	Debris	Flow	Recent-landslide	5.00000000
MT70	Ethekweni_69	31.08099	-29.70337	2931CA	Earth	Flow	Recent-landslide	5.00000000
MT71	Ethekweni_70	31.09012	-29.61822	2931CA	Earth	Flow	Recent-landslide	500.00000000
MT72	The KwaDukusa	31.27903	-29.36736	2931AD	Earth	Flow	Recent-landslide	50000.00000000
MT73	Umvoti_5	30.74260	-29.14057	2930BA	Debris	Undifferentiated	Recent-landslide	50000.00000000
MT74	Maphumulo	31.06290	-29.12270	2931AA	Earth	Flow	Recent-landslide	500.00000000
MT75	Umvoti_6	30.76375	-29.10222	2930BB	Debris	Undifferentiated	Recent-landslide	50000.00000000
MT76	Umvoti_4	30.78107	-29.07246	2930BB	Debris	Undifferentiated	Recent-landslide	500.00000000
MT77	Umvoti_3	30.74195	-29.05190	2930BA	Debris	Undifferentiated	Recent-landslide	50000.00000000
MT78	Umvoti_2	30.53567	-29.11061	2930BA	Earth	Flow	Recent-landslide	5.00000000
MT79	Umvoti_1	30.50631	-28.98118	2830DC	Earth	Flow	Recent-landslide	500.00000000
MT8	Ethekweni_8	30.80828	-30.17583	3030BB	Earth	Flow	Recent-landslide	500.00000000
MT80	Umlalazi_2	31.53755	-28.96023	2831DC	Earth	Flow	Recent-landslide	5.00000000
MT81	Umlalazi_1	31.18571	-28.84994	2831CC	Earth	Flow	Recent-landslide	5.00000000
MT82	uMhalathuze	31.86421	-28.76449	2831DD	Earth	Flow	Recent-landslide	5.00000000
MT83	Msinga_1	30.45060	-28.51103	2830CB	Debris	Flow	Recent-landslide	500.00000000
MT84	Msinga_2	30.47897	-28.56912	2830CB	Debris	Flow	Recent-landslide	500.00000000
MT85	Okhahlamba_3	29.50128	-28.44119	2829BC	Debris	Undifferentiated	Recent-landslide	500.00000000
MT86	Okhahlamba_1	29.05659	-28.57602	2829CA	Debris	Flow	Recent-landslide	500.00000000
MT87	Okhahlamba_5	29.05668	-28.58416	2829CA	Debris	Flow	Recent-landslide	500.00000000
MT88	Okhahlamba_2	29.05840	-28.58889	2829CA	Debris	Flow	Recent-landslide	500.00000000
MT89	Okhahlamba_4	29.07066	-28.60457	2829CA	Debris	Flow	Recent-landslide	500.00000000
MT9	KZ5a5	30.15040	-30.09906	3030AA	Debris	Translational	Recent-landslide	5.00000000
MT90	Ethekweni_67	30.98484	-29.76514	2930DD & 2931CC	Debris	Rotational	Recent-landslide	500.00000000
MT91	Ethekweni_63	30.98471	-29.77322	2930DD & 2931CC	Debris	Rotational	Recent-landslide	50000.00000000
MT92	Ethekweni_66	30.99089	-29.77278	2930DD & 2931CC	Debris	Undifferentiated	Recent-landslide	500.00000000

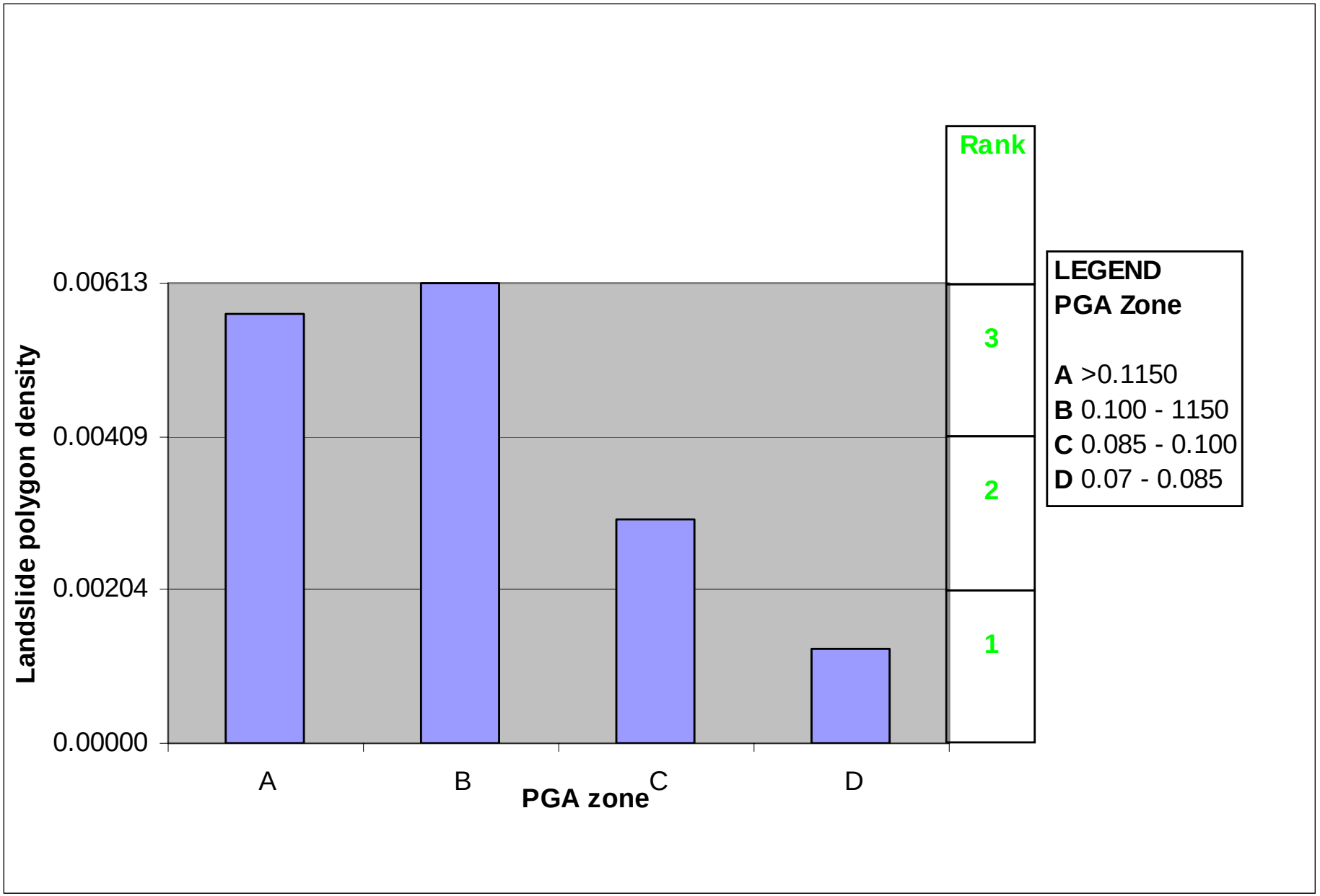
MT93	Ethekweni_65	31.00728	-29.77028	2930DD & 2931CC	Debris	Translational	Recent-landslide	500.00000000
MT94	Ethekweni_64	31.00947	-29.77510	2930DD & 2931CC	Debris	Undifferentiated	Recent-landslide	50000.00000000
MT95	Ethekweni_54	31.01362	-29.77314	2930DD & 2931CC	Debris	Undifferentiated	Recent-landslide	50000.00000000
MT96	Ethekweni_62	31.01397	-29.76947	2930DD & 2931CC	Debris	Undifferentiated	Recent-landslide	500.00000000
MT97	Ethekweni_61	31.01827	-29.76618	2930DD & 2931CC	Debris	Translational	Recent-landslide	50000.00000000
MT98	Ethekweni_60	31.01841	-29.77270	2930DD & 2931CC	Debris	Flow	Recent-landslide	5.00000000
MT99	Ethekweni_59	31.03511	-29.76074	2930DD & 2931CC	Earth	Rotational	Recent-landslide	500.00000000
NPR1	Ethekweni_49	30.85167	-29.96222	2930DD & 2931CC	Debris	Rotational	Recent-landslide	500.00000000
NPR2	Ethekweni_48	30.90778	-29.97000	2930DD & 2931CC	Debris	Translational	Recent-landslide	500.00000000
RCNB_01	Draaihoek_1	30.28055	-29.66337	2930CB		Undifferentiated	Landslide	50011.76600000
RCNB_02	Draaihoek_2	30.27585	-29.66717	2930CB		Undifferentiated	Landslide	24898.46800000
RCNB_03	Pietermarizburg_3	30.31468	-29.69509	2930CB		Undifferentiated	Landslide	18727.85900000
RCNB_04	Pietermarizburg_4	30.33371	-29.71714	2930CB		Undifferentiated	Landslide	78170.36400000
RCNB_05	Pietermarizburg_5	30.36553	-29.71805	2930CB		Undifferentiated	Landslide	12525.11200000
RCNB_06	Pietermarizburg_6	30.30046	-29.71884	2930CB		Undifferentiated	Landslide	48055.82400000
RCNB_07	Sinathingi_1	30.27534	-29.68147	2930CB		Undifferentiated	Landslide	21952.89100000
RCNB_08	Sinathingi_1	30.27875	-29.68066	2930CB		Undifferentiated	Landslide	15364.50700000
RCNB_10	Pietermarizburg_8	30.26176	-29.69654	2930CB		Undifferentiated	Landslide	35772.88500000
RCNB_11	Pietermarizburg_9	30.26276	-29.59769	2930CB		Undifferentiated	Landslide	5.00000000
RCNB_12	Pietermarizburg_10	30.26527	-29.59603	2930CB		Undifferentiated	Landslide	5.00000000
RCNB_13	Pietermarizburg_11	30.26424	-29.61986	2930CB		Undifferentiated	Landslide	5.00000000
RCNB_14	Pietermarizburg_12	30.26456	-29.62510	2930CB		Undifferentiated	Landslide	5.00000000
RCNB_15	Pietermarizburg_13	30.29343	-29.62759	2930CB		Undifferentiated	Landslide	5.00000000
RCNB_16	Pietermarizburg_14	30.28068	-29.63123	2930CB		Undifferentiated	Landslide	5.00000000
RCNB_17	Pietermarizburg_15	30.27216	-29.63185	2930CB		Undifferentiated	Landslide	5.00000000
RCNB_18	Pietermarizburg_16	30.28060	-29.63124	2930CB		Undifferentiated	Landslide	5.00000000
RCNB_19	Pietermarizburg_17	30.31045	-29.66089	2930CB		Undifferentiated	Landslide	5.00000000
RCNB_20	Pietermarizburg_18	30.32666	-29.67044	2930CB		Undifferentiated	Landslide	5.00000000
RCNB_21	Pietermarizburg_19	30.28384	-29.67125	2930CB		Undifferentiated	Landslide	5.00000000
RCNB_22	Pietermarizburg_20	30.27627	-29.67605	2930CB		Undifferentiated	Landslide	5.00000000
RCNB_23	Pietermarizburg_21	30.27247	-29.67460	2930CB		Undifferentiated	Landslide	5.00000000
RCNB_24	Pietermarizburg_22	30.26063	-29.68558	2930CB		Undifferentiated	Landslide	5.00000000
RCNB_25	Pietermarizburg_23	30.25572	-29.68947	2930CB		Undifferentiated	Landslide	5.00000000
RCNB_26	Pietermarizburg_24	30.25191	-29.69130	2930CB		Undifferentiated	Landslide	5.00000000
RCNB_27	Pietermarizburg_25	30.26059	-29.70101	2930CB		Undifferentiated	Landslide	5.00000000
RCNB_28	Pietermarizburg_26	30.33502	-29.62568	2930CB		Undifferentiated	Landslide	5.00000000
RCNB_29	Otto's Bluff	30.37838	-29.52279	2930CB	Debris	Undifferentiated	Palaeo-landslide	9085745.23561000
RCNB_30	Pietermarizburg_27	30.33815	-29.51181	2930CB		Undifferentiated	Landslide	3577581.28666000
RCNB_31	Pietermarizburg_28	30.38507	-29.54811	2930CB		Undifferentiated	Landslide	5511316.54698000
RCNB_32	Pietermarizburg_29	30.33420	-29.55676	2930CB		Undifferentiated	Landslide	2854100.15550000
RCNB_33	Pietermarizburg_30	30.33805	-29.57711	2930CB		Undifferentiated	Landslide	7117045.35862000
RCNB_34	Pietermarizburg_31	30.31317	-29.58990	2930CB		Undifferentiated	Landslide	1301246.73812000
RCNB_35	Pietermarizburg_32	30.32745	-29.59413	2930CB		Undifferentiated	Landslide	311539.69603000
RCNB_36	World's View	30.32186	-29.60656	2930CB	Debris	Undifferentiated	Palaeo-landslide	4142491.88990000
RCNB_37	Pietermarizburg_33	30.49102	-29.59613	2930CB		Undifferentiated	Landslide	65079.59114640
RCNB_38	Pietermarizburg_34	30.49713	-29.59712	2930CB		Undifferentiated	Landslide	44116.77161800
RCNB_39	Pietermarizburg_35	30.48054	-29.60454	2930CB		Undifferentiated	Landslide	106679.93414000
RCNB_40	Pietermarizburg_36	30.30519	-29.62210	2930CB		Undifferentiated	Landslide	5694569.64096000
RCNB_41	Pietermarizburg_37	30.33476	-29.61227	2930CB		Undifferentiated	Landslide	39545.68319310
RCNB_42	Pietermarizburg_38	30.25286	-29.61611	2930CB		Undifferentiated	Landslide	116093.28973400
RCNB_43	Pietermarizburg_39	30.25863	-29.62925	2930CB		Undifferentiated	Landslide	308217.33731100
RCNB_44	Pietermarizburg_40	30.28703	-29.63505	2930CB		Undifferentiated	Landslide	1339229.60858000
RCNB_45	Pietermarizburg_41	30.26552	-29.63120	2930CB		Undifferentiated	Landslide	122167.83469200
RCNB_46	Pietermarizburg_42	30.27241	-29.63432	2930CB		Undifferentiated	Landslide	234527.21177300
RCNB_47	Pietermarizburg_43	30.26384	-29.63804	2930CB		Undifferentiated	Landslide	404513.81992600
RCNB_48	Pietermarizburg_44	30.25273	-29.65893	2930CB		Undifferentiated	Landslide	456921.03385400
RCNB_49	Pietermarizburg_45	30.26127	-29.66491	2930CB		Undifferentiated	Landslide	400361.05301800
RCNB_50	Pietermarizburg_46	30.26032	-29.67808	2930CB		Undifferentiated	Landslide	513351.81993300
RCNB_51	Pietermarizburg_47	30.26042	-29.69104	2930CB		Undifferentiated	Landslide	2153646.35776000
RCNB_52	Pietermarizburg_48	30.28415	-29.70886	2930CB		Undifferentiated	Landslide	5705426.60822000
RCNB_53	Pietermarizburg_49	30.25095	-29.70288	2930CB		Undifferentiated	Landslide	46916.11702940
RCNB_54	Pietermarizburg_50	30.25055	-29.72640	2930CB		Undifferentiated	Landslide	1317618.26703000
RCNB_55	Pietermarizburg_51	30.32022	-29.72621	2930CB		Undifferentiated	Landslide	270839.65783800
RCNB_56	Pietermarizburg_52	30.26269	-29.73861	2930CB		Undifferentiated	Landslide	65619.49455820
RCNB_9	Pietermarizburg_7	30.28421	-29.68844	2930CB		Undifferentiated	Landslide	26414.40400000
WEB149	Ethekweni_Mayat_place	30.97509	-29.80976	2930DD & 2931CC	Debris	Translational	Recent-landslide	88155.34600000
X1	eDumbe	30.90860	-27.31490	2730BD	Debris	Flow	Recent-landslide	500.00000000
X2	Ethekweni_47	30.71065	-29.77966		Debris	Rotational	Recent-landslide	5.00000000

APPENDIX 2: GRAPHS SHOWING RANKING VALUES OF ALL INITIALLY CONSIDERED LANDSLIDE CAUSAL FACTORS

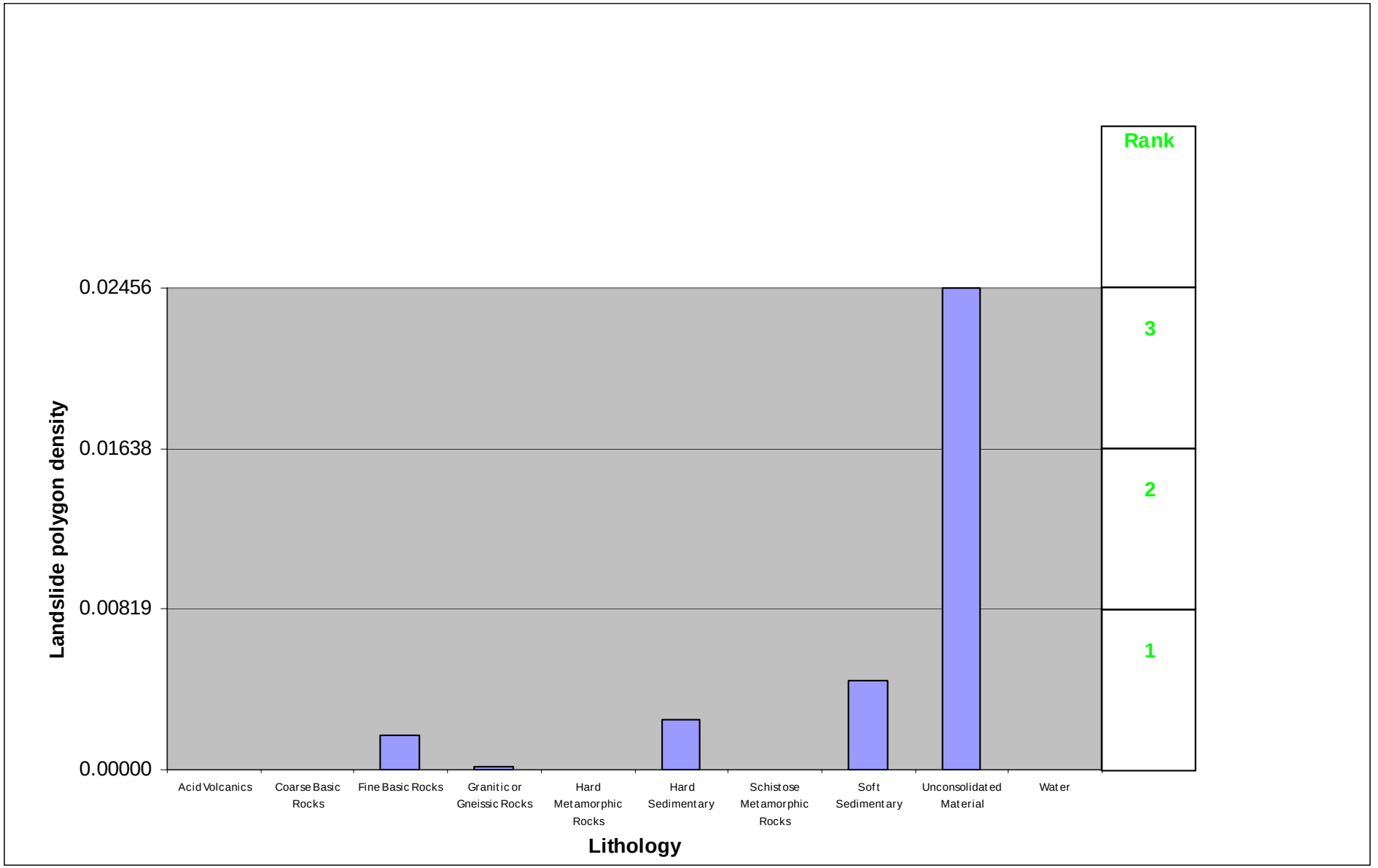
2a Slope Angle


Rank
3
2
1
0.01549
0.01033
0.00516
0.00000
Landslide polygon density
A
B
C
D
Slope Class
LEGEND
Slope angle class
A >18°
B 12 -18°
C 6 -12°
D 0 - 6°

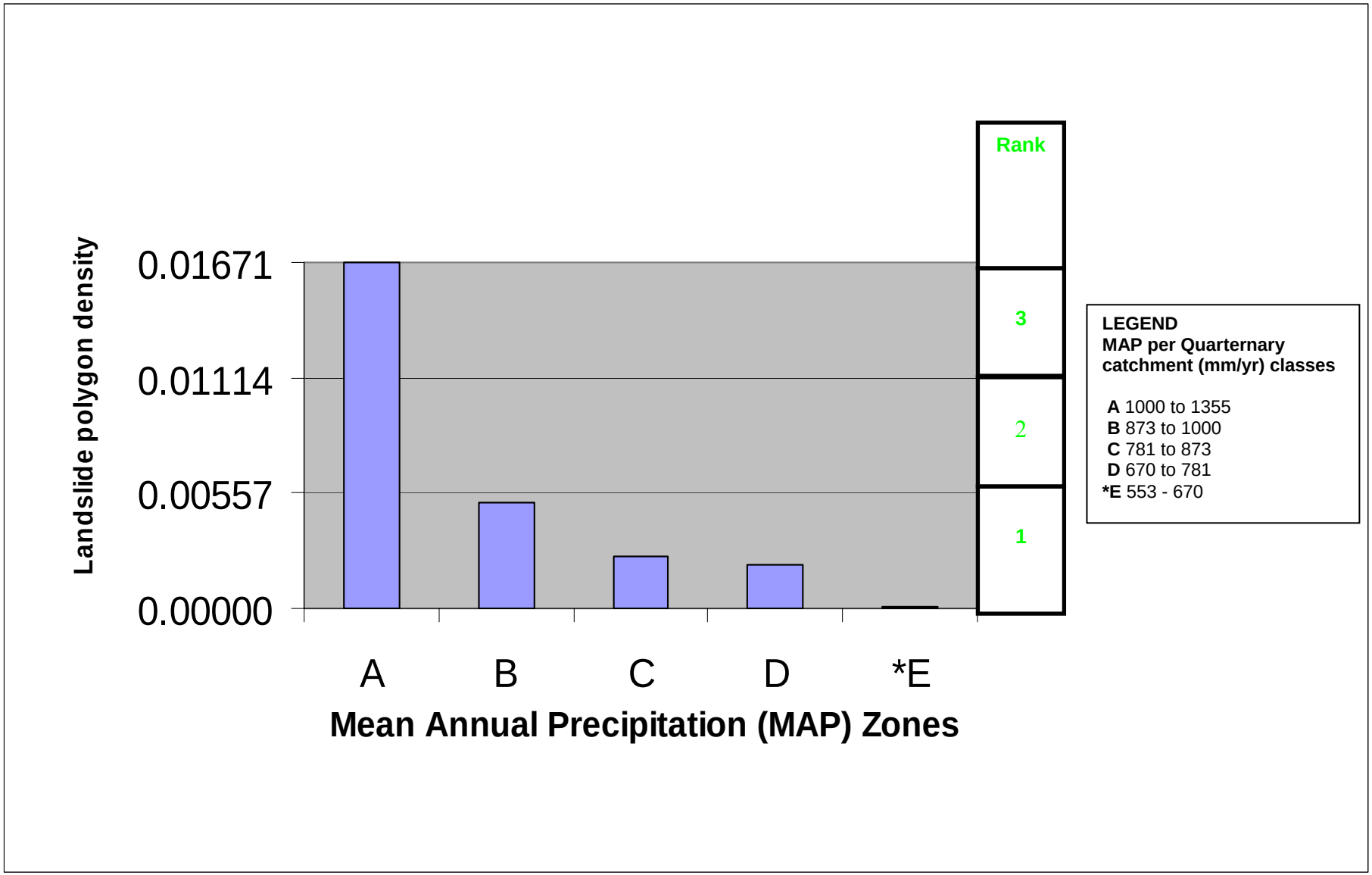
2b Seismicity


Rank
3
2
1
LEGEND
PGA Zone
A >0.1150
B 0.100 - 1150
C 0.085 - 0.100
D 0.07 - 0.085
0.00613
0.00409
0.00204
0.00000
Landslide polygon density
A
B
C
D
PGA zone

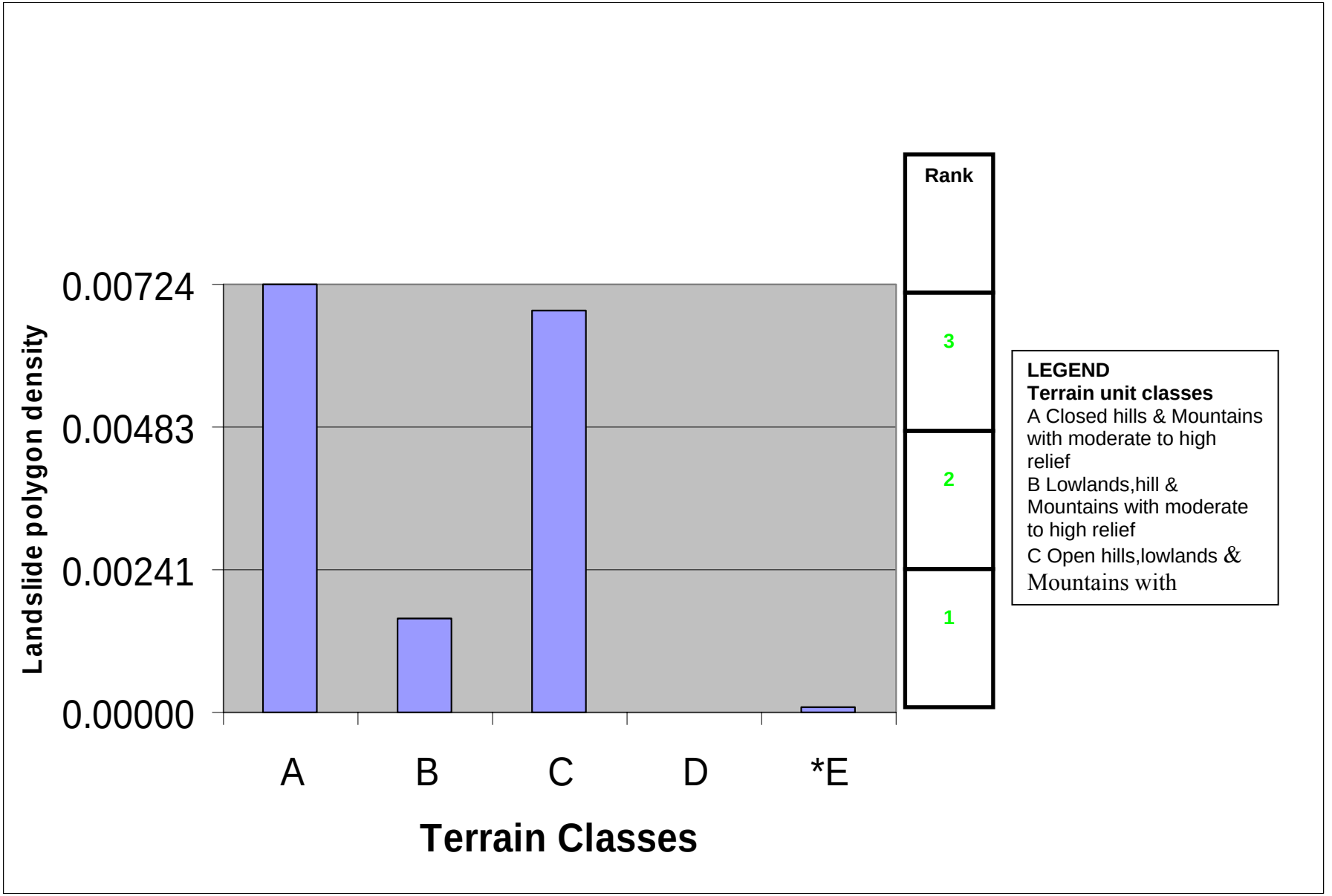
2c Geology


Rank
3
2
1
0.02456
0.01638
0.00819
0.00000
Landslide polygon density
Acid Volcanics
Coarse Basic Rocks
Fine Basic Rocks
Granitic or Gneissic Rocks
Hard Metamorphic Rocks
Hard Sedimentary
Schistose Metamorphic Rocks
Soft Sedimentary
Unconsolidated Material
Water
Lithology

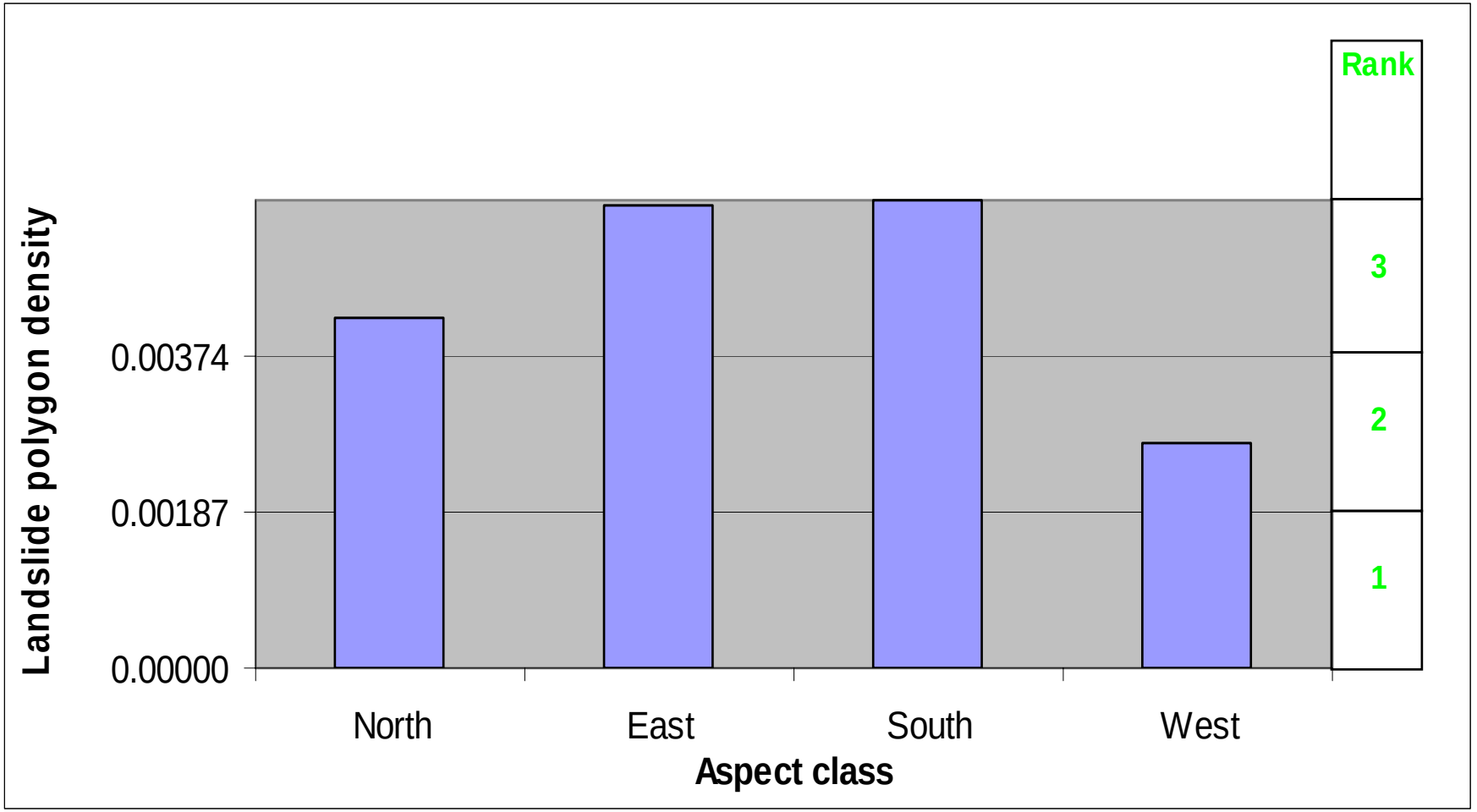
2d Rainfall


Landslide polygon density
0.01671
0.01114
0.00557
0.00000
A
B
C
D
*E
Mean Annual Precipitation (MAP) Zones
Rank
3
2
1
LEGEND
MAP per Quarternary catchment (mm/yr) classes
A 1000 to 1355
B 873 to 1000
C 781 to 873
D 670 to 781
*E 553 - 670

2e Terrain morphology


Landslide polygon density
0.00724
0.00483
0.00241
0.00000
A
B
C
D
*E
Terrain Classes
Rank
3
2
1
LEGEND
Terrain unit classes
A Closed hills & Mountains with moderate to high relief
B Lowlands,hill & Mountains with moderate to high relief
C Open hills,lowlands & Mountains with

2f Aspect


Rank
3
2
1
Landslide polygon density
0.00374
0.00187
0.00000
North
East
South
West
Aspect class

APPENDIX 3: CONSISTENCY RATIO CALCULATION

HOME
WHAT'S NEW
ABOUT CCI
- Who We Are
- CCI In Action
- Virtual Tour

SERVICES
LEARNING OPPORTUNITIES
CCI LIBRARY
PUBLICATIONS
- The Bookstore
- Conservation Information Database
- CCI Newsletter
- CCI Notes
- Technical Bulletins

RESOURCES
- Preserving my Heritage Website
- BCIN
- Links of Interest

TOOLS
- Preservation Framework Online
- Analytical Hierarchy Process (AHP) Program
- Downloads

FEEDBACK
TELL A COLLEAGUE ABOUT THE SITE

Analytical Hierarchy Process (AHP) Program

Matrix Method

Apply the desired weights to your criteria in the matrix below. Begin by finding the first criterion in the lefthand column. Follow along the row to the right until you come to the criterion you wish to compare it to, and enter the desired value. Acceptable values range from -9 (absolutely less important) to +9 (absolutely more important). After entering all of your values, click Calculate. The results will appear in the graph on the right.

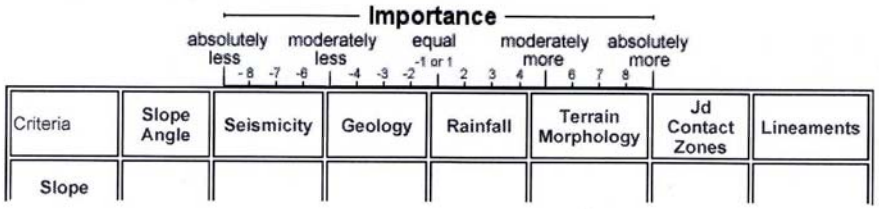
Crit.	X	Y	Z
X			
Y			
Z			

Results



Consistancy Ratio: 0.048

The small matrix above provides an example. In this case, criterion Y is being compared to criterion Z. If criterion Y is absolutely less important than criterion Z, a value of -9 would be appropriate. If criterion Y is moderately more important the criterion Z, a value of +5 would be appropriate. And so on.



Angle		5	6	6	5	5	8
Seismicity			1	2	3	3	7
Geology				2	1	-1	5
Rainfall					1	-1	4
Terrain Morphology						-2	4
Jd Contact Zones							5
Lineaments							

Calculate

Last Updated: 2005-5-13

Important Notices

APPENDIX 4: ANALYTICAL HIERARCHY PROCESS CALCULATION

AHP Calculation

n*(n-1)/2 = 7*(7-1)/2= 21

Enter pairwise responses into the importance table

	SLOPE ANGLE	SEISMICITY	GEOLOGY	RAINFALL	TERRAIN MORPHOLOGY	DOLERITE CONTACT ZONES	LINEAMENTS
SLOPE ANGLE	1	5	6	6	5	5	8
SEISMICITY	"1/5"	1	1	2	3	3	7
GEOLOGY	"1/6"	"1/1"	1	2	1	-1	5
RAINFALL	"1/6"	"1/2"	"1/2"	1	1	-1	4
TERRAIN MORPHOLOGY	"1/5"	"1/3"	"1/1"	"1/1"	1	-2	4
DOLERITE CONTACT ZONES	"1/5"	"1/3"	"1/-1"	"1/-1"	"1/-2"	1	5
LINEAMENTS	"1/8"	"1/7"	"1/5"	"1/4"	"1/4"	"1/5"	1

Calculate weights

Step 1: Complete matrix calculating reciprocal values

	SLOPE ANGLE	SEISMICITY	GEOLOGY	RAINFALL	TERRAIN MORPHOLOGY	DOLERITE CONTACT ZONES	LINEAMENTS
SLOPE ANGLE	1	5	6	6	5	5	8
SEISMICITY	0.2	1	1	2	3	3	7
GEOLOGY	0.166666667	1	1	2	1	1	5
RAINFALL	0.166666667	0.5	0.5	1	1	1	4
TERRAIN MORPHOLOGY	0.2	0.333333333	1	1	1	0.50	4
DOLERITE CONTACT ZONES	0.2	0.333333333	1	1	2	1	5
LINEAMENTS	0.125	0.142857143	0.2	0.25	0.25	0.2	1

Step 2: Sum column values

	SLOPE ANGLE	SEISMICITY	GEOLOGY	RAINFALL	TERRAIN MORPHOLOGY	DOLERITE CONTACT ZONES	LINEAMENTS
SLOPE ANGLE	1	5	6	6	5	5	8
SEISMICITY	0.2	1	1	2	3	3	7
GEOLOGY	0.166666667	1	1	2	1	1	5
RAINFALL	0.166666667	0.5	0.5	1	1	1	4
TERRAIN MORPHOLOGY	0.2	0.333333333	1	1	1	0.5	4
DOLERITE CONTACT ZONES	0.2	0.333333333	1	1	2	1	5
LINEAMENTS	0.125	0.142857143	0.2	0.25	0.25	0.2	1
	2.058	8.310	10.700	13.250	13.250	11.700	34.000

Step 3: Divide matrix values by column sums

	SLOPE ANGLE	SEISMICITY	GEOLOGY	RAINFALL	TERRAIN MORPHOLOGY	DOLERITE CONTACT ZONES	LINEAMENTS
SLOPE ANGLE	0.49	0.60	0.56	0.45	0.38	0.43	0.24
SEISMICITY	0.10	0.12	0.09	0.15	0.23	0.26	0.21
GEOLOGY	0.08	0.12	0.09	0.15	0.08	0.09	0.15
RAINFALL	0.08	0.06	0.05	0.08	0.08	0.09	0.12
TERRAIN MORPHOLOGY	0.10	0.04	0.09	0.08	0.08	0.04	0.12
DOLERITE CONTACT ZONES	0.10	0.04	0.09	0.08	0.15	0.09	0.15
LINEAMENTS	0.06	0.02	0.02	0.02	0.02	0.02	0.03
	1.00	1.00	1.00	1.00	1.00	1.00	1.00

Step 4: Sum row values

	SLOPE ANGLE	SEISMICITY	GEOLOGY	RAINFALL	TERRAIN MORPHOLOGY	DOLERITE CONTACT ZONES	LINEAMENTS		Weight using Arithmetic mean method
SLOPE ANGLE	0.49	0.60	0.56	0.45	0.38	0.43	0.24	3.14	0.44873
SEISMICITY	0.10	0.12	0.09	0.15	0.23	0.26	0.21	1.15	0.16437
GEOLOGY	0.08	0.12	0.09	0.15	0.08	0.09	0.15	0.75	0.10767
RAINFALL	0.08	0.06	0.05	0.08	0.08	0.09	0.12	0.54	0.07742
TERRAIN MORPHOLOGY	0.10	0.04	0.09	0.08	0.08	0.04	0.12	0.54	0.07744
DOLERITE CONTACT ZONES	0.10	0.04	0.09	0.08	0.15	0.09	0.15	0.69	0.09853
LINEAMENTS	0.06	0.02	0.02	0.02	0.02	0.02	0.03	0.18	0.02584
	1.00	1.00	1.00	1.00	1.00	1.00	1.00	*7.00*	1.00000
							Minimum Value		0.02584

Note: Complete steps 1-4 for each participant, then average the weights and determine the minimum value for calculating the overall weights (step 5)

Step 5: Divide each weight by the minimum value

		Overall Weights	% Weight	AHP Weight (Value between 0&1)	Maximum Susceptibility Coefficient (M)
SLOPE ANGLE		17.36833	44.873286	0.44873	1.346196591
SEISMICITY		6.3621	16.437413	0.16437	0.493122375
GEOLOGY		4.1675	10.767392	0.10767	0.323021763
RAINFALL		2.9965	7.7419013	0.07742	0.23225704
TERRAIN MORPHOLOGY		2.9972	7.7437721	0.07744	0.232313163
DOLERITE CONTACT ZONES		3.8135	9.8526079	0.09853	0.295578237
LINEAMENTS		1.0000	2.5836277	0.02584	0.077508832
		38.7053	100	1.00000	3